JOURNAL OF MATHEMATICAL PHYSICS VOLUME 10, NUMBER 1 JANUARY 1969

High-Frequency Scattering by a Transparent Sphere. I. Direct Reflection and Transmission

H. M. NUSSENZVEIG
Department of Physics and Astronomy, University of Rochester, Rochester, New York

(Received 15 April 1968)

This is Paper I of a series on high-frequency scattering of a scalar plane wave by a transparent sphere (square potential well or barrier). It is assumed that $(ka)^{\frac{1}{3}} \gg 1$, $|N-1|^{\frac{1}{2}}(ka)^{\frac{1}{3}} \gg 1$, where k is the wavenumber, a is the radius of the sphere, and N is the refractive index. By applying the modified Watson transformation, previously employed for an impenetrable sphere, the asymptotic behavior of the exact scattering amplitude in any direction is obtained, including several angular regions not treated before. The distribution of Regge poles is determined and their physical interpretation is given. The results are helpful in explaining the reason for the difference in the analytic properties of scattering amplitudes for cutoff potentials and potentials with tails. Following Debye, the scattering amplitude is expanded in a series, corresponding to a description in terms of multiple internal reflections. In Paper I, the first term of the Debye expansion, associated with direct reflection from the surface, and the second term, associated with direct transmission (without any internal reflection), are treated, both for $N > 1$ and for $N < 1$. The asymptotic expansions are carried out up to (not including) correction terms of order $(ka)^{-2}$. For $N > 1$, the behavior of the first term is similar to that found for an impenetrable sphere, with a forward diffraction peak, a lit (geometrical reflection) region, and a transition region where the amplitude is reduced to generalized Fock functions. For $N < 1$, there is an additional shadow boundary, associated with total reflection, and a new type of surface waves is found. They are related to Schmidt head waves, but their sense of propagation disagrees with the geometrical theory of diffraction. The physical interpretation of this result is given. The second term of the Debye expansion again gives rise to a lit region, a shadow region, and a Fock-type transition region, both for $N > 1$ and for $N < 1$. In the former case, surface waves make shortcuts across the sphere, by critical refraction. In the latter one, they excite new surface waves by internal diffraction.

1. INTRODUCTION

This is the first in a series of papers dealing with the scattering of a plane wave by a transparent sphere at high frequencies. [A preliminary account of this work[1] and a survey of the main results[2] have already been given.] The assumptions are

$$\beta^{\frac{1}{3}} \gg 1, \quad |N-1|^{\frac{1}{2}}\beta^{\frac{1}{3}} \gg 1, \tag{1.1}$$

where

$$\beta = ka \tag{1.2}$$

is the dimensionless parameter associated with the wavenumber k and the radius a of the sphere, and N is the refractive index.

The lower limit on β for which the results are applicable depends on the degree of accuracy desired. It is hoped that they provide useful quantitative information down to $\beta \sim 100$ and at least qualitative information down to $\beta \sim 10$.

The sphere is assumed to be perfectly transparent, so that N is real. Both $N > 1$ and $N < 1$ are considered, but more attention is devoted to the former case. Additional limitations on N will be set in Paper II.[3] Extension of the results to complex values of N, to account for absorption, should not be unduly difficult.

As a rule, we shall also exclude

$$N \gg 1, \quad N \ll 1, \tag{1.3}$$

although the results can be at least partially applied in these cases. The reason for the second limitation in (1.1) will be discussed in Sec. 2. We note here that it implies

$$2\,|N-1|\,\beta \gg \beta^{\frac{1}{3}} \gg 1, \tag{1.4}$$

where the left-hand side is the phase shift of a central ray going through the sphere. This excludes the domain of Rayleigh–Gans scattering (where the Born approximation is applicable) and part of the anomalous diffraction region. The terminology is explained in Van de Hulst's beautiful book (Ref. 4, p. 133). In Van de Hulst's chart of the N–β domain (Ref. 4, Fig. 20), the region we treat corresponds to the right-hand side of the square, excluding the neighborhood of the corners.

For the sake of simplicity, we discuss only the scattering of a scalar field in the first two papers of this series. The whole treatment can be extended to electromagnetic scattering, as will be shown in the third paper.[5]

[1] H. M. Nussenzveig, Bull. Am. Phys. Soc. **11**, 372 (1966).
[2] H. M. Nussenzveig, to appear in *Proceedings of the Theoretical Physics Conference for R. E. Peierls's 60th Birthday.*
[3] H. M. Nussenzveig, J. Math. Phys. **10**, 125 (1969) (following paper), to be referred to hereafter as II.
[4] H. C. Van de Hulst, *Light Scattering by Small Particles* (John Wiley & Sons, New York, 1957).
[5] H. M. Nussenzveig (to be published); hereafter referred to as III.

The scalar wavefunction may be interpreted either as the velocity potential of sound waves or as the Schrödinger wavefunction in quantum mechanics. In the latter case, the problem corresponds to the scattering of nonrelativistic particles of momentum $p = \hbar k$ by a square potential well or barrier of radius a and depth (height) given by V_0,

$$V(r) = -V_0 \quad (0 \leq r < a);$$
$$V(r) = 0 \quad (r > a). \tag{1.5}$$

The refractive index is given by

$$N = [1 + (2mV_0/\hbar^2k^2)]^{\frac{1}{2}}, \tag{1.6}$$

where m is the mass of the particle. Note that $N > 1$ corresponds to a well and $N < 1$ to a barrier. This analogy, of course, is valid only at fixed energy, i.e., fixed k. For a fixed V_0, N is frequency-dependent (dispersion), while fixed N corresponds to an energy-dependent potential (V_0 proportional to the energy).

The extension of the present model to complex N may be of some interest in connection with the optical model in nuclear and high-energy physics. Of course, it would still be unrealistic in several respects: at high energies, inelastic and relativistic effects become important, and the simple potential-well picture no longer applies. Furthermore, some of the effects to be described depend on the existence of a sharp edge in the potential, which again might be unrealistic for nuclear forces. Nevertheless, we shall see that at least some of these effects appear to have analogs in the nuclear case.

We are dealing with a classic problem in scattering theory, the literature on which ranges over several decades.[6] An excellent survey up to 1957 is given by Van de Hulst.[4]

The exact solution of the electromagnetic problem in the form of a partial-wave series is usually associated with Mie.[7] As is well known, this series converges very slowly at high frequencies. One can then associate with the lth partial wave an "impact parameter"

$$p_l = (l + \tfrac{1}{2})/k, \tag{1.7}$$

and partial waves with $p_l \lesssim a$ are appreciably distorted, so that one has to keep at least β terms in the series. Experience with numerical computations has shown that the actual number of terms that must be retained is

$$l_+ \sim \beta + c\beta^{\frac{1}{3}}, \tag{1.8}$$

where c is a constant of order unity (empirically, $c \gtrsim 3$).

[6] N. A. Logan, Proc. I.E.E.E. **53**, 73 (1965).
[7] G. Mie, Ann. Physik **25**, 377 (1908).

This result can be understood in terms of the penetration of the centrifugal barrier up to the surface. The effective potential for radial motion is

$$U(r) = V(r) + \hbar^2 l(l + 1)/2mr^2, \tag{1.9}$$

where $V(r)$ is given by (1.5). [Actually, in order to apply the WKB approximation, $l(l + 1)$ should be replaced by $(l + \frac{1}{2})^2$.[8]] The discontinuity at $r = a$ gives rise to a barrier, and $p_l > a$, according to (1.7), corresponds to an energy below the top of this barrier. The transmissivity of the barrier up to $r = a - 0$ is then given by[8]

$$T_l = \frac{4N}{1 + N^2} \exp(2\psi_l), \tag{1.10}$$

where

$$\psi_l = -\int_\beta^{l+\frac{1}{2}} [(l + \tfrac{1}{2})^2 - x^2]^{\frac{1}{2}} \frac{dx}{x}. \tag{1.11}$$

In particular, near the top of the barrier, we find that

$$\psi_l \approx -\tfrac{1}{3}[2(l + \tfrac{1}{2} - \beta)/\beta^{\frac{1}{3}}]^{\frac{3}{2}}, \tag{1.12}$$

so that the transmissivity for $p_l > a$ is appreciable only within the range $\beta < l < l_+$.

The difficulty in employing the partial-wave expansion at high frequencies is apparent from (1.8). Nevertheless, in view of the practical importance of the problem, numerical computations have been carried out in this way up to values of β of the order of a few hundred. Besides the fact that computer calculations are no substitute for a physical understanding of the behavior of the solution, however, there are also practical difficulties: The results are very rapidly varying functions of β, N, and the scattering angle, so that very closely spaced points would be required for accurate interpolation.

Several approximation methods have been proposed to overcome these difficulties; they are reviewed in Ref. 4. The "localization principle" (1.7) leads to a subdivision of the terms of the partial-wave series into three domains:

(i) $$0 \leq l \lesssim l_- \sim \beta - c\beta^{\frac{1}{3}}; \tag{1.13}$$

(ii) $$l_- \lesssim l \lesssim l_+; \tag{1.14}$$

(iii) $$l_+ \lesssim l. \tag{1.15}$$

Partial waves in the domain (iii) are damped faster than exponentially by the centrifugal barrier and give a negligible contribution. The domain (i) gives rise to the forward diffraction peak, as well as to the contributions of reflected and refracted rays, according to geometrical optics (Ref. 4, Chap. 12).

[8] M. V. Berry, Proc. Phys. Soc. (London) **88**, 285 (1966).

The domain (ii) will be called the *edge domain*, because it corresponds to incident rays passing close to the "edge" of the sphere. We have already seen that the transmissivity of the centrifugal barrier is still appreciable for $\beta < l < l_+$. The domain $l_- < l < \beta$ corresponds to near-grazing incidence, so that strong reflection occurs, as well as strong interference between incident and reflected waves (Ref. 4, Sec. 17.21). We shall see that the edge domain gives rise to some of the most interesting effects.

According to classical mechanics, a particle with $l + \frac{1}{2} \sim \beta$ would have vanishing radial velocity at $r = a$, and it might be expected to circle indefinitely around the scatterer, a phenomenon known as *orbiting*.[9] We shall see that the edge domain indeed gives rise to surface waves, circling around the sphere any number of times. In addition, for $N > 1$, they can also penetrate through the sphere, leading to several striking effects, as will be seen later.

The most far-reaching attempts to derive the high-frequency asymptotic behavior of the exact solution have been based upon Watson's transformation.[10–12] However, the results have never gone much beyond other previously known approximations, and they have been subject to several limitations. Only some disconnected angular regions have been treated, with no discussion of the transition between them. In particular, the neighborhood of the forward and backward directions, where several important diffraction effects take place, has not been treated.

Light scattering by water droplets in the atmosphere gives rise to two of the most beautiful natural phenomena: the rainbow and the glory. The best approximate theory of the rainbow so far available is still Airy's classic theory,[13] despite the fact that it is known to suffer from several shortcomings (Ref. 4, p. 249). No satisfactory quantitative treatment of the glory has ever been given.

A modified form of the Watson transformation has recently been developed and applied by the author to the problem of scattering by an impenetrable sphere (Ref. 14, hereafter referred to as N). This method enables one to derive the asymptotic behavior of the exact solution at any distance from the sphere and in any direction, including near-forward and near-backward directions.

In the present series of papers, the modified Watson transformation is applied to the transparent sphere problem. We shall consider only the scattering amplitude; the behavior of the wavefunction in the near region is not discussed. The main result is that the asymptotic high-frequency behavior of the exact scattering amplitude in any direction can be determined by this method. The different types of transition regions that occur are discussed. In particular, an improved treatment of the rainbow and a quantitative theory of the glory will be given.

In Sec. 2, the distribution of poles of the S function in the complex angular-momentum plane is determined. Their physical interpretation is discussed and their relation to the usual Regge poles that appear in potential scattering is examined. This helps to clarify a long-standing puzzle in scattering theory, namely, the question of why cutoff potentials and potentials with exponential tails give rise to scattering amplitudes having widely different analytic properties. However, it is found that the Watson transformation, applied directly to the partial-wave expansion, is not at all helpful, because the residue series associated with the poles of the S function, in contrast with the case of an impenetrable sphere, are not rapidly convergent.

This difficulty is circumvented in Sec. 3, by means of a procedure first applied by Debye[15] in the case of a circular cylinder. The interaction of the incident wave with the sphere is decomposed into an infinite series of interactions with the surface, analogous to the multiple internal reflection treatment of the Fabry–Perot interferometer. The terms of this Debye expansion are also closely related with the rays appearing in the geometrical-optics (ray-tracing) method that undergo multiple internal reflections. The poles in the complex-angular-momentum plane associated with the terms of the Debye expansion are determined. It is found that, in contrast with the poles of the S function, they give rise to rapidly convergent residue series. The relation with previous treatments of the problem is also discussed.

The modified Watson transformation can be applied to each term of the Debye expansion. The asymptotic behavior of each term, as in the impenetrable sphere problem, is usually dominated by contributions of two types: (a) *saddle-point contributions:* these are associated with geometrical-optic rays and the WKB expansion, and they are related with partial waves in the domain (i); (b) *residue-series contributions:* these correspond to surface waves, and they are related with partial waves in the edge domain (ii).

Each class of rays gives rise to "shadow" and "lit" regions for the corresponding term of the Debye

[9] K. W. Ford and J. A. Wheeler, Ann. Phys. (N.Y.) **7**, 259 (1959).
[10] B. Van der Pol and H. Bremmer, Phil. Mag. **24**, 141, 825 (1937).
[11] P. Beckmann, Z. Naturforsch. **12a**, 960 (1957).
[12] S. I. Rubinow, Ann. Phys. (N.Y.) **14**, 305 (1961).
[13] G. B. Airy, Trans. Cambridge Phil. Soc. **6**, 379 (1838).
[14] H. M. Nussenzveig, Ann. Phys. (N.Y.) **34**, 23 (1965).
[15] P. J. Debye, Physik. Z. **9**, 775 (1908).

expansion. In lit regions, the amplitude is usually (though not always) dominated by the geometrical-optic contributions, whereas the surface-wave contributions are usually dominant in shadow regions. For $N > 1$, each term gives rise to different shadow boundaries, but for $N < 1$ there exists a shadow boundary common to all terms of the Debye expansion.

For each term, we also find transition regions between light and shadow, and the most interesting diffraction phenomena occur in these regions. In addition to "Fock-type" transition regions, such as were found for an impenetrable sphere (N, Fig. 14), we shall find new types of transition regions, such as those associated with the rainbow and the glory. In terms of the particle picture, shadow regions are classically forbidden, and transition effects may be interpreted as a sort of "inertial barrier" penetration.

As to the convergence of the Debye expansion, the geometrical-optic contributions usually converge quite rapidly, because of the attenuation due to successive internal reflections, provided that we exclude the cases (1.3). The surface-wave contributions do not converge so rapidly, because of their high internal reflection coefficient. Nevertheless, we shall be able to estimate their combined effect, and we shall see that, for $N > 1$, they give rise to rapid intensity fluctuations, which become quite large in the case of the glory.

The present paper is concerned with the evaluation of the first two terms in the Debye expansion. The behavior of these terms is discussed both for $N > 1$ and for $N < 1$. In Sec. 4, we consider the first term, which corresponds to rays reflected directly from the surface. For $N > 1$, the results are quite similar to those found for an impenetrable sphere. For $N < 1$, however, we find a new type of diffracted rays, that cannot be interpreted according to the usual formulation of Keller's geometrical theory of diffraction.[16] The physical interpretation of these terms is given. In Sec. 5, the second term of the Debye expansion, corresponding to rays directly transmitted through the sphere, without any internal reflection, is treated in a similar manner.

Paper II is concerned mainly with the third term, and it contains the theory of the rainbow and the glory (for the scalar problem). The effect of higher-order terms will also be discussed. The conclusions for both papers will be given at the end of Paper II.

[16] J. B. Keller, in "Calculus of Variations and its Applications," *Proceedings of Symposia in Applied Mathematics*, L. M. Graves, Ed. (McGraw-Hill, New York, 1958), Vol. 8, p. 27.

2. THE POLES OF THE S FUNCTION

The total scattering amplitude $F(k, \theta)$ is given by the partial-wave expansion

$$F(k, \theta) = \frac{1}{ik} \sum_{l=0}^{\infty} (l + \tfrac{1}{2})[S_l(k) - 1]P_l(\cos\theta), \quad (2.1)$$

where S_l is the S function and P_l is the lth Legendre polynomial. We shall find it convenient to work with a dimensionless scattering amplitude $f(\beta, \theta)$, defined by

$$f(\beta, \theta) = F(k, \theta)/a. \quad (2.2)$$

The continuity conditions for the wavefunction and its normal derivative at the boundary lead to the well-known expression (cf. e.g., Ref. 17):

$$S_l = -\frac{h_l^{(2)}(\beta)}{h_l^{(1)}(\beta)}\left[\frac{\ln' h_l^{(2)}(\beta) - N \ln' j_l(\alpha)}{\ln' h_l^{(1)}(\beta) - N \ln' j_l(\alpha)}\right], \quad (2.3)$$

where ln′ denotes the logarithmic derivative, j_l and h_l are spherical Bessel and Hankel functions, and we have introduced, in addition to (1.2), the dimensionless parameter α associated with the internal wave number:

$$\alpha = Nka = N\beta. \quad (2.4)$$

Applying Poisson's sum formula [N, Eq. (9.57)] to Eq. (2.1), we find

$$f(\beta, \theta) = \frac{i}{\beta} \sum_{m=-\infty}^{\infty} (-1)^m \times \int_0^{\infty} [1 - S(\lambda, \beta)]P_{\lambda-\frac{1}{2}}(\cos\theta)e^{2im\pi\lambda}\lambda\, d\lambda, \quad (2.5)$$

where

$$S(\lambda, \beta) = -\frac{H_\lambda^{(2)}(\beta)}{H_\lambda^{(1)}(\beta)}\left(\frac{[2\,\beta] - N[\alpha]}{[1\,\beta] - N[\alpha]}\right), \quad (2.6)$$

and we have introduced the following notations:

$$[x] = \ln' J_\lambda(x), \quad (2.7)$$

$$[1\,x] = \ln' H_\lambda^{(1)}(x), \quad (2.8)$$

$$[2\,x] = \ln' H_\lambda^{(2)}(x). \quad (2.9)$$

We have also gone over from spherical to cylindrical Bessel and Hankel functions. The physical values of λ are $\lambda = l + \frac{1}{2}$, $l = 0, 1, 2, \cdots$.

The ordinary Watson transformation [N, Eqs. (2.7) and (2.11)] yields

$$f(\beta, \theta) = \frac{i}{2\beta}\int_C [1 - S(\lambda, \beta)]P_{\lambda-\frac{1}{2}}(\cos\theta)e^{-i\pi\lambda}\frac{\lambda\, d\lambda}{\cos(\pi\lambda)} \quad (2.10)$$

[17] H. M. Nussenzveig, Nucl. Phys. **11**, 499 (1959).

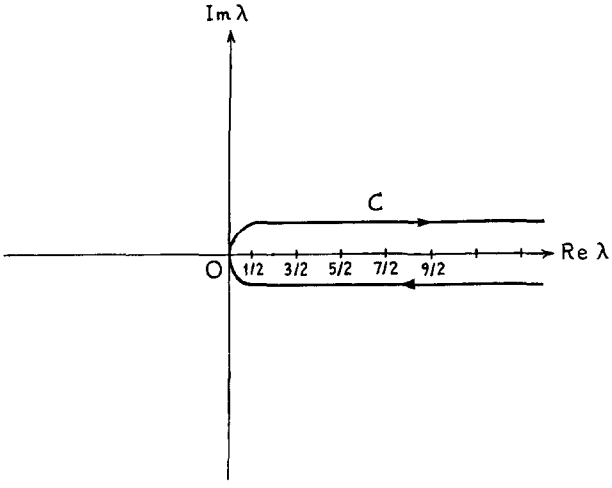

FIG. 1. The contour C.

or, equivalently,

$$f(\beta, \theta) = \frac{1}{2\beta} \int_C [1 - S(\lambda, \beta)] P_{\lambda-\frac{1}{2}}(-\cos\theta) \frac{\lambda \, d\lambda}{\cos(\pi\lambda)}, \tag{2.11}$$

where C is the contour shown in Fig. 1.

The representation (2.10) is equivalent to (2.5), as we see by employing, along the upper half of C, the expansion

$$\frac{1}{\cos(\pi\lambda)} = 2 \sum_{m=0}^{\infty} (-1)^m \exp[i(2m+1)\pi\lambda] \tag{2.12}$$

and, along the lower half,

$$\frac{1}{\cos(\pi\lambda)} = -2 \sum_{m=-\infty}^{-1} (-1)^m \exp[i(2m+1)\pi\lambda]. \tag{2.13}$$

By substituting the same expansions in (2.11), we find that (2.5) is also equivalent to

$$f(\beta, \theta) = \frac{1}{\beta} \sum_{m=-\infty}^{\infty} (-1)^m \int_0^{\infty} [1 - S(\lambda, \beta)] P_{\lambda-\frac{1}{2}}(-\cos\theta) \times \exp[i(2m+1)\pi\lambda] \lambda \, d\lambda. \tag{2.14}$$

In order to apply the modified Watson transformation (N, Sec. IX.D) directly to (2.5), we have to locate the poles of the meromorphic function $S(\lambda, \beta)$ in the complex λ plane. According to (2.6), they are the roots of

$$[1\ \beta] = N[\alpha]. \tag{2.15}$$

By interpreting N in accordance with (1.6), they may also be identified with the Regge poles for a square potential well ($N > 1$) or barrier ($N < 1$).

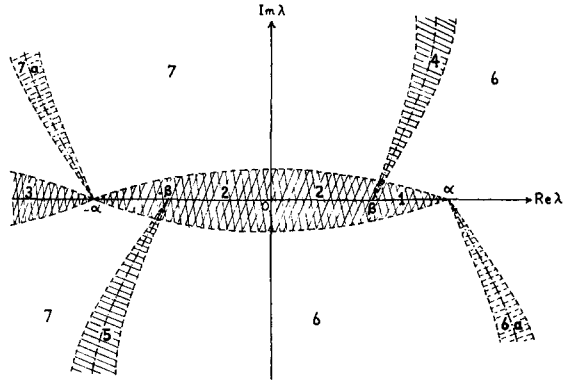

FIG. 2. Subdivision of the λ plane into regions (regions 6a and 7a refer only to Sec. 3B).

The Regge poles associated with the square-well potential have been investigated by many authors.[18–21] For $N < 1$, they have also been investigated in connection with the scattering by a dielectric cylinder.[22]

A detailed discussion of the pole distribution turns out not to be very relevant for the present problem, although some features of it will be required later on. On the other hand, such a discussion is very instructive in connection with the analytic properties of scattering amplitudes in potential scattering. The reader who is not interested in this connection may proceed directly to Sec. 3.

Instead of solving (2.15) to determine the poles $\lambda_n(\beta)$ of $S(\lambda, \beta)$ for fixed (physical) β, one can also fix λ at a physical value, $\lambda = l + \frac{1}{2}$, and solve with respect to β, to find the poles $\beta_n(l)$ in the complex β plane. This has been done explicitly for the lowest values of l.[17] The two sets of poles are related to each other (Ref. 21, Chap. 14), and we shall make use of the known results on the poles β_n to help in the physical interpretation of the poles λ_n.

We are interested mainly in the Regge-pole distribution for $\beta \gg 1$. The case $N > 1$ will be considered first. The physical interpretation of the results becomes simpler for $N \gg 1$, corresponding to an optically very dense material or to a very deep potential well. Accordingly, we shall assume that

$$\alpha \gg \beta \gg 1. \tag{2.16}$$

To solve (2.15), we replace the cylindrical functions by their asymptotic expansions, given in N (Appendix A). Corresponding to N, Fig. 15, the λ plane is subdivided into seven regions, as shown in Fig. 2.

[18] C. J. Bollini and J. J. Giambiagi, Nuovo Cimento **26**, 619 (1962); **28**, 341 (1963).
[19] A. O. Barut and F. Calogero, Phys. Rev. **128**, 1383 (1962).
[20] A. Z. Patashinskii, V. L. Pokrovskii, and I. M. Khalatnikov, Sov. Phys.—JETP **17**, 1387 (1963).
[21] R. G. Newton, *The Complex j-Plane* (W. A. Benjamin, New York, 1964), Chap. 12.
[22] W. Streifer and R. D. Kodis, Quart. Appl. Math. **23**, 27 (1965).

(In the present section, regions 6a and 7a are not to be distinguished from 6 and 7, respectively; this distinction will arise only in Sec. 3B.)

Outside of the shaded regions, we find:

$$[\alpha] \approx (\lambda^2 - \alpha^2)^{\frac{1}{2}}/\alpha, \tag{2.17}$$

$$[1\ \beta] \approx -(\lambda^2 - \beta^2)^{\frac{1}{2}}/\beta, \quad \text{in region 6,} \tag{2.18}$$

$$[1\ \beta] \approx (\lambda^2 - \beta^2)^{\frac{1}{2}}/\beta, \quad \text{in region 7,} \tag{2.19}$$

so that (2.15) becomes $(\lambda^2 - \alpha^2)^{\frac{1}{2}} = \pm(\lambda^2 - \beta^2)^{\frac{1}{2}}$, and therefore has no solutions.

The solutions must be located in the shaded regions, where either the left- or the right-hand side of (2.15) is rapidly varying, because they contain the zeros of $H_\lambda^{(1)}(\beta)$ or $J_\lambda(\alpha)$.

Let us begin with regions 1, 2, and 3, where the zeros of $J_\lambda(\alpha)$ are located. In 1 and 2, for

$$\alpha - |\lambda| \gg \alpha^{\frac{1}{3}}, \tag{2.20}$$

we have, according to N, Eq. (A16):

$$[\alpha] \approx -\frac{(\alpha^2 - \lambda^2)^{\frac{1}{2}}}{\alpha} \tan\left[\varphi(\lambda, \alpha) - \frac{\pi}{4}\right], \tag{2.21}$$

where

$$\varphi(\lambda, x) = (x^2 - \lambda^2)^{\frac{1}{2}} - \lambda \cos^{-1}(\lambda/x), \tag{2.22}$$

with

$$(x^2 - \lambda^2)^{\frac{1}{2}} > 0, \quad 0 < \cos^{-1}(\lambda/x) < \pi/2, \quad \text{for} \quad -x < \lambda < x. \tag{2.23}$$

In region 1, for

$$|\lambda| - \beta \gg \beta^{\frac{1}{3}}, \tag{2.24}$$

Eq. (2.18) is valid as a first approximation; however, in this approximation, we would find poles located on the real axis. To get the imaginary part of the poles, which is a small correction, we need an improved approximation for $[1\ \beta]$ in region 1. Under the condition (2.24), we have[23]

$$H_\lambda^{(1)}(\beta) \approx (2/\pi)^{\frac{1}{2}}(\lambda^2 - \beta^2)^{-\frac{1}{4}} \times \{\exp[\psi(\lambda, \beta)] - i \exp[-\psi(\lambda, \beta)]\}, \tag{2.25}$$

where [cf. N, Eq. (A2)]:

$$\psi(\lambda, x) = (\lambda^2 - x^2)^{\frac{1}{2}} - \lambda \ln\left[\frac{\lambda}{x} + \frac{(\lambda^2 - x^2)^{\frac{1}{2}}}{x}\right]. \tag{2.26}$$

The branches of the many-valued functions that have to be taken are specified in N (Appendix A). In region 1, with (2.24), we have

$$\operatorname{Re} \psi(\lambda, \beta) < 0, \quad |\psi(\lambda, \beta)| \gg 1, \tag{2.27}$$

so that

$$[1\ \beta] \approx -\frac{(\lambda^2 - \beta^2)^{\frac{1}{2}}}{\beta}\{1 - 2i \exp[2\psi(\lambda, \beta)]\}, \tag{2.28}$$

where the exponential term is the small correction to (2.18) that is required to determine the imaginary part of the poles.

Substituting (2.21) and (2.28) in (2.15), we find

$$\tan\left[\varphi(\lambda, \alpha) - \frac{\pi}{4}\right] = \left(\frac{\lambda^2 - \beta^2}{\alpha^2 - \lambda^2}\right)^{\frac{1}{2}}\{1 - 2i \exp[2\psi(\lambda, \beta)]\}. \tag{2.29}$$

Let

$$\lambda_n = \xi_n + i\eta_n \tag{2.30}$$

be the roots of (2.29), where $|\eta_n/\xi_n| \ll 1$. Then, to a very good approximation,

$$\varphi(\xi_n, \alpha) \approx n\pi + \frac{\pi}{4} + \tan^{-1}\left[\left(\frac{\xi_n^2 - \beta^2}{\alpha^2 - \xi_n^2}\right)^{\frac{1}{2}}\right], \tag{2.31}$$

$$\eta_n \approx \frac{2[(\alpha^2 - \xi_n^2)(\xi_n^2 - \beta^2)]^{\frac{1}{2}}}{(\alpha^2 - \beta^2)\cos^{-1}(\xi_n/\alpha)} \exp[2\psi(\xi_n, \beta)], \tag{2.32}$$

where n takes on integer values. To determine the real part of the poles, the real transcendental equation (2.31) must be solved. The corresponding imaginary part is then given by (2.32). In particular, for

$$\beta \ll \xi_n \ll \alpha, \tag{2.33}$$

these equations simplify to

$$\alpha - (\xi_n + \tfrac{1}{2})(\pi/2) \approx n\pi, \tag{2.34}$$

$$\eta_n \approx \frac{4\xi_n}{\pi\alpha}\left(\frac{e\beta}{2\xi_n}\right)^{2\xi_n}. \tag{2.35}$$

Thus, we find in region 1 a series of poles located very close to the real axis. The spacing between two consecutive poles, according to (2.31), is given by

$$\Delta\xi_n \approx \pi/\cos^{-1}(\xi_n/\alpha) \quad (\approx 2 \quad \text{for} \quad \xi_n \ll \alpha). \tag{2.36}$$

According to (2.35), the poles get closer to the real axis as ξ_n increases.

These poles have a simple physical interpretation in terms of resonances. Optically, they correspond to the "free modes of vibration of a dielectric sphere" [see Refs. 24 (p. 73) and 25]. Their long lifetime is made possible by the high internal reflectivity, due to the large refractive index, and by the high centrifugal barrier, due to the large angular momentum. The resonance appears when the corresponding pole lies close to a physical value of λ.

In the quantum-mechanical interpretation, (2.16) corresponds to a very deep potential well, and the poles (2.30) correspond to resonances lying below the top of the centrifugal barrier. Under these conditions,

[23] G. N. Watson, *Theory of Bessel Functions* (Cambridge University Press, Cambridge, England, 1962), 2nd ed., p. 267.

[24] P. J. Debye, Ann. Physik Ser. 4, **30**, 57 (1909).

[25] G. Beck and P. Wenzel, Z. Physik **84**, 335 (1933).

the effective potential (1.9) represents a deep well surrounded by a high barrier, thus giving rise to sharp resonances.

The corresponding poles in the β plane are obtained by setting $\lambda = l + \frac{1}{2}$ in (2.29) and solving for β. We find that $\operatorname{Re}\beta_n$ is determined by the well-known resonance condition (Ref. 26, p. 382):

$$N \operatorname{Re}\beta_n - (l + \tfrac{1}{2})\frac{\pi}{2} \approx n\pi, \tag{2.37}$$

which is equivalent to (2.34). We also find a result analogous to (2.32) for $\operatorname{Im}\beta_n$:

$$\operatorname{Im}\beta_n \propto \exp[2\psi(l + \tfrac{1}{2}, \operatorname{Re}\beta_n)] = \exp(2\psi_l) = v_l, \tag{2.38}$$

where ψ_l is given by (1.11) and v_l represents the penetration factor of the centrifugal barrier in the WKB approximation [cf. Eq. (1.10) and Ref. 26, p. 361]. This leads to the usual expression for the width Γ_n of the resonance (Ref. 26, p. 389).

In region 2, also assuming (2.24), we have, by N, Eq. (A16),

$$[1\ \beta] \approx i(\beta^2 - \lambda^2)^{\frac{1}{2}}/\beta, \tag{2.39}$$

so that (2.15) becomes

$$\tan[\varphi(\lambda, \alpha) - \pi/4] \approx -i\left(\frac{\beta^2 - \lambda^2}{\alpha^2 - \lambda^2}\right)^{\frac{1}{2}}, \tag{2.40}$$

or, since $\beta \ll \alpha$,

$$\varphi(\lambda_n, \alpha) \approx n\pi + \frac{\pi}{4} - i\left(\frac{\beta^2 - \lambda_n^2}{\alpha^2 - \lambda_n^2}\right)^{\frac{1}{2}}. \tag{2.41}$$

In particular, for $|\lambda_n| \ll \beta$, this gives

$$\lambda_n \approx \frac{2\alpha}{\pi} - \left(2n + \frac{1}{2}\right) + \frac{2i}{\pi N}, \quad |\lambda_n| \ll \beta. \tag{2.42}$$

This corresponds to another series of poles with spacing $|\Delta\lambda_n| \approx 2$, not so close to the real axis and with almost constant imaginary part. Their real part is again determined by the resonance condition (2.34).

These poles are associated with broad resonances above the top of the centrifugal barrier. For the corresponding poles in the β plane, we find

$$\operatorname{Im}\beta_n \approx -1. \tag{2.43}$$

This again agrees with the usual expression (Ref. 26, p. 389) for the resonance width, with the barrier penetration factor v_l set equal to unity, so that the width is determined only by the refractive index. For $l = 0$, these poles have been discussed in Ref. 17.

In region 3, setting

$$\lambda = -\mu, \tag{2.44}$$

we find, by N, Eq. (A15),

$$[\alpha] \approx -\frac{(\mu^2 - \alpha^2)^{\frac{1}{2}}}{\alpha} \times \left\{\frac{2\sin(\pi\mu) - \cos(\pi\mu)\exp[2\psi(\mu, \alpha)]}{2\sin(\pi\mu) + \cos(\pi\mu)\exp[2\psi(\mu, \alpha)]}\right\}, \tag{2.45}$$

and, since $H^{(1)}_{-\mu}(x) = e^{i\pi\mu}H^{(1)}_{\mu}(x)$, Eq. (2.28) gives

$$[1\ \beta] \approx -\frac{(\mu^2 - \beta^2)^{\frac{1}{2}}}{\beta}\{1 - 2i\exp[2\psi(\mu, \beta)]\}. \tag{2.46}$$

Substituting into (2.15), we find, for $\mu \gg \alpha$,

$$\left[\frac{\alpha^2 - \beta^2}{2\mu^2} - 2i\left(\frac{e\beta}{2\mu}\right)^{2\mu}\right]\sin(\pi\mu) \approx -\left[\left(\frac{e\alpha}{2\mu}\right)^{2\mu} - i\left(\frac{e^2\alpha\beta}{4\mu^2}\right)^{2\mu}\right]\cos(\pi\mu),$$

so that the roots are located very close to the integers, $\mu_n = n - \epsilon_n$, $|\epsilon_n| \ll 1$, and we finally get

$$\lambda_n = -\mu_n \approx -n + \frac{2n^2}{\pi(\alpha^2 - \beta^2)}\left(\frac{e\alpha}{2n}\right)^{2n} \times \left[1 + \frac{4in^2}{(\alpha^2 - \beta^2)}\left(\frac{e\beta}{2n}\right)^{2n}\right]. \tag{2.47}$$

Thus, in region 3, there is an infinite number of poles, which approach the negative integers faster than exponentially as $|\lambda_n| \to \infty$.

In region 4, let us consider first the neighborhood of $\lambda = \beta$. Let

$$\lambda = \beta + e^{i\pi/3}\xi/\gamma, \tag{2.48}$$

where we have introduced the parameter

$$\gamma = (2/\beta)^{\frac{1}{3}} \ll 1, \tag{2.49}$$

which is very small according to (1.1), and we assume that $|\xi| = \mathcal{O}(1)$. The asymptotic behavior of the cylindrical functions under these conditions is given in Appendix A. It follows from (A1) and (A2) that

$$[1\ \beta] \approx e^{-i\pi/3}\gamma\ \mathrm{Ai}'(-\xi)/\mathrm{Ai}(-\xi), \tag{2.50}$$

where $\mathrm{Ai}(z)$ is the Airy function.

On the other hand, for $\operatorname{Im}\lambda \gg 1$, Eq. (2.21) gives

$$[\alpha] \approx i(\alpha^2 - \lambda^2)^{\frac{1}{2}}/\alpha, \tag{2.51}$$

so that (2.15) becomes

$$\mathrm{Ai}(-\xi)/\mathrm{Ai}'(-\xi) \approx -e^{i\pi/6}\gamma/M, \tag{2.52}$$

where we have introduced the abbreviation

$$M = (N^2 - 1)^{\frac{1}{2}}, \quad N > 1. \tag{2.53}$$

According to (2.52), the roots lie close to the zeros x_n of $\mathrm{Ai}(-x)$. Let

$$\xi_n = x_n - \epsilon_n, \quad \mathrm{Ai}(-x_n) = 0. \tag{2.54}$$

[26] J. M. Blatt and V. F. Weisskopf, *Theoretical Nuclear Physics* (John Wiley & Sons, New York, 1952).

Then, (2.52) yields

$$\epsilon_n \approx -e^{i\pi/6}\gamma/M, \tag{2.55}$$

so that (2.48) becomes

$$\lambda_n \approx \beta + e^{i\pi/3}(x_n/\gamma) + i/M. \tag{2.56}$$

The first two terms of the (2.56) coincide with those found for the Regge poles for an impenetrable sphere [N, Eq. (3.5)]. Thus, as in that case, the poles (2.56) must be associated with surface waves, with an angular damping factor given by Im λ_n (N, Sec. V). The second term of (2.56) contains the radiation damping due to propagation along a curved surface. Since this effect depends only on the geometry (radius of curvature), it is not surprising that it coincides with that found for an impenetrable sphere. The third term in (2.56) is the only one that depends on the refractive index. It represents the additional damping due to refraction of the surface waves into the sphere. This is a small correction, provided that the refractive index is not too close to unity, as expressed in the second condition (1.1). We now see the physical meaning of that condition: it implies that *the damping of the surface waves is determined mainly by the geometry, and is not greatly perturbed by penetration into the sphere.*

Finally, let us consider the asymptotic behavior of the poles for large $|\lambda|$ in region 4. According to N, Eq. (3.7), we then have

$$[1\ \beta] \approx \frac{(\lambda^2-\beta^2)^{\frac{1}{2}}}{\beta}\coth\left[\psi(\lambda,\beta) - i\frac{\pi}{4}\right], \tag{2.57}$$

while $[\alpha]$ is still given by (2.17). Thus, for $|\lambda| \gg \alpha^2$, Eq. (2.15) becomes

$$\coth\left[\lambda \ln\left(\frac{2\lambda}{e\beta}\right) + i\frac{\pi}{4}\right] \approx -1 + (N^2-1)\frac{\beta^2}{2\lambda^2}. \tag{2.58}$$

Let

$$\lambda_n = \rho_n \exp\,[i(\pi/2 - \epsilon_n)], \quad \rho_n \gg \alpha^2. \tag{2.59}$$

Then, equating real and imaginary parts of (2.58), we get

$$\rho_n \ln\,(2\rho_n/e\beta) \approx n\pi, \tag{2.60}$$

$$\epsilon_n \approx \frac{\pi}{2\ln\,(2\rho_n/e\beta)} - \frac{1}{n\pi}\ln\left(\frac{2\rho_n}{M\beta}\right). \tag{2.61}$$

The solution of (2.60) has already been given in N, Eq. (3.12):

$$\rho_n \approx \frac{n\pi}{\ln\,(2n\pi/e\beta)} + \cdots. \tag{2.62}$$

Substituting these results in (2.59), we see that the asymptotic behavior of these poles is again very similar to that found for an impenetrable sphere [N, Eq. (3.13)]. Both Re λ_n and Im λ_n approach infinity with n, but

$$\text{Re}\ \lambda_n/\text{Im}\ \lambda_n = \mathcal{O}[(\ln n)^{-1}]. \tag{2.63}$$

The results for the poles in region 5 are very similar to those found for region 4.

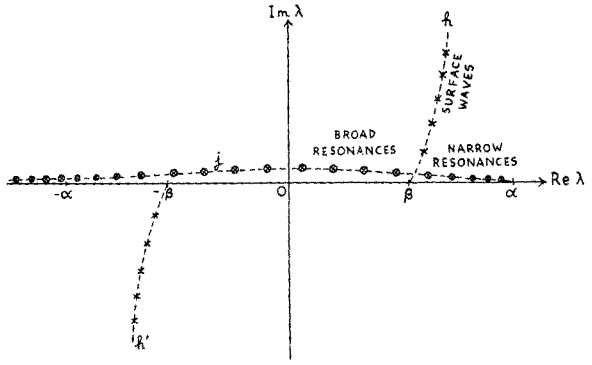

FIG. 3. The Regge poles of $S(\lambda, \beta)$ for $\alpha \gg \beta \gg 1$. The physical interpretation of the poles in the first quadrant is also indicated. ⊗—Class I poles; ×—Class II poles.

The complete pole distribution for $\alpha \gg \beta \gg 1$ is schematically shown in Fig. 3. We see that the poles fall into two sharply differentiated classes: those located near the real axis, along the curve j, will be called *Class I poles*, whereas those located along the curves h and h' will be called *Class II poles.*

The Regge trajectories for these two classes of poles also show quite different behavior.[20] For Class I poles (called "physical" in Ref. 20), they behave similarly to the well-known pattern of Regge trajectories for Yukawa-type potentials.[21] For a sufficiently deep well, the "right-most" poles in the right half-plane move along the real axis at negative energies, giving rise to bound states, and they leave the real axis, going into the first quadrant, at positive energies, giving rise to resonances. At finite energy, there is only a finite number of Class I poles in the right half-plane. However, in contrast with Yukawa-type potentials, the trajectories do not turn back as $\beta \to \infty$, but proceed to infinity in the right half-plane.

The trajectories of Class II poles (called "unphysical" in Ref. 20) behave quite differently. At finite energy, there is an infinite number of these poles, with unbounded real parts, in the first quadrant. As $\beta \to 0$, they all move towards the origin, so that they have "0-type" trajectories, in contrast with Class-I poles, which have "C-type" trajectories (cf. Ref. 21, pp. 66, 99, 100).

The physical origin of the different behavior of the two classes of poles is now clear. Class I poles are associated with the "interior" of the potential, i.e.,

with its behavior for $r < a$. This is why they resemble the usual Regge poles for Yukawa-type potentials. Class II poles, on the other hand, are by no means unphysical. They are associated with surface waves, as has been discussed in detail in N. They are insensitive to the behavior of the potential in the internal region, and are almost entirely determined by the geometrical shape of the surface.

These results help us to understand the origin of a very puzzling feature in dispersion theory, namely, the radically different analytic behavior of scattering amplitudes for cutoff potentials and for potentials with tails extending to infinity (e.g., Yukawa type). One can argue that cutting off an exponentially decreasing potential at sufficiently large distances should produce negligibly small physical effects, and yet it drastically alters the analytic behavior. This has always been regarded as an unphysical aspect of dispersion theory, reflecting the instability of analytic continuation.

It is now seen that the effect is at least partially due to the appearance of surface waves as soon as a cutoff is made. For Yukawa-type potentials, it is the finiteness of the number of Regge poles in the right half-plane that leads to polynomial boundedness of the scattering amplitude in momentum transfer and therefore to the Mandelstam representation. For cutoff potentials, the existence of an infinite number of Class II poles in the right half-plane at any finite energy gives rise to an essential singularity at infinity in the momentum transfer plane, so that the Mandelstam representation is no longer valid.[27]

It can still be argued that a sufficiently rapid exponential decrease is physically indistinguishable from a sharp cutoff, and should therefore give rise to effects resembling those of surface waves. However, this can only be true over a bounded energy range. In fact, "sufficiently rapid" means that the range of the exponential is much shorter than the wavelength, which ceases to be true at sufficiently high energy. On the other hand, cutoff potentials can support surface waves at arbitrarily high energy. This is related with the existence of an infinite number of Class II poles.

Finally, let us briefly consider the pole distribution for $N < 1$. We restrict ourselves to the case $N \ll 1$ (corresponding to a very high potential barrier), so that

$$\beta \gg \alpha \gg 1. \tag{2.64}$$

A detailed investigation of the pole distribution for $N < 1$ has been made by Streifer and Kodis.[22] Figure 4, based on their results, gives a schematic representation of the pole distribution when (2.64) is valid.

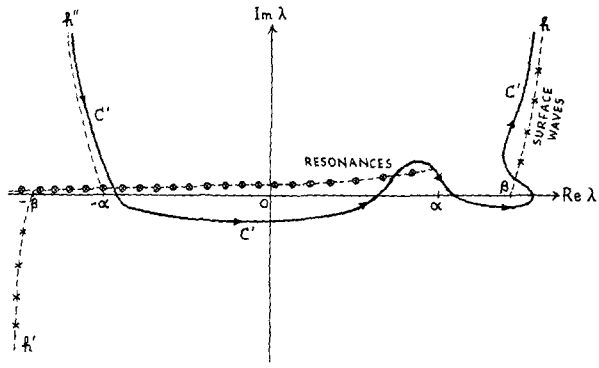

FIG. 4. The Regge poles of $S(\lambda, \beta)$ for $\beta \gg \alpha \gg 1$. The physical interpretation of the poles in the first quadrant is also indicated. ⊗—Class I poles; ×—Class II poles. C' is the path used by Chen (cf. Sec. 3D).

The main difference with respect to Fig. 3 is that narrow resonances now occur also at low values, rather than only at high values of the angular momentum. In fact, for $|\lambda| \ll \alpha$, the poles are approximately given by [cf. Eq. (2.42)]:

$$\lambda_n \approx (2\alpha/\pi) - (2n + \tfrac{1}{2}) + (2i/\pi)N, \tag{2.65}$$

which is close to the real axis for $N \ll 1$.

These poles correspond to Fabry–Perot type resonances immediately above the top of the barrier. The corresponding poles in the β plane, for $l = 0$, are given by Ref. 17 [Eq. (18)].

In the second quadrant, the poles again tend to approach the negative integers; (2.47) remains valid for $N < 1$.

3. THE DEBYE EXPANSION

A. Derivation

If we try to apply the modified Watson transformation, as developed in N (Sec. IX.D), directly to (2.5), we are immediately confronted with the following difficulty: in contrast with the case of an impenetrable sphere, a large number of Regge poles lie close to the real axis (cf. Figs. 3 and 4). Therefore, if we succeeded in reducing (2.5) to rapidly convergent contour integrals plus series of residues at the Regge poles, as in N, the residue series would still be slowly convergent. According to (2.36), the number of poles located very close to the real axis in the first quadrant is of the order of $(N - 1)\beta$. Thus, the minimum number of terms to be retained in the residue series (even without considering the infinite number of poles in the second quadrant) would be of the same order as in the original partial-wave series. Physically, this corresponds to the fact that a large number of partial waves can be near resonance at high frequency.

[27] H. M. Nussenzveig, Ann. Phys. (N.Y.) **21**, 344 (1963).

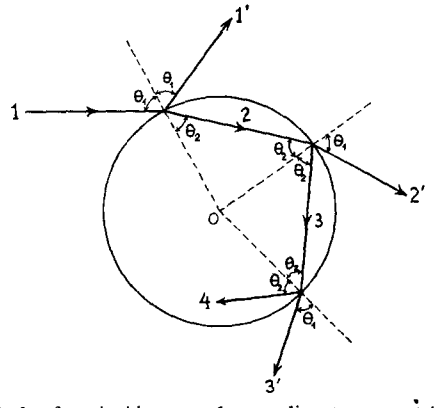

FIG. 5. Path of an incident ray 1 according to geometrical optics ($N > 1$).

Another way to see the origin of this difficulty, which also provides a clue to its solution, is to consider the contour integrals resulting from the transformation. In N, these contour integrals were evaluated by the saddle-point method, and the saddle-point contributions were found to correspond, in first approximation, to the results given by geometrical optics.

In order to apply geometrical optics to the present problem, we have to consider the path followed by a ray incident upon the sphere. This path is indicated in Fig. 5. An incident ray 1 is partially reflected (ray 1') and partially transmitted into the sphere (ray 2). Ray 2 in its turn undergoes partial internal reflection (ray 3) and partial transmission to the external region (ray 2'), and so on. This gives rise to an infinite series of multiple internal reflections, analogous to multiple-beam formation in a plane–parallel plate. The geometrical-optic solution outside of the sphere is constructed by superposing the contribution from the incident ray 1 with that from the directly reflected ray 1' and those from all transmitted rays 2', 3', $\cdots$.

Thus, in contrast with the impenetrable-sphere case, where only direct reflection takes place, each incident ray generates an infinite series of geometrical-optic rays, which should correspond to an infinite number of saddle points. In the geometrical-optic description, the total interaction of a ray with the sphere is broken up into an infinite number of interactions with the surface.

This is the clue to the resolution of the difficulty: in order to have a parallel with geometrical optics, we must look for *a description in terms of surface interactions*. This was first done by Debye[15] for a circular cylinder; his procedure was applied to the sphere by Van der Pol and Bremmer.[10]

For each multipole order l, we consider an incoming spherical wave of this order that strikes the surface of the sphere at $r = a$ and is partially reflected and partially transmitted. In order to evaluate the reflection and transmission coefficients of the interface purely in terms of a surface interaction, we must regard it as an interface between two unbounded media, by solving the radial equation in a fictitious one-dimensional space, in which r ranges from $-\infty$ to ∞. If 1 and 2 denote the interior and exterior of the sphere, respectively, there will then be only a transmitted wave in medium 1, so that we have

$$\psi_{2,l} = A\left[\frac{h_l^{(2)}(kr)}{h_l^{(2)}(\beta)} + R_{22}(l,\beta)\frac{h_l^{(1)}(kr)}{h_l^{(1)}(\beta)}\right], \quad (3.1)$$

$$\psi_{1,l} = AT_{21}(l,\beta)\frac{h_l^{(2)}(Nkr)}{h_l^{(2)}(\alpha)}, \quad (3.2)$$

where $\psi_{i,l}$ denotes the radial wavefunction in medium i for multipole order l, $R_{22}(l,\beta)$ is the external spherical reflection coefficient, and $T_{21}(l,\beta)$ is the spherical transmission coefficient from 2 to 1. The wavefunction and its radial derivative must be continuous at the interface; the coefficients are determined by this condition. Letting

$$l + \tfrac{1}{2} = \lambda, \quad (3.3)$$

we find

$$R_{22}(\lambda,\beta) = -\frac{[2\,\beta] - N[2\,\alpha]}{[1\,\beta] - N[2\,\alpha]}, \quad (3.4)$$

$$\begin{aligned} T_{21}(\lambda,\beta) &= 1 + R_{22}(\lambda,\beta) \\ &= \frac{[1\,\beta] - [2\,\beta]}{[1\,\beta] - N[2\,\alpha]} \\ &= \frac{4i}{\pi\beta H_\lambda^{(1)}(\beta)H_\lambda^{(2)}(\beta)([1\,\beta] - N[2\,\alpha])}, \end{aligned} \quad (3.5)$$

where we have employed the notations (2.8), (2.9), as well as the Wronskian relation

$$\begin{aligned} &W[H_\lambda^{(1)}(z), H_\lambda^{(2)}(z)] \\ &\quad = H_\lambda^{(1)}(z)H_\lambda^{(2)}(z)([2\,z] - [1\,z]) = -4i/\pi z. \end{aligned} \quad (3.6)$$

Similarly, by considering an outgoing spherical multipole wave of order l in medium 1, we can determine the internal spherical reflection coefficient R_{11} and the spherical transmission coefficient T_{12} from 1 to 2:

$$R_{11}(\lambda,\beta) = -\frac{[1\,\beta] - N[1\,\alpha]}{[1\,\beta] - N[2\,\alpha]}, \quad (3.7)$$

$$\begin{aligned} T_{12}(\lambda,\beta) &= 1 + R_{11}(\lambda,\beta) \\ &= \frac{N([1\,\alpha] - [2\,\alpha])}{[1\,\beta] - N[2\,\alpha]} \\ &= \frac{4i}{\pi\beta H_\lambda^{(1)}(\alpha)H_\lambda^{(2)}(\alpha)([1\,\beta] - N[2\,\alpha])}. \end{aligned} \quad (3.8)$$

For real λ, we have (reciprocity):

$$|R_{11}(\lambda, \beta)| = |R_{22}(\lambda, \beta)|, \quad \lambda \text{ real.} \tag{3.9}$$

On the other hand, for any λ, real or complex, it follows from the reflection properties of the cylindrical functions with respect to the index [cf. N, Eq. (2.15)] that all the coefficients are even functions of λ:

$$R_{ii}(-\lambda, \beta) = R_{ii}(\lambda, \beta); \quad T_{ij}(-\lambda, \beta) = T_{ij}(\lambda, \beta); \quad i, j = 1, 2. \tag{3.10}$$

The conservation of energy (or probability, in the quantum-mechanical interpretation) yields

$$|R_{22}(\lambda, \beta)|^2 + \left| \frac{H_\lambda^{(2)}(\beta)}{H_\lambda^{(2)}(\alpha)} T_{21}(\lambda, \beta) \right|^2 = |R_{11}(\lambda, \beta)|^2 + \left| \frac{H_\lambda^{(1)}(\alpha)}{H_\lambda^{(1)}(\beta)} T_{12}(\lambda, \beta) \right|^2 = 1. \tag{3.11}$$

These relations are valid for any real λ, as may also be verified directly from the definitions of the spherical reflection and transmission coefficients, with the help of (3.6). Actually, the first equality in (3.11) already follows from (3.5) and (3.8).

In the limit as the radius of the sphere goes to infinity, the above coefficients approach the well-known Fresnel reflection and transmission coefficients for a plane interface at perpendicular incidence, as they should:

$$R_{22} \to -\frac{N-1}{N+1}, \quad T_{21} \to \frac{2}{N+1}, \quad R_{11} \to \frac{N-1}{N+1}, \quad T_{12} \to \frac{2N}{N+1}, \quad a \to \infty. \tag{3.12}$$

In order to expand the S function in terms of surface interactions, we first subtract from (2.6) the external reflection coefficient (3.4), rewriting the result as follows:

$$\frac{H_\lambda^{(1)}(\beta)}{H_\lambda^{(2)}(\beta)} S(\lambda, \beta) - R_{22}(\lambda, \beta) = N T_{21}(\lambda\ \beta) \frac{([\alpha] - [2\,\alpha])}{([1\ \beta] - N[\alpha])} = \frac{N T_{21}(\lambda, \beta) H_\lambda^{(1)}(\alpha)([1\ \alpha] - [2\,\alpha])}{H_\lambda^{(1)}(\alpha)([1\ \beta] - N[1\ \alpha]) + H_\lambda^{(2)}(\alpha)([1\ \beta] - N[2\,\alpha])}. \tag{3.13}$$

With the help of (3.8), this becomes

$$\frac{H_\lambda^{(1)}(\beta)}{H_\lambda^{(2)}(\beta)} S(\lambda, \beta) = R_{22}(\lambda, \beta) + \frac{H_\lambda^{(1)}(\alpha)}{H_\lambda^{(2)}(\alpha)} \frac{T_{21}(\lambda, \beta) T_{12}(\lambda, \beta)}{[1 - \rho(\lambda, \beta)]}, \tag{3.14}$$

where

$$\rho(\lambda, \beta) = \frac{H_\lambda^{(1)}(\alpha)}{H_\lambda^{(2)}(\alpha)} R_{11}(\lambda, \beta). \tag{3.15}$$

The Debye expansion is now obtained by expanding the inverse of the denominator in (3.14) into a geometric series:

$$S(\lambda, \beta) = \frac{H_\lambda^{(2)}(\beta)}{H_\lambda^{(1)}(\beta)} \left\{ R_{22}(\lambda, \beta) + T_{21}(\lambda, \beta) T_{12}(\lambda, \beta) \frac{H_\lambda^{(1)}(\alpha)}{H_\lambda^{(2)}(\alpha)} \sum_{p=1}^{\infty} [\rho(\lambda, \beta)]^{p-1} \right\}. \tag{3.16}$$

This expansion has a very simple physical interpretation. The over-all phase factor $H_\lambda^{(2)}(\beta)/H_\lambda^{(1)}(\beta)$ expresses the fact that the interaction takes place at $r = a$ (rather than at $r = 0$). The first term R_{22} represents direct reflection from the surface. The pth term corresponds to transmission into the sphere (factor T_{21}), followed by going back and forth between $r = a$ and $r = 0$ p times [factors $H_\lambda^{(1)}(\alpha)/H_\lambda^{(2)}(\alpha)$ in ρ], with $p - 1$ internal reflections at the surface (factors R_{11} in ρ) and a final transmission to the outside (factor T_{12}). The origin acts as a perfect reflector (due to the regularity of the wavefunction at $r = 0$). *The pth term of the Debye expansion represents the effect of $p + 1$ surface interactions.*

Before applying the Debye expansion, we must first make sure that it converges. For any finite real λ, this follows immediately from (3.15) and (3.11):

$$|\rho(\lambda, \beta)| = |R_{11}(\lambda, \beta)| < 1, \quad \lambda \text{ real.} \tag{3.17}$$

In fact, the denominator of (3.8) has no poles for real λ, so that $|T_{12}|$ is strictly positive.

On the other hand, as $\lambda \to \infty$, it follows from the asymptotic behavior of T_{12}, given in Appendix B, and from N (Appendix A), that

$$\frac{H_\lambda^{(1)}(\alpha)}{H_\lambda^{(1)}(\beta)} T_{12}(\lambda, \beta) \approx -4i \frac{\lambda^2}{\alpha^2 - \beta^2} \left(\frac{e\beta}{2\lambda}\right)^{2\lambda} \left(\frac{e\alpha}{2\lambda}\right)^{2\lambda} \to 0, \quad \lambda \to \infty, \tag{3.18}$$

so that

$$\lim_{\lambda \to \pm\infty} |\rho(\lambda, \beta)| = 1. \tag{3.19}$$

Thus, in order to substitute the Debye expansion in (3.5), where the integrals range from 0 to ∞, we must interpret the integrals in (2.5) as limits of finite integrals:

$$\int_0^\infty d\lambda = \lim_{\Lambda \to \infty} \int_0^\Lambda d\lambda. \tag{3.20}$$

For any finite Λ, according to (3.17), the expansion

is justified, so that we get

$$f(\beta, \theta) = f_0(\beta, \theta) + \sum_{p=1}^{\infty} f_p(\beta, \theta), \tag{3.21}$$

where

$$f_0(\beta, \theta) = \frac{i}{\beta} \sum_{m=-\infty}^{\infty} (-1)^m \int_0^{\infty} \left[1 - \frac{H_\lambda^{(2)}(\beta)}{H_\lambda^{(1)}(\beta)} R_{22}\right] \times P_{\lambda-\frac{1}{2}}(\cos\theta) \exp(2im\pi\lambda)\lambda \, d\lambda, \tag{3.22}$$

$$f_p(\beta, \theta) = -\frac{i}{\beta} \sum_{m=-\infty}^{\infty} (-1)^m \int_0^{\infty} U(\lambda, \beta)[\rho(\lambda, \beta)]^{p-1} \times P_{\lambda-\frac{1}{2}}(\cos\theta) \exp(2im\pi\lambda)\lambda \, d\lambda, \quad p \geq 1, \tag{3.23}$$

where we have introduced

$$U(\lambda, \beta) = T_{21}(\lambda, \beta) \frac{H_\lambda^{(1)}(\alpha) H_\lambda^{(2)}(\beta)}{H_\lambda^{(2)}(\alpha) H_\lambda^{(1)}(\beta)} T_{12}(\lambda, \beta) = U(-\lambda, \beta), \tag{3.24}$$

and all integrals in (3.23) are to be interpreted in accordance with (3.20). Actually, when we discuss the asymptotic behavior of the integrand of (3.23) (cf. Sec. 5A and Appendix B), we shall see that it tends to zero faster than exponentially for $\lambda - \beta \gg \beta^{\frac{1}{3}}$, just like the integrand of (2.5), so that contributions to (3.20) are very rapidly damped beyond this point and we do not have to worry about the effect of (3.19). This corresponds to the negligible contribution from the partial waves in the domain (1.15).

Alternatively, one can also substitute (3.16) in (2.14) [or apply to each term of (3.21) the same transformation that led from (2.5) to (2.14)], with the result:

$$f_0(\beta, \theta) = \frac{1}{\beta} \sum_{m=-\infty}^{\infty} (-1)^m \int_0^{\infty} \left[1 - \frac{H_\lambda^{(2)}(\beta)}{H_\lambda^{(1)}(\beta)} R_{22}\right] \times P_{\lambda-\frac{1}{2}}(-\cos\theta) \exp[i(2m+1)\pi\lambda]\lambda \, d\lambda, \tag{3.25}$$

$$f_p(\beta, \theta) = -\frac{1}{\beta} \sum_{m=-\infty}^{\infty} (-1)^m \int_0^{\infty} U(\lambda, \beta)[\rho(\lambda, \beta)]^{p-1} \times P_{\lambda-\frac{1}{2}}(-\cos\theta) \exp[i(2m+1)\pi\lambda]\lambda \, d\lambda, \quad p \geq 1. \tag{3.26}$$

Although the Debye expansion is convergent with the interpretation (3.20), what matters in practice is whether or not it is rapidly convergent. There are two questions involved: first, whether the application of the modified Watson transformation leads to rapidly convergent results in the evaluation of *each term* in the expansion [in contrast with its direct application to (2.5)]; secondly, how rapidly the Debye expansion itself converges.

We shall defer till later a discussion of the second point. As for the first one, the trouble with (2.5) was the slow convergence of residue series due to the existence of many Regge poles close to the real axis. In order to find out what happens for (3.21), our first task is to determine the distribution of poles in the λ plane associated with each term.

B. The Poles for the Debye Expansion

According to (3.22)–(3.26) and (3.4)–(3.8), the same set of poles is associated with each term in the Debye expansion. The poles are the roots of

$$[1\ \beta] = N[2\ \alpha], \tag{3.27}$$

which differs from (2.15) by the replacement $[\alpha] \to [2\ \alpha]$, corresponding to the transition from standing waves to travelling waves within the sphere, in accordance with the physical interpretation of the Debye expansion. Although the poles are the same for all terms, their order varies from term to term: they are of order $p + 1$ for the pth term ($p = 0, 1, 2, \cdots$).

As we have seen in connection with (2.15), the roots of (3.27) are located in those regions of the λ plane where either the left or the right-hand side is rapidly varying, i.e., close to the zeros of $H_\lambda^{(1)}(\beta)$ (regions 4 and 5, Fig. 2) or to those of $H_\lambda^{(2)}(\alpha)$ (regions 6a and 7a, Fig. 2). We shall denote by λ_n the poles in region 4 and by λ_n' those in region 6a. (As the Regge poles λ_n discussed in Sec. 2 will no longer be considered from now on, no confusion should arise.) These considerations already suggest that there will not be many poles close to the real axis.

Since $[1\ \beta]$ and $[2\ \alpha]$ are even functions of λ [cf. N, Eq. (2.15)], the pole distribution is symmetric with respect to the origin, so that it suffices to determine the poles located in the right half-plane.

In region 4, Eq. (2.50) is valid, whereas we have

$$[2\ \alpha] \approx -i(\alpha^2 - \lambda^2)^{\frac{1}{2}}/\alpha, \quad \text{if} \quad N > 1, \qquad \approx -(\lambda^2 - \alpha^2)^{\frac{1}{2}}/\alpha, \quad \text{if} \quad N < 1, \tag{3.28}$$

assuming that $|\alpha - \beta| \gg \beta^{\frac{1}{3}}$ [cf. (1.4)]. We then find

$$\lambda_n \approx \beta + e^{i\pi/3}(x_n/\gamma) - i/M, \quad N > 1, \tag{3.29}$$

where M has been defined by (2.53). The corresponding result for $N < 1$ is obtained by the substitution

$$M \to -iM', \quad N < 1, \tag{3.30}$$

where we define

$$M' = (1 - N^2)^{\frac{1}{2}} \quad (N < 1). \tag{3.31}$$

As we found in connection with (2.56), the dependence on the refractive index is a small correction when (1.1)

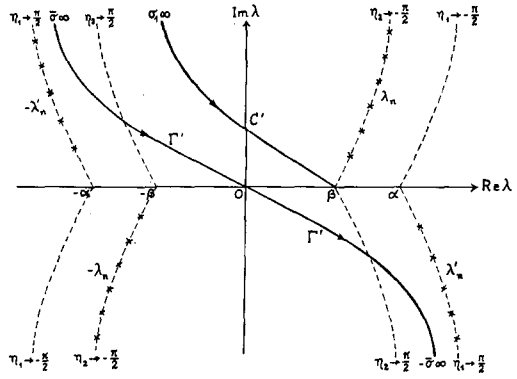

FIG. 6. The poles associated with the Debye expansion for $N > 1$. The path C' refers to (4.10) and the path Γ' to (4.18).

is valid, so that the poles λ_n are still very close to those found for an impenetrable sphere.

Similarly, in region 6a, with

$$\lambda = \alpha + e^{-i\pi/3}(\alpha/2)^{\frac{1}{3}}\xi, \tag{3.32}$$

we find [cf. Eqs. (A1) and (A2)]

$$[2\,\alpha] \approx e^{i\pi/3}(2/\alpha)^{\frac{1}{3}}\mathrm{Ai}'(-\xi)/\mathrm{Ai}(-\xi), \tag{3.33}$$

and

$$\begin{aligned}[1\,\beta] &\approx -(\lambda^2 - \beta^2)^{\frac{1}{2}}/\beta, \quad \text{if} \quad N > 1, \\ &\approx i(\beta^2 - \lambda^2)^{\frac{1}{2}}/\beta, \quad \text{if} \quad N < 1,\end{aligned} \tag{3.34}$$

so that the same procedure yields

$$\lambda'_n \approx \alpha + e^{-i\pi/3}N^{\frac{1}{3}}(x_n/\gamma) + N/M, \quad N > 1, \tag{3.35}$$

to which the substitution (3.30) is to be applied for $N < 1$.

The pole distribution for $N > 1$ is illustrated in Fig. 6. The asymptotic behavior of the poles λ_n as $n \to \infty$ is given by expressions very similar to (2.59)–(2.62), and analogous results (with obvious modifications) hold for the poles λ'_n.

Although the above approximations turn out to be adequate for most purposes in the present paper, we shall later require a better approximation to the poles λ_n. Complete asymptotic expansions for both λ_n and λ'_n have been derived by Streifer and Kodis.[28] Their results for λ_n are reproduced in Appendix A, together with the Schöbe asymptotic expansions for the cylindrical functions, on which their work is based. The case excluded by (1.1), in which $|N - 1| \sim \beta^{-\frac{2}{3}}$, has also been discussed in Ref. 28.

C. Discussion

The poles λ_n shown in Fig. 6 do not differ very much from those found for an impenetrable sphere, so that we expect them to be also associated with surface waves.

The poles λ'_n are located in the fourth quadrant, where ordinary Regge poles cannot appear at positive energy (Ref. 21, p. 51); their appearance is due entirely to the Debye expansion. However, except for their location in different quadrants, the pole distributions for λ_n and λ'_n have several features in common. This suggests that the poles λ'_n may be also associated with surface waves. It will be seen in Sec. 4E that this interpretation is indeed correct.

The next step will be to apply the modified Watson transformation to each term in the Debye expansion. As has already been mentioned in Sec. 1, the dominant contributions to the asymptotic behavior of each term are usually of the same type as for an impenetrable sphere, i.e., saddle-point contributions and residue-series contributions. The former correspond to the geometrical-optic rays in Fig. 5, so that for each term there is a finite (and, at least for the first few terms, small) number of saddle points. The latter, according to Fig. 6, are rapidly convergent, since the imaginary parts of λ_n and λ'_n increase rapidly with n. Thus, the modified Watson transformation leads to rapidly convergent asymptotic expansions for each term of the Debye series, in contrast with (2.5).

There remains to discuss the second problem referred to above, namely, the rapidity of convergence of the Debye series itself. Insofar as saddle-point contributions are concerned, they converge as rapidly as the corresponding geometrical-optic contributions, shown in Fig. 5. Their rate of convergence is determined by the damping produced at each internal reflection, i.e., by the Fresnel reflection coefficient at the interface. (If the sphere is not perfectly transparent, there is an additional damping of successive terms due to absorption, which increases the rapidity of convergence.) This in turn depends on the refractive index and on the angle θ_2 in Fig. 5, i.e., on the impact parameter of the incident ray. If we exclude the cases $N \gg 1$, $N \ll 1$, as in (1.3), the reflection coefficient is small for most directions, leading to fairly rapid convergence.

In the case of water, for instance, which will be of particular interest later on, we have $N \approx 1.33$, and it has been estimated by Van de Hulst (Ref. 4, p. 231) that more than 98.5% of the total intensity goes into the rays 1', 2', and 3' of Fig. 5, corresponding to the first three terms of the Debye expansion. The remaining 1.5% must be distributed among higher-order terms and residue-series contributions.

Thus, in this case, residue-series contributions account only for a small fraction of the total intensity.

[28] W. Streifer and R. D. Kodis, Quart. Appl. Math. **21**, 285 (1964).

This does not preclude them from being large within narrow angular domains, concentrated about special directions As will be seen in Paper II, this indeed happens in the glory region, where residue-series contributions become dominant over those associated with geometrical-optic rays.

We shall postpone the discussion of the rapidity of convergence of the Debye expansion for the residue-series contributions until we have found out more about their physical interpretation. It can already be expected, however, that they will converge much more slowly than the saddle-point contributions. In fact, as one increases the impact parameter of the incident ray, the reflection coefficient tends to increase, approaching unity in the limiting case of total reflection. This happens at glancing incidence for $N > 1$ and at critical incidence for $N < 1$. While the corresponding incident rays are totally reflected in the geometrical-optics approximation, it will be seen later that they are precisely the limiting rays responsible for the excitation of surface waves. According to the above discussion, high reflectivity implies slow convergence of the surface-wave contributions.

We can also note that $|\rho(\lambda, \beta)|$ in (3.17) is very close to unity within the edge domain (1.14), from which the residue-series contributions originate. Different damping mechanisms also arise in this case. In spite of the relatively slow convergence, however, it is possible to estimate the total residue-series contribution and to find out its physical effects. We shall return to the discussion of this point in Paper II (Sec. 6D).

D. Relation to Previous Treatments

Van de Hulst (Ref. 4, Chap. 12) applies the Debye expansion directly to the partial-wave series. He shows that the geometrical-optic contributions may be obtained by applying the principle of stationary phase to the domain (1.13); the forward diffraction peak also arises from this domain. He also gives a heuristic discussion of the contributions from the edge domain (1.14) (Ref. 4, Chap. 17).

The Debye expansion combined with the Watson transformation has been employed by several authors. The results agree insofar as geometrical-optic contributions are concerned, but they differ considerably in dealing with the remaining contributions.

For $N > 1$, the treatments most closely related to the present one are those given by Van der Pol and Bremmer,[10] Rubinow,[12] and Chen.[29] However, although the method is potentially more powerful, the results do not go beyond the derivation of the geometrical-optics approximation and the evaluation of some residue-series contributions within limited angular domains. No discussion of the domain of validity of the results is given, and the transition regions between different angular domains are not considered. In particular, the neighborhood of the forward and backward directions is not treated. Rubinow and Chen relate their results with Keller's geometrical theory of diffraction. However, the contribution from the poles λ_n' is omitted in their work.

Several investigations of the transparent cylinder or sphere problem have been made by Franz and Beckmann,[11,30–32] who propose somewhat different methods in each of them. They criticize Van der Pol and Bremmer for substituting the Debye expansion directly in the partial-wave series, claiming that $|\rho|$ is necessarily greater than unity for some partial wave near $\lambda = \alpha$, so that the expansion diverges. However, in view of (3.17), this criticism is unjustified: $|\rho| < 1$ for any real λ, and in particular at the physical points $\lambda = l + \frac{1}{2}$. It is true that $|\rho| \to 1$ as $\lambda \to \pm\infty$ [cf. Eq. (3.19)], but this also happens for Franz and Beckmann's contours, as will be seen below, so that an interpretation similar to (3.20) is required, although they are apparently unaware of this.

The starting point of their method is the representation (2.11); actually, they treat Green's function rather than the scattering amplitude. They then deform the lower half of the contour C (Fig. 1) into the lower half-plane, bringing it down to the negative imaginary axis[11] or to the negative real axis.[31,32] The Debye expansion is carried out along the modified contour.

This modification has a twofold purpose: (i) to find a contour along which $|\rho| < 1$. As shown in Appendix B (Fig. 21) one then has

$$\lim_{|\lambda| \to \infty} \rho = 0$$

along the lower part of the modified contour, and it can be shown that $|\rho| < 1$ along the negative imaginary axis. (ii) To avoid the appearance of contributions from the poles λ_n'. In fact, $S(\lambda, \beta)$ has no poles in the fourth quadrant, so that no poles are captured when the lower part of C sweeps across this quadrant, and the Debye expansion is only made afterwards. Franz and Beckmann claim that the residue series at the poles λ_n' have no physical interpretation, so that the poles are unphysical and should not contribute to the solution.

[29] Y. M. Chen, J. Math. Phys. **5**, 820 (1964).

[30] W. Franz and P. Beckmann, Trans. IRE, **AP-4**, 203 (1956).

[31] P. Beckmann and W. Franz, Z. Naturforsch. **12a**, 257 (1957).

[32] W. Franz, "Theorie der Beugung elektromagnetischer Wellen," Erg., Angew. Math., Band 4, §§16 and 19 (Springer-Verlag, Berlin, 1957).

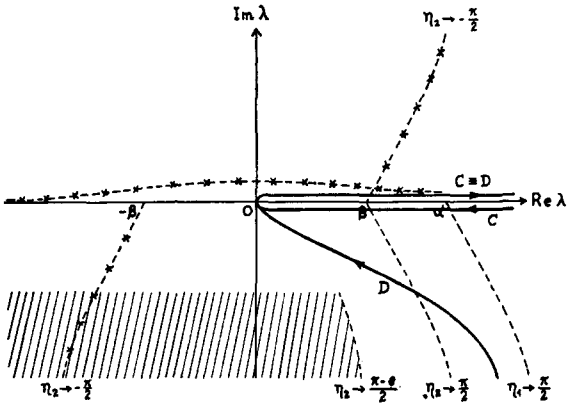

FIG. 7. Modification of the contour C in (2.11) according to Franz and Beckmann. The integrand tends to infinity in the shaded regions, to zero elsewhere, apart from the poles ×. The parameters η_1 and η_2 are defined by (B2).

To find out whether the modification proposed by Franz and Beckman is allowed, we must consider the asymptotic behavior of the integrand of (2.11) as $|\lambda| \to \infty$, which follows from Appendix B (Fig. 18) and from N [Eq. (C8)]. The behavior differs from that shown in Fig. 18 essentially by a factor $\lambda^{\frac{1}{2}}e^{i\lambda\theta}$ for $\operatorname{Im}\lambda > 0$ and $\lambda^{\frac{1}{2}}e^{-i\lambda\theta}$ for $\operatorname{Im}\lambda < 0$. It follows that the integrand tends to zero everywhere, except in the shaded region of Fig. 7.

Thus, while it is not possible to deform the lower half of C onto the negative imaginary axis, as proposed by Beckmann,[11] it is possible to move it across the line of poles λ'_n (curve $\eta_1 \to \pi/2$) and into the region where $\rho \to 0$ as $|\lambda| \to \infty$ (cf. Fig. 21, Appendix B). This leads to the contour D shown in Fig. 7.

Furthermore, after making the Debye expansion on D, it is possible, for the first term of the expansion, to deform the part of D located in the upper half-plane in order to obtain a path symmetric about the origin, which is another requirement in Franz and Beckmann's method. [If we had started from (2.10) instead of (2.11), it would have been possible to deform the lower part of C onto the negative imaginary axis. However, the last requirement could not then be satisfied, because the integrand of (2.10) (as well as the corresponding first term in the Debye expansion) diverges as $|\lambda| \to \infty$ over a portion of the upper half-plane, in such a way that no equivalent contour symmetric about the origin can be found.]

However, a modified contour, such as they propose, is not only unnecessary, but also inappropriate. In fact, as was shown above, the condition $|\rho| < 1$ is already satisfied along any bounded portion of C; it is unnecessary to get away from C in order to make use of the Debye expansion. It is true that $\rho \to 0$ along the part of D located in the lower half-plane, but we still have $|\rho| \to 1$ as $|\lambda| \to \infty$ along the upper portion of D. This is unavoidable, as shown in Appendix B (Fig. 21).

Furthermore, it is neither possible nor desirable to get rid of the contributions from the poles λ'_n. This can be seen already for the first term of the Debye expansion. As will be shown in Sec. 4, different representations are required for $\theta \gg \gamma$ and for $\theta \ll \gamma$. Franz and Beckmann's representation, avoiding the poles λ'_n, might be employed for $\theta \gg \gamma$. However, it cannot be continued to the domain $\theta \ll \gamma$ without including contributions from these poles.

For $N > 1$, we shall see that the contributions from the poles λ'_n are negligibly small (and consequently harmless). However, this is by no means so for $N < 1$. In this case, as will be seen in Sec. 4, the residue series at the poles λ'_n play an important role, and they have a clearcut physical interpretation. It will also be shown (cf. Sec. 4E) that there is no possible way to avoid them, since the contour that gives rise to the saddle-point contributions necessarily sweeps across the poles λ'_n as the scattering angle varies from 0 to π. We conclude that Franz and Beckmann's method is not suitable for the present problem.

For $N < 1$, there appears to be no treatment related to the present one. Chen's procedure for a cylinder, in this case,[33] is to deform the path of integration, before making the Debye expansion, into the path C' shown in Fig. 4, thereby capturing the residues at Regge poles located to the left and to the right of C', as well as at the poles located close to $\lambda = \alpha$ (exactly how many such poles are to be enclosed is not specified). He then applies the Debye expansion on C' and claims that all the integrals over C' can be evaluated by the saddle-point method (without further residue-series contributions, because C' is kept within the lines on which λ_n and λ'_n are located), yielding the geometrical-optic contributions. However, apart from the fact that C' is not suitable for saddle-point evaluation, it is contained within the region where $|\rho| \to \infty$ (cf. Fig. 21, Appendix B), so that the Debye expansion diverges. Thus, Chen's method cannot be applied.

Christiansen[34] starts with a contour similar to that employed by Beckmann[11]; after subtracting out the direct-reflection term, he deforms the path of integration for the remaining term [second term on the right in Eq. (3.14)] into the first quadrant, capturing the residues at the corresponding Regge poles.

[33] Y. M. Chen, J. Math. Phys. **6**, 1332 (1965).

[34] P. L. Christiansen, Report No. 1, Laboratory of Applied Mathematical Physics, Technical University of Denmark, Lingby, 1965.

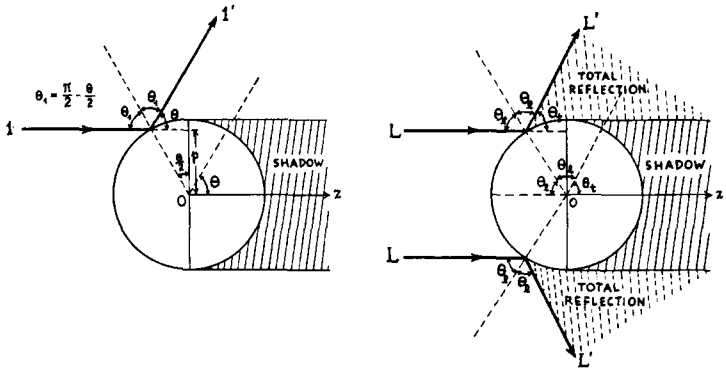

FIG. 8. Structure of the lit and shadow regions in the geometrical-optics approximation, for the first term of the Debye expansion. (a) $N > 1$; p is the impact parameter of the incident ray that is geometrically reflected in the direction θ. (b) $N < 1$; in this case, there is an additional shadow, bounded by the critically reflected rays L' (θ_l = critical angle for total reflection).

He then makes the Debye expansion over the resulting path of integration and applies the saddle-point method. Here again the Debye expansion is divergent on the resulting path. Furthermore, all Regge poles in the first quadrant (Fig. 4) contribute (not only those near $\lambda = \alpha$), and we have seen that the corresponding residue series, for $\alpha \gg 1$, converge no better than the partial-wave expansion.

4. THE FIRST TERM OF THE DEBYE EXPANSION

A. Preliminary Considerations

The first term of the Debye expansion is given by either one of the equivalent representations (3.22) or (3.25). In the geometrical-optics approximation, it is associated with rays directly reflected from the surface, without penetrating into the sphere, like the ray 1′ in Fig. 5.

To each term of the Debye expansion, associated with a certain class of rays, there correspond, in the geometrical-optics approximation, one or more "lit regions" and one or more "shadow regions," the latter being inaccessible to rays of this class (though not necessarily to rays of other classes!). The structure of these regions for the first term of the Debye expansion is shown in Fig. 8.

For $N > 1$, at finite distance, we have the geometrical shadow of the sphere, just as for an impenetrable sphere. For the scattering amplitude, which represents the field at infinity, this corresponds to the single direction $\theta = 0$ [Fig. 8(a)].

For $N < 1$, there is an additional shadow, bounded by the reflected rays L' corresponding to the critically incident rays L, that fall upon the surface at the critical angle,

$$\theta_l = \sin^{-1} N, \quad N < 1. \tag{4.1}$$

Beyond this region [Fig. 8(b)], total reflection occurs. It will be seen in Sec. 5 that the complementary region, $\theta > \pi - 2\theta_l$, is a shadow region for transmitted rays, and this remains true for all terms of the Debye expansion.

We shall see that around each shadow boundary there is a domain of angular width $\Delta\theta$, where the transition from the lit region to the shadow takes place. For an impenetrable sphere (N), such transitions were found to be described by "Fock-type" functions, and the corresponding angular width was given by (N, Fig. 14):

$$\Delta\theta \sim \gamma, \tag{4.2}$$

where γ is defined by (2.49). Transitions of this type will be called "normal." The scattering amplitude is given by different approximations within a transition region and on either side of it.

We shall consider first the case $N > 1$. The structure of the first term should then be very similar to that found for an impenetrable sphere, since the corresponding class of rays does not penetrate within the sphere. According to Fig. 8(a), different approximations should hold for $0 \leq \theta \leqslant \Delta\theta$ and for $\Delta\theta \ll \theta \leq \pi$; for an impenetrable sphere, $\Delta\theta$ was given by (4.2) (N, Sec. IX.D), and the same is true here.

The corresponding representations for $f_0(\beta, \theta)$ can be derived from (3.22) and (3.25) by the same procedure applied in N (Sec. IX.D). Let us define

$$S_0(\lambda, \beta) = \frac{H_\lambda^{(2)}(\beta)}{H_\lambda^{(1)}(\beta)} R_{22}(\lambda, \beta) = e^{2i\pi\lambda} S_0(-\lambda, \beta). \tag{4.3}$$

Then, as in N [Eq. (9.59)], it follows from (3.22) that

$$f_0(\beta,\theta)=\frac{i}{\beta}\sum_{m=0}^{\infty}(-1)^m \times\left\{\int_{-\infty}^{0}[e^{2i\pi\lambda}-S_0(\lambda,\beta)]P_{\lambda-\frac{1}{2}}(\cos\theta)e^{2im\pi\lambda}\lambda\,d\lambda +\int_0^{\infty}[1-S_0(\lambda,\beta)]P_{\lambda-\frac{1}{2}}(\cos\theta)e^{2im\pi\lambda}\lambda\,d\lambda\right\}. \quad (4.4)$$

The asymptotic behavior of $R_{22}(\lambda,\beta)$ as $|\lambda|\to\infty$ follows from Appendix B (Fig. 19). We find that $R_{22}\to -1$ in all regions, except for $-\pi/2<\eta_2<\pi/2$, where $R_{22}\to 0$ like λ^{-2}. Thus, except in this region, we have

$$S_0(\lambda,\beta)\approx S_{\text{imp}}(\lambda,\beta)=-H_\lambda^{(2)}(\beta)/H_\lambda^{(1)}(\beta), \quad \text{as} \quad |\lambda|\to\infty, \quad (4.5)$$

where $S_{\text{imp}}(\lambda,\beta)$ is the S function for an impenetrable sphere [N, Eq. (3.1)].

Combining the above results with those given in N for the asymptotic behavior of $S_{\text{imp}}(\lambda,\beta)$, we find that $e^{2i\pi\lambda}-S_0(\lambda,\beta)$ tends to zero at least as fast as $e^{i\pi\lambda}$ in the second quadrant, so that the path of integration in the first integral of (4.4) may be shifted to the positive imaginary axis. To do this, we have to sweep across the poles $-\lambda_n'$ (Fig. 6), so that we get a corresponding residue-series contribution. Let

$$r_{0n}'=\text{residue } S_0(\lambda,\beta)\big|_{\lambda=\lambda_n'}.$$

Then, according to (4.3), we have

$$\text{residue } S_0(\lambda,\beta)\big|_{\lambda=-\lambda_n'}=-e^{-2i\pi\lambda_n'}r_{0n}', \quad (4.6)$$

so that we find

$$f_0(\beta,\theta)=\frac{i}{\beta}\sum_{m=0}^{\infty}(-1)^m \times\left\{\int_{i\infty}^{0}[e^{2i\pi\lambda}-S_0(\lambda,\beta)]P_{\lambda-\frac{1}{2}}(\cos\theta)e^{2im\pi\lambda}\lambda\,d\lambda +\int_0^{\infty}[1-S_0(\lambda,\beta)]P_{\lambda-\frac{1}{2}}(\cos\theta)e^{2im\pi\lambda}\lambda\,d\lambda\right\} +\frac{2\pi}{\beta}\sum_{m=0}^{\infty}(-1)^m\sum_n\lambda_n'r_{0n}' \times\exp[-2i(m+1)\pi\lambda_n']P_{\lambda_n'-\frac{1}{2}}(\cos\theta). \quad (4.7)$$

Writing

$$e^{2i\pi\lambda}-S_0(\lambda,\beta)=e^{2i\pi\lambda}-1+1-S_0(\lambda,\beta)$$

in the sum from $m=1$ to ∞, and employing N [Eq. (9.61)], we get, just as in N [Eqs. (9.62)–(9.65)],

$$\begin{aligned}f_0(\beta,\theta)=&-\frac{i}{\beta}\int_{i\infty}^{0}S_0(\lambda,\beta)P_{\lambda-\frac{1}{2}}(\cos\theta)\lambda\,d\lambda\\&+\frac{i}{\beta}\int_0^{\infty}[1-S_0(\lambda,\beta)]P_{\lambda-\frac{1}{2}}(\cos\theta)\lambda\,d\lambda\\&+\frac{2i}{\beta}\int_{i\infty}^{0}\frac{e^{2i\pi\lambda}}{1+e^{2i\pi\lambda}}P_{\lambda-\frac{1}{2}}(\cos\theta)\lambda\,d\lambda\\&+\frac{2\pi}{\beta}\sum_{m=0}^{\infty}(-1)^m\sum_n\lambda_n'r_{0n}'\\&\times\exp[-2i(m+1)\pi\lambda_n']P_{\lambda_n'-\frac{1}{2}}(\cos\theta)\\&+\frac{i}{\beta}\sum_{m=1}^{\infty}(-1)^m\left(\int_{i\infty}^{0}+\int_0^{\infty}\right)[1-S_0(\lambda,\beta)]\\&\times e^{2im\pi\lambda}P_{\lambda-\frac{1}{2}}(\cos\theta)\lambda\,d\lambda. \quad (4.8)\end{aligned}$$

It follows from (4.3)–(4.5) that the asymptotic behavior of $1-S_0(\lambda,\beta)$ in the first quadrant is the same as that for an impenetrable sphere, so that, as in N [Eq. (9.65)], the path of integration in the last term of (4.8) can be closed at infinity, reducing it to a residue series at the poles λ_n in the first quadrant (Fig. 6). Similarly, we can split the path of integration in the second term of (4.8) at $\lambda=\beta$ and combine it with the first term, as in N [Eqs. (9.67)–(9.69)], so that we finally get

$$f_0(\beta,\theta)=f_{01}+f_{02}+f_{03}+\tilde{f}_{0,\text{res}}+\tilde{f}_{0,\text{res}}', \quad (4.9)$$

where

$$\begin{aligned}f_{01}(\beta,\theta)+f_{02}(\beta,\theta)=&-\frac{i}{\beta}\int_{\sigma_1\infty}^{\beta}S_0(\lambda,\beta)P_{\lambda-\frac{1}{2}}(\cos\theta)\lambda\,d\lambda\\&+\frac{i}{\beta}\int_\beta^{\infty}[1-S_0(\lambda,\beta)]P_{\lambda-\frac{1}{2}}(\cos\theta)\lambda\,d\lambda, \quad (4.10)\end{aligned}$$

$$f_{03}(\beta,\theta)=\frac{i}{\beta}\int_0^{\beta}P_{\lambda-\frac{1}{2}}(\cos\theta)\lambda\,d\lambda+\Delta_1, \quad (4.11)$$

$$\Delta_1(\beta,\theta)=\frac{2i}{\beta}\int_{i\infty}^{0}\frac{e^{2i\pi\lambda}}{1+e^{2i\pi\lambda}}P_{\lambda-\frac{1}{2}}(\cos\theta)\lambda\,d\lambda, \quad (4.12)$$

$$\tilde{f}_{0,\text{res}}(\beta,\theta)=\frac{2\pi}{\beta}\sum_{m=1}^{\infty}(-1)^m\sum_n\lambda_nr_{0n} \times\exp(2im\pi\lambda_n)P_{\lambda_n-\frac{1}{2}}(\cos\theta), \quad (4.13)$$

$$\tilde{f}_{0,\text{res}}'(\beta,\theta)=\frac{2\pi}{\beta}\sum_{m=0}^{\infty}(-1)^m\sum_n\lambda_n'r_{0n}' \times\exp[-2i(m+1)\pi\lambda_n']P_{\lambda_n'-\frac{1}{2}}(\cos\theta), \quad (4.14)$$

and

$$r_{0n}=\text{residue } S_0(\lambda,\beta)\big|_{\lambda=\lambda_n}. \quad (4.15)$$

The path C' from $\sigma_1\infty$ to β is shown in Fig. 6. According to the above discussion on the behavior of $S_0(\lambda, \beta)$, the path must begin at infinity to the left of $\eta_2 \to -(\pi - \theta)/2$ (cf. also Fig. 10); in particular, any direction $\sigma_1\infty$ in the second quadrant may be chosen.

The representation (4.9)–(4.14) is exact and, just like its counterpart N, Eq. (9.78), it will be employed for

$$0 \leq \theta \lesssim \gamma. \tag{4.16}$$

To obtain the counterpart of N, Eq. (9.79), we might proceed just as in N, by transforming (4.7), but it is simpler to start from (3.25). By the same procedure that led from (2.11) to (2.14), we find that (3.25) is equivalent to

$$f_0(\beta, \theta) = \frac{1}{2\beta}\int_C [1 - S_0(\lambda, \beta)]P_{\lambda-\frac{1}{2}}(-\cos\theta)\frac{\lambda\, d\lambda}{\cos(\pi\lambda)}, \tag{4.17}$$

where C is the contour shown in Fig. 1.

The asymptotic behavior of the integrand as $|\lambda| \to \infty$ is essentially the same as that of (2.11), illustrated in Fig. 7. Thus, we can deform the lower half of C into the lower half of the contour Γ' shown in Fig. 6, going from $-\bar{\sigma}\infty$ to 0 (Γ' is symmetric about the origin). This gives rise to a residue-series contribution from the poles λ'_n. Similarly, the upper half of C can be deformed into the upper half of Γ', from 0 to $\bar{\sigma}\infty$, giving rise to a residue-series contribution from the poles λ_n. The result is

$$\begin{aligned} f_0(\beta, \theta) = &-\frac{1}{2\beta}\int_{\Gamma'}[1 - S_0(\lambda, \beta)]P_{\lambda-\frac{1}{2}}(-\cos\theta) \\ &\times \frac{\lambda\, d\lambda}{\cos(\pi\lambda)} - \frac{i\pi}{\beta}\sum_n \lambda_n r_{0n}\frac{P_{\lambda_n-\frac{1}{2}}(-\cos\theta)}{\cos(\pi\lambda_n)} \\ &- \frac{i\pi}{\beta}\sum_n \lambda'_n r'_{0n}\frac{P_{\lambda_n'-\frac{1}{2}}(-\cos\theta)}{\cos(\pi\lambda'_n)}. \end{aligned} \tag{4.18}$$

The integral can be split into two, corresponding to the two terms within square brackets (both are convergent for $\theta > 0$). The first of the resulting integrals identically vanishes, because its integrand is odd. The second integral can again be split into two according to the identity [N, Eq. (C5)]:

$$\begin{aligned} P_{\lambda-\frac{1}{2}}(-\cos\theta) = &\, ie^{-i\pi\lambda}P_{\lambda-\frac{1}{2}}(\cos\theta) \\ &- 2i\cos(\pi\lambda)Q^{(1)}_{\lambda-\frac{1}{2}}(\cos\theta). \end{aligned} \tag{4.19}$$

Again, both integrals are separately convergent for $\theta > 0$, and the first one identically vanishes due to the antisymmetry of the integrand [cf. Eq. (4.3)]. Finally, substituting (2.12) in the first residue series of (4.18) and (2.13) in the second one, we get

$$f_0(\beta, \theta) = f_{0,g} + f_{0,\mathrm{res}} + f'_{0,\mathrm{res}}, \tag{4.20}$$

where

$$f_{0,g}(\beta, \theta) = -\frac{i}{\beta}\int_{\Gamma'} S_0(\lambda, \beta)Q^{(1)}_{\lambda-\frac{1}{2}}(\cos\theta)\lambda\, d\lambda, \tag{4.21}$$

$$\begin{aligned} f_{0,\mathrm{res}}(\beta, \theta) = &-\frac{2\pi i}{\beta}\sum_{m=0}^{\infty}(-1)^m\sum_n \lambda_n r_{0n} \\ &\times \exp[i(2m+1)\pi\lambda_n]P_{\lambda_n-\frac{1}{2}}(-\cos\theta), \end{aligned} \tag{4.22}$$

and

$$\begin{aligned} f'_{0,\mathrm{res}}(\beta, \theta) = &-\frac{2\pi i}{\beta}\sum_{m=0}^{\infty}(-1)^m\sum_n \lambda'_n r'_{0n} \\ &\times \exp[-i(2m+1)\pi\lambda'_n]P_{\lambda_n'-\frac{1}{2}}(-\cos\theta). \end{aligned} \tag{4.23}$$

In view of the symmetry property (4.3), we may rewrite (4.21) as (cf. N, Eqs. (9.75)–(9.76)]:

$$\begin{aligned} f_{0,g}(\beta, \theta) = &\frac{i}{\beta}\int_{\bar{\sigma}\infty}^{0} S_0(\lambda, \beta)P_{\lambda-\frac{1}{2}}(-\cos\theta) \\ &\times e^{-i\pi\lambda}\tan(\pi\lambda)\lambda\, d\lambda, \end{aligned} \tag{4.24}$$

thus rendering manifest the regularity of all the above expressions at $\theta = \pi$.

The exact representation (4.20)–(4.24) is the counterpart of N, Eq. (9.79), and it will be employed for

$$\gamma \ll \theta \leq \pi. \tag{4.25}$$

Together with (4.9)–(4.14), it allows us to determine the asymptotic behavior of $f_0(\beta, \theta)$ for $0 \leq \theta \leq \pi$ and $N > 1$. The case $N < 1$ will be discussed in Sec. 4E.

B. Behavior for $N > 1$, $\theta \gg \gamma$, $\pi - \theta \gg \beta^{-\frac{1}{2}}$

Let us consider first the behavior of $f_0(\beta, \theta)$ for $N > 1$ and θ not too close to 0 or π. As in N [Eq. (9.9)], we shall see that the approximations below are valid for

$$\theta \gg \gamma, \quad \pi - \theta \gg \beta^{-\frac{1}{2}}. \tag{4.26}$$

In this domain, we employ (4.20)–(4.24).

Let us discuss first the behavior of (4.21), which is quite similar to that of N, Eq. (9.8), representing the directly reflected wave in the geometrical-optics approximation. As in N, Eq. (9.8), the main contribution to (4.21) arises from the neighborhood of a saddle point, located at [cf. N, Eq. (9.2)]

$$\bar{\lambda} = kp = \beta\cos(\theta/2). \tag{4.27}$$

The physical interpretation is the same as in N (Fig. 11): p is the impact parameter of the incident ray that is geometrically reflected from the surface in the direction θ; this is also shown in Fig. 8(a). We may again employ the approximation N, Eq. (6.14) for

$H_\lambda^{(2)}(\beta)/H_\lambda^{(1)}(\beta)$ and N, Eq. (C7) for $Q_{\lambda-\frac{1}{2}}^{(1)}(\cos\theta)$. There remains only to approximate R_{22} in (4.3).

In the neighborhood of $\lambda = \bar{\lambda}$, we can employ the Debye asymptotic expansion N, Eq. (A16), to evaluate $[1\,\beta]$, $[2\,\beta]$, and $[2\,\alpha]$ in (3.4), with the following result:

$$\beta[1\,\beta] = i(\beta^2 - \lambda^2)^{\frac{1}{2}} - \frac{\beta^2}{2(\beta^2 - \lambda^2)} + \mathcal{O}\left[\frac{\beta^2}{(\beta^2 - \lambda^2)^{\frac{3}{2}}}\right]. \tag{4.28}$$

To obtain $[2\,\beta]$, it suffices to replace i by $-i$, and $[2\,\alpha]$ is obtained by replacing β by α. Substituting these approximations in (3.4), we find

$$R_{22}(\lambda, \beta) \approx -\left(\frac{(\alpha^2 - \lambda^2)^{\frac{1}{2}} - (\beta^2 - \lambda^2)^{\frac{1}{2}}}{(\alpha^2 - \lambda^2)^{\frac{1}{2}} + (\beta^2 - \lambda^2)^{\frac{1}{2}}}\right) \times \left[1 + \frac{i\lambda^2}{(\beta^2 - \lambda^2)^{\frac{1}{2}}(\alpha^2 - \lambda^2)} + \cdots\right]. \tag{4.29}$$

Finally, substituting all the above approximations in (4.21) and making the change of variable

$$\lambda = \beta \cos w, \tag{4.30}$$

we get

$$f_{0,g}(\beta, \theta) = -e^{i\pi/4}\left(\frac{\beta}{2\pi \sin\theta}\right)^{\frac{1}{2}} \times \int B(w, \beta, \theta) \exp\left[i\beta\delta(w, \theta)\right] dw, \tag{4.31}$$

where

$$\delta(w, \theta) = 2\left[\left(w - \frac{\theta}{2}\right)\cos w - \sin w\right], \tag{4.32}$$

$$B(w, \beta, \theta) = \sin w(\cos w)^{\frac{1}{2}}\left(\frac{\sqrt{N^2 - \cos^2 w} - \sin w}{\sqrt{N^2 - \cos^2 w} + \sin w}\right) \times \left\{1 + \frac{i}{4\beta}\left[\frac{1}{\sin w} + \frac{\cot\theta}{2\cos w} + \frac{5}{3}\frac{\cos^2 w}{\sin^3 w} + \frac{4\cos^2 w}{\sin w(N^2 - \cos^2 w)}\right] + \mathcal{O}(\beta^{-2})\right\}, \tag{4.33}$$

and the path of integration is the image of Γ' (Fig. 6) in the w plane. For the application of the saddle-point method, the path is shifted so as to cross the real axis at the saddle point (4.27), i.e., at $\bar{w} = \theta/2$, $0 < \bar{w} < \pi/2$, at an angle of $-\pi/4$ with the real axis.

The formula for the saddle-point evaluation of (4.31), including the first correction term, has already been given in N [Eq. (6.21)]:

$$f_{0,g}(\beta, \theta) = -\frac{Be^{i\delta\beta}}{(|\delta''|\sin\theta)^{\frac{1}{2}}}\left\{1 - \frac{i}{2\beta\,|\delta''|}\left[\frac{B''}{B} + \frac{B'}{B}\frac{\delta'''}{|\delta''|} + \frac{5}{12}\left(\frac{\delta'''}{\delta''}\right)^2 + \frac{1}{4}\frac{\delta''''}{|\delta''|}\right] + \mathcal{O}(\beta^{-2})\right\}, \tag{4.34}$$

where B, δ, and their derivatives are to be evaluated at the saddle point $\bar{w} = \theta/2$. Substituting (4.32) and (4.33) in (4.34), we finally get

$$f_{0,g}(\beta, \theta) = -\frac{1}{2}\left(\frac{\sqrt{N^2 - \cos^2(\theta/2)} - \sin(\theta/2)}{\sqrt{N^2 - \cos^2(\theta/2)} + \sin(\theta/2)}\right) \times \exp\left(-2i\beta\sin(\theta/2)\right)\left\{1 + \frac{i}{2\beta}\left[\frac{1}{\sin^3(\theta/2)} - \frac{2N^2 - \cos^2(\theta/2)}{(N^2 - \cos^2(\theta/2))^{\frac{3}{2}}}\right] + \mathcal{O}(\beta^{-2})\right\}. \tag{4.35}$$

The main term of (4.35) is well known [cf. Ref. 12, Eq. (39)]. In the limit $N \to i\infty$, which would formally correspond to an impenetrable sphere, both the main term and the first correction term agree with the result found in N [Eq. (9.4)]. The main term differs from that result only by the replacement of the reflection coefficient $R = -1$ for an impenetrable sphere by the Fresnel reflection coefficient corresponding to the angle of incidence $\theta_1 = (\pi - \theta)/2$ [Fig. 8(a)]:

$$R = -\frac{\sin(\theta_1 - \theta_2)}{\sin(\theta_1 + \theta_2)} = -\frac{\sqrt{N^2 - \cos^2(\theta/2)} - \sin(\theta/2)}{\sqrt{N^2 - \cos^2(\theta/2)} + \sin(\theta/2)}. \tag{4.36}$$

Let us consider next the residue-series contribution from the poles λ_n, given by (4.22). The poles λ_n are given by (3.29), with sufficiently good approximation for our present purpose (a more accurate expansion is given in Appendix A). The residues r_{0n} follow from (4.15), (4.3), and (3.4):

$$r_{0n} = 4i/\{\pi\beta[H_{\lambda_n}^{(1)}(\beta)]^2\,\dot{d}(\lambda_n, \beta)\} \tag{4.37}$$

where

$$d(\lambda, \beta) = [1\,\beta] - N[2\,\alpha], \tag{4.38}$$

and the dot denotes a derivative with respect to λ; we have also made use of (3.6).

The asymptotic expansion of all functions required for the evaluation of (4.37) is given in Appendix A. If we keep only the dominant term in each expansion, we find

$$r_{0n} \approx e^{-i\pi/6}/2\pi\gamma a_n'^2, \tag{4.39}$$

where we have introduced the abbreviation

$$a_n' = \mathrm{Ai}'(-x_n), \tag{4.40}$$

and x_n is defined by (2.54). If necessary, higher-order

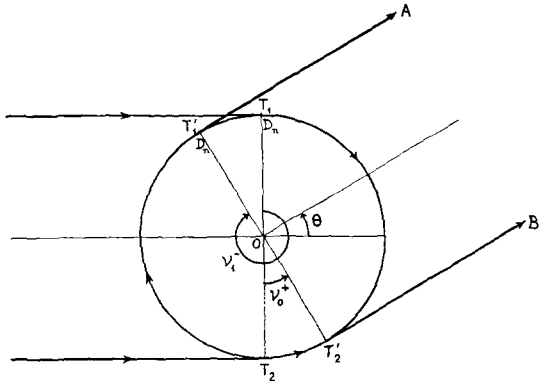

FIG. 9. Diffracted rays $T_1T_1'A$ and $T_2T_2'B$ in the direction θ.

corrections to (4.39) can easily be computed, with the help of Appendix A.

Substituting $P_{\lambda_n-\frac{1}{2}}(-\cos\theta)$ in (4.22) by its asymptotic expansion N, Eq. (C8), we finally get

$$f_{0,\mathrm{res}}(\beta,\theta)=\frac{1}{\beta}\left(\frac{2\pi}{\sin\theta}\right)^{\frac{1}{2}}\Bigg\{e^{-i\pi/4}\sum_n\sqrt{\lambda_n}\,r_{0n}\exp(i\lambda_n\nu_0^+)+\sum_{m=1}^{\infty}(-1)^m\sum_n\sqrt{\lambda_n}\,r_{0n}\times\left[\exp\left(i\lambda_n\nu_m^-+i\frac{\pi}{4}\right)+\exp\left(i\lambda_n\nu_m^+-i\frac{\pi}{4}\right)\right]\Bigg\},\tag{4.41}$$

where

$$\nu_m^{\pm}=2m\pi\pm\theta,\quad m=0,1,2,\cdots.\tag{4.42}$$

In particular, in the lowest-order approximation, in which r_{0n} is given by (4.39), the above result becomes formally identical to N, Eq. (9.5), the only difference (apart from notation) being in the expression for the poles λ_n.

The physical interpretation of this result is again the same as in N: the incident rays tangential to the sphere at T_1 and T_2 (Fig. 9) excite surface waves that travel around the sphere any number of times, giving rise to diffracted rays in the direction θ. The angles $\nu_m^{\pm}$ correspond to the total arc described along the surface (Fig. 9).

In the language of the geometrical theory of diffraction,[35] we can rewrite (4.41) as follows:

$$f_{0,\mathrm{res}}(\beta,\theta)=\frac{1}{(\sin\theta)^{\frac{1}{2}}}\Bigg\{-i\sum_n D_n^2\exp(i\lambda_n\nu_0^+)+\sum_{m=1}^{\infty}(-1)^m\sum_n D_n^2\times[\exp(i\lambda_n\nu_m^-)-i\exp(i\lambda_n\nu_m^+)]\Bigg\},\tag{4.43}$$

[35] B. R. Levy and J. B. Keller, Commun. Pure Appl. Math. **12**, 159 (1959).

where

$$D_n^2=e^{i\pi/4}(2\pi\lambda_n)^{\frac{1}{2}}r_{0n}/\beta\tag{4.44}$$

is the square of the *diffraction coefficient*. (Our diffraction coefficient differs from that of Levy and Keller[35] by an extra factor $a^{-\frac{1}{2}}$, to render it dimensionless.) One factor D_n corresponds to the excitation of a diffracted ray (e.g., at T_1, Fig. 9), and the other one to its reconversion into a tangentially emerging ray (e.g., at T_1', Fig. 9).

In the first-order approximation (4.39), Eq. (4.44) becomes

$$D_n^2\approx\frac{e^{i\pi/12}}{(2\pi\beta)^{\frac{1}{2}}\gamma a_n'^2}=\frac{e^{i\pi/12}}{2\sqrt{\pi}\,a_n'^2}\left(\frac{2}{\beta}\right)^{\frac{1}{6}}.\tag{4.45}$$

This is identical to the result for an impenetrable sphere [cf. N, Eq. (9.5), and Ref. 35, p. 170]. [Chen's result for a cylinder [Ref. 29, Eq. (1.42)], although apparently different, can be shown to be equivalent to (4.45), by employing Ref. 29, Eq. (1.44).] Thus, to first order, not only the decay exponents, but also the diffraction coefficients associated with this class of rays are the same as those for an impenetrable sphere.

Finally, let us consider $f_{0,\mathrm{res}}'(\beta,\theta)$, which is given by (4.23). The expression for r_{0n}' differs from (4.37) only by the replacement of λ_n by λ_n'. Taking into account (3.33)–(3.35), we find

$$r_{0n}'\approx 2i(N/M)\exp(2M\beta-2\lambda_n'\cosh^{-1}N)\tag{4.46}$$

and, similarly to (4.41),

$$f_{0,\mathrm{res}}'(\beta,\theta)\approx\frac{1}{\beta}\left(\frac{2\pi}{\sin\theta}\right)^{\frac{1}{2}}\times\sum_{m=0}^{\infty}(-1)^m\sum_n\sqrt{\lambda_n'}\,r_{0n}'\exp(-2im\pi\lambda_n')\times\{\exp[-i\lambda_n'(2\pi-\theta)-i(\pi/4)]-\exp[-i\lambda_n'\theta+i(\pi/4)]\}.\tag{4.47}$$

Since $\mathrm{Im}\,\lambda_n'<0$, this is again a superposition of rapidly damped surface waves; however, as $\mathrm{Re}\,\lambda_n'>0$, they travel around the sphere in the opposite sense to those in (4.41).

In order to estimate the order of magnitude of this contribution, we may substitute λ_n' by (3.35), taking into account only the contributions from the first few poles. We then find

$$f_{0,\mathrm{res}}'(\beta,\theta)\approx 2\frac{N^{\frac{3}{2}}}{M}\left(\frac{2\pi}{\beta\sin\theta}\right)^{\frac{1}{2}}\exp[-2\beta(N\cosh^{-1}N-M)]\times\sum_{m=0}^{\infty}(-1)^m\sum_n\exp[-2e^{-i\pi/3}x_n\cosh^{-1}N(\alpha/2)^{\frac{1}{3}}]\times\exp(-2im\pi\lambda_n')\{\exp[-i\lambda_n'\theta-i(\pi/4)]+\exp[-i\lambda_n'(2\pi-\theta)+i(\pi/4)]\}.\tag{4.48}$$

Due to the presence of the over-all exponential factor outside of the sum, as well as the rapidly damped exponentials within the sum, $f'_{0,\mathrm{res}}(\beta, \theta)$ is exponentially small in comparison with $f_{0,\mathrm{res}}(\beta, \theta)$ [cf. Eq. (4.41)], and may therefore be neglected. This is true even for N close to unity, provided that condition (1.1) is verified.

Although $f'_{0,\mathrm{res}}(\beta, \theta)$ is completely negligible for $N > 1$, it will be seen in Sec. 4E that this is no longer true for $N < 1$. The result found in that case has a well-defined physical interpretation. It will then become clear that (4.48) represents the analytic continuation of that result to $N > 1$, in which process real rays are replaced by imaginary rays, giving rise to the real exponentials in (4.48). Thus, there is no reason either for calling this contribution unphysical or for trying to avoid it, as was done by Franz and Beckmann (cf. Sec. 3D).

Finally, let us show that the domain of validity of the above approximations is indeed given by (4.26). This follows from the following facts: (i) The Debye asymptotic expansion (4.28) employed in the neighborhood of $\bar{\lambda}$ is no longer valid when $\beta - \bar{\lambda} = \mathcal{O}(\gamma)$, i.e., by (4.27), when $\theta \leqslant \gamma$. Correspondingly, the WKB expansion (4.35) is rapidly convergent only for $\theta \gg \gamma$. (ii) The asymptotic expansions of the Legendre functions employed above are valid only for $\pi - \theta \gg \beta^{-\frac{1}{2}}$.

C. Behavior for $N > 1$, $\pi - \theta \leqslant \beta^{-\frac{1}{2}}$

The procedure to be employed near the backward direction is exactly the same as in N (Sec. IX.C). We start from (4.24) to compute $f_{0,g}(\beta, \theta)$. The only difference with respect to N [Eq. (9.45)] is an additional factor $-R_{22}(\lambda, \beta)$ in the integrand. Since the main contribution to the integral arises from $|\lambda| \leqslant \beta^{\frac{1}{2}}$ [N, Eq. (9.48); there was a misprint in this equation: the exponent should read $\frac{1}{2}$ instead of $-\frac{1}{2}$], we expand $-R_{22}$ in powers of λ, keeping only terms that yield corrections up to $\mathcal{O}(\beta^{-1})$. The result [cf. Eq. (4.29)] is

$$-R_{22}(\lambda, \beta) = \left(\frac{N-1}{N+1}\right)\left(1 + \frac{\lambda^2}{N\beta^2} + \cdots\right). \quad (4.49)$$

Let

$$\theta = \pi - \epsilon, \quad \epsilon \leqslant \beta^{-\frac{1}{2}}. \quad (4.50)$$

Then, proceeding exactly as in N (Sec. IX.C), and employing precisely the same notation, we find that $f_{0,g}(\beta, \pi - \epsilon)$ is given by N [Eq. (9.51)], multiplied by the over-all correction factor $(N-1)/(N+1)$, and with the following additional term within the square brackets:

$$-\frac{i}{N\beta}\int_0^\infty \exp(-x^2) J_0(\omega x) \tan(\pi\alpha x) x^3\, dx$$
$$= \frac{1}{2N\beta}\left(1 + i\beta\frac{\epsilon^2}{4}\right)\exp\left(i\beta\frac{\epsilon^2}{4}\right) + \mathcal{O}(\beta^{-2}), \quad (4.51)$$

which arises from the term $\lambda^2/(N\beta^2)$ in (4.49). The integral has been evaluated by the procedure given in N, Appendix F.

Thus, we finally obtain, in the place of N [Eq. (9.53)],

$$f_{0,g}(\beta, \pi - \epsilon)$$
$$= -\frac{1}{2}\left(\frac{N-1}{N+1}\right)\exp\left[-2i\beta\left(1 - \frac{\epsilon^2}{8}\right)\right]$$
$$\times\left[1 + \frac{i}{2\beta} - \frac{i\beta\epsilon^4}{192} - \frac{i}{N\beta}\left(1 + i\beta\frac{\epsilon^2}{4}\right) + \mathcal{O}(\beta^{-2})\right],$$
$$0 \leq \epsilon \leqslant \beta^{-\frac{1}{2}}. \quad (4.52)$$

This coincides with the expansion of (4.35) in powers of ϵ^2, within the domain $\epsilon \leqslant \beta^{-\frac{1}{2}}$. Thus, precisely as in N, we see that (4.35) is uniformly valid up to $\theta = \pi$. In the backward direction, we get the reflection coefficient (3.12).

The only modification that is necessary in $f_{0,\mathrm{res}}$ and $f'_{0,\mathrm{res}}$ is the substitution of the asymptotic expansion [N, Eq. (C8)] of the Legendre functions by the uniform asymptotic expansion [N, Eq. (C11)]. Finally, putting together all these results in (4.20), we obtain

$$f_0(\beta, \theta) \approx -\frac{1}{2}\left(\frac{[N^2 - \cos^2(\theta/2)]^{\frac{1}{2}} - \sin(\theta/2)}{[N^2 - \cos^2(\theta/2)]^{\frac{1}{2}} + \sin(\theta/2)}\right)\exp(-2i\beta\sin(\theta/2))$$
$$\times\left\{1 + \frac{i}{2\beta}\left[\frac{1}{\sin^3(\theta/2)} - \frac{2N^2 - \cos^2(\theta/2)}{[N^2 - \cos^2(\theta/2)]^{\frac{3}{2}}}\right] + \mathcal{O}(\beta^{-2})\right\}$$
$$-\frac{e^{i\pi/3}}{\gamma}\left(\frac{\pi - \theta}{\sin\theta}\right)^{\frac{1}{2}}\sum_{m=0}^{\infty}(-1)^m\sum_n (a'_n)^{-2}\exp[i(2m+1)\pi\lambda_n]J_0[\lambda_n(\pi - \theta)]$$
$$+ 4\pi\frac{N^2}{M}\left(\frac{\pi - \theta}{\sin\theta}\right)^{\frac{1}{2}}\exp[-2\beta(N\cosh^{-1}N - M)]$$
$$\times\sum_{m=0}^{\infty}(-1)^m\sum_n\exp[-2e^{-i\pi/3}\cosh^{-1}N(\alpha/2)^{\frac{1}{3}}x_n]\exp[-i(2m+1)\pi\lambda'_n]J_0[\lambda'_n(\pi - \theta)],$$
$$N > 1, \quad \gamma \ll \theta \leq \pi, \quad (4.53)$$

which is uniformly valid throughout the whole domain (4.25). We have employed the approximation (4.39) for r_{0n}; a better approximation may be obtained, if necessary, from (4.37) and Appendix A.

The contribution from the residue series $f_{0,\mathrm{res}}$ is very small, except perhaps at the lower end of the range $\gamma \ll \theta$; that from the residue series $f'_{0,\mathrm{res}}$ is always negligible when (1.1) is satisfied.

D. Behavior for $N > 1$, $0 \leq \theta \leqslant \gamma$

In the domain $0 \leq \theta \leqslant \gamma$, we employ the representation (4.9)–(4.14). Let us evaluate first the contribution from (4.10). As we have seen in connection with the analogous terms in N, the main contribution to the integrals in (4.10) arises from the neighborhood of $\lambda = \beta$, so that we may employ the asymptotic expansions given in Appendix A.

In particular, it follows from (A11) and from the corresponding expansion for $H_\lambda^{(2)}(x)$ (obtained by changing $i \to -i$ everywhere) that

$$\frac{H_\lambda^{(2)}(\beta)}{H_\lambda^{(1)}(\beta)} = e^{2i\pi/3}\frac{\bar{A}(\zeta)}{A(\zeta)} + \frac{e^{i\pi/6}\zeta^2}{120\pi A^2(\zeta)}\gamma^2 + \mathcal{O}(\gamma^4), \quad (4.54)$$

where

$$\zeta = \gamma(\lambda - \beta), \quad (4.55)$$

and we have introduced the abbreviations

$$A(\zeta) = \mathrm{Ai}\,(e^{2i\pi/3}\zeta), \quad \bar{A}(\zeta) = \mathrm{Ai}\,(e^{-2i\pi/3}\zeta). \quad (4.56)$$

We have also made use of the Wronskian relation (Ref. 36, p. 446):

$$W[A(\zeta), \bar{A}(\zeta)] = i/2\pi. \quad (4.57)$$

Similarly, employing (3.4), (A11), (A12), and the analogue of (4.28) for [2 α], we find

$$-R_{22}(\lambda, \beta) = 1 - \frac{\gamma}{2\pi M\bar{A}A} - \frac{e^{i\pi/6}A'}{2\pi M^2\bar{A}A^2}\gamma^2 - \frac{1}{2\pi M\bar{A}A}\left[\left(\frac{2}{15} + \frac{1}{2M^2}\right)\zeta + \frac{e^{i\pi/3}}{M^2}\frac{A'^2}{A^2} - \frac{\zeta^2}{60}\left(2e^{-i\pi/3}\frac{A'}{A} - \frac{i}{2\pi\bar{A}A}\right)\right]\gamma^3 + \mathcal{O}(\gamma^4), \quad (4.58)$$

where

$$A' = \mathrm{Ai}'\,(e^{2i\pi/3}\zeta). \quad (4.59)$$

Finally, combining (4.3) with (4.54) and (4.58), we find

$$-S_0(\lambda, \beta) = e^{2i\pi/3}\frac{\bar{A}}{A} + \frac{e^{-i\pi/3}}{2\pi MA^2}\gamma + \frac{1}{2\pi}\left(\frac{e^{i\pi/6}}{60}\frac{\zeta^2}{A^2} + \frac{e^{-i\pi/6}}{M^2}\frac{A'}{A^3}\right)\gamma^2 + \frac{e^{-i\pi/3}}{2\pi M}\left[\left(\frac{2}{15} + \frac{1}{2M^2}\right)\frac{\zeta}{A^2} + \frac{e^{i\pi/3}}{M^2}\frac{A'^2}{A^4} - \frac{e^{-i\pi/3}}{30}\frac{A'}{A^3}\zeta^2\right]\gamma^3 + \mathcal{O}(\gamma^4). \quad (4.60)$$

The corresponding expansion for $1 - S_0(\lambda, \beta)$ can be obtained by noting that [cf. N, Eq. (D3)]:

$$1 - e^{2i\pi/3}\frac{\bar{A}}{A} = e^{i\pi/3}\frac{\mathrm{Ai}\,(\zeta)}{A}. \quad (4.61)$$

In the angular domain under consideration, the uniform asymptotic expansion [N, Eq. (C11)] of the Legendre function becomes

$$P_{\lambda-\frac{1}{2}}(\cos\theta) = (\theta/\sin\theta)^{\frac{1}{2}}J_0 + \mathcal{O}(\gamma^4), \quad (4.62)$$

where we have employed the abbreviation

$$J_0 = J_0(\beta\theta + (\theta/\gamma)\zeta) = J_0[\beta\theta(1 + \tfrac{1}{2}\zeta\gamma^2)]. \quad (4.63)$$

Substituting the above results in(4.10), we obtain

$$f_{01}(\beta, \theta) + f_{02}(\beta, \theta) = \frac{i}{\gamma}\left(\frac{\theta}{\sin\theta}\right)^{\frac{1}{2}}\left\{e^{2i\pi/3}\int_{\sigma_1\infty}^{0}(1 + \tfrac{1}{2}\zeta\gamma^2)\frac{\bar{A}}{A}J_0\,d\zeta + e^{i\pi/3}\int_0^\infty(1 + \tfrac{1}{2}\zeta\gamma^2)\frac{\mathrm{Ai}\,(\zeta)}{A}J_0\,d\zeta + \frac{e^{-i\pi/3}}{2\pi M}\gamma\int_\Gamma\frac{J_0}{A^2}d\zeta + \frac{\gamma^2}{2\pi}\left(\frac{e^{i\pi/6}}{60}\int_\Gamma\frac{\zeta^2}{A^2}J_0\,d\zeta + \frac{e^{-i\pi/6}}{M^2}\int_\Gamma\frac{A'}{A^3}J_0\,d\zeta\right) + \frac{e^{-i\pi/3}\gamma^3}{2\pi M}\left[\left(\frac{2}{15} + \frac{N^2}{2M^2}\right)\int_\Gamma\frac{\zeta}{A^2}J_0\,d\zeta + \frac{e^{i\pi/3}}{M^2}\int_\Gamma\frac{A'^2}{A^4}J_0\,d\zeta - \frac{e^{-i\pi/3}}{30}\int_\Gamma\zeta^2\frac{A'}{A^3}J_0\,d\zeta\right] + \mathcal{O}(\gamma^4)\right\}, \quad (4.64)$$

where

$$\int_\Gamma = \int_{\sigma_1\infty}^0 + \int_0^\infty. \quad (4.65)$$

As we have seen in connection with (4.10), $\sigma_1\infty$ may be any direction in the second quadrant. It is convenient to choose it in such a way that the integrands in (4.64) decrease as rapidly as possible away from $\zeta = 0$. It follows from the asymptotic behavior of the Airy function [N, Eq. (D4)] that the best choice is

$$\sigma_1 = e^{2i\pi/3}, \quad (4.66)$$

[36] *Handbook of Mathematical Functions*, M. Abramowitz and I. A. Stegun, Eds. (National Bureau of Standards, Washington, 1964).

so that the path Γ is composed of a straight line from $e^{2i\pi/3}\infty$ to 0 and the positive real axis from 0 to ∞, as in N (Fig. 10). All the integrands in (4.64) then behave like

$$\exp\left(-\tfrac{4}{3}|\zeta|^{\frac{3}{2}}\right)$$

for large $|\zeta|$, so that only the domain $|\zeta| \leqslant 1$ gives an appreciable contribution.

The first two integrals in (4.64) correspond to the Fock-type functions that appeared in N [Eq. (9.13)]. Both these and the remaining integrals can be reduced, by partial integration, to *generalized Fock functions*, defined by

$$F_{m,n}(\beta,\theta) = \frac{e^{i\pi/6}}{2\pi}\int_\Gamma \frac{\zeta^m}{\mathrm{Ai}^2(e^{2i\pi/3}\zeta)} J_n(\beta\theta + (\theta/\gamma)\zeta)\, d\zeta, \tag{4.67}$$

where m and n are integers. The reduction is performed in Appendix C. Taking into account (C3)–(C7), Eq. (4.64) becomes

$$\begin{aligned} f_{01}(\beta,\theta) + f_{02}(\beta,\theta) &= i\left(\frac{\theta}{\sin\theta}\right)^{\frac{1}{2}}\Bigg[-\frac{J_1(\beta\theta)}{\theta} + \frac{1}{\theta}\left(1+\frac{\theta^2}{2M^2}\right)F_{0,1} \\ &\quad + \frac{\gamma^2}{2\theta}F_{1,1} - \frac{i}{M}\left(1+\frac{e^{-i\pi/3}\theta^2}{12M^2}\right)F_{0,0} \\ &\quad + \frac{\gamma}{60}F_{2,0} - \frac{i(4N^2-3)\gamma^2}{6M^3}F_{1,0} \\ &\quad - \frac{e^{i\pi/6}\theta^2}{12M^3}F_{0,2} + \frac{i\theta\gamma}{60M}F_{2,1} + \mathcal{O}(\gamma^3)\Bigg]. \end{aligned} \tag{4.68}$$

On the other hand, $f_{03}(\beta,\theta)$, as defined in (4.11)–(4.12), has already been evaluated in N [Eqs. (9.21) and (9.70)]:

$$f_{03}(\beta,\theta) = i\left(\frac{\theta}{\sin\theta}\right)^{\frac{1}{2}}\frac{J_1(\beta\theta)}{\theta} + \mathcal{O}(\gamma^3), \tag{4.69}$$

which corresponds to the well-known forward diffraction peak.

The residue-series contributions are given by (4.13) and (4.14), where the Legendre function may be replaced by N, Eq. (C11). Taking into account (4.39) and (4.46), and adding the results to (4.68) and (4.69), we finally get from (4.9)

$$\begin{aligned} f_0(\beta,\theta) &= i\left(\frac{\theta}{\sin\theta}\right)^{\frac{1}{2}}\Bigg\{\frac{1}{\theta}\left(1+\frac{\theta^2}{2M^2}\right)F_{0,1} + \frac{\gamma^2}{2\theta}F_{1,1} - \frac{i}{M}\left(1+\frac{e^{-i\pi/3}\theta^2}{12M^2}\right)F_{0,0} + \frac{\gamma}{60}F_{2,0} \\ &\quad - \frac{i(4N^2-3)\gamma^2}{6M^3}F_{1,0} - \frac{e^{i\pi/6}\theta^2}{12M^3}F_{0,2} + \frac{i\theta\gamma}{60M}F_{2,1} + \mathcal{O}(\gamma^3) - \frac{e^{i\pi/3}}{\gamma} \\ &\quad \times \sum_{m=1}^{\infty}(-1)^m \sum_n (a_n')^{-2}\exp(2im\pi\lambda_n)J_0(\lambda_n\theta) + \frac{4\pi N^2}{M}\exp\left[-2\beta(N\cosh^{-1}N - M)\right] \\ &\quad \times \sum_{m=0}^{\infty}(-1)^m \sum_n \exp\left[-2i(m+1)\pi\lambda_n'\right]\exp\left[-2e^{-i\pi/3}\cosh^{-1}N(\alpha/2)^{\frac{1}{3}}x_n\right]J_0(\lambda_n'\theta), \quad N>1, \quad 0 \leq \theta \leqslant \gamma. \end{aligned} \tag{4.70}$$

For $N \to i\infty$, this reduces to the result found for an impenetrable sphere in N [Eq. (9.42)], where only the first two terms of (4.64) were taken into account.

In particular, within the diffraction peak region $0 \leq \theta \ll \gamma$, we can expand the generalized Fock functions in power series in the small parameter θ/γ, by substituting in (4.67) the Taylor expansion

$$J_n(\beta\theta + (\theta/\gamma)\zeta) = \sum_{p=0}^{\infty} J_n^{(p)}(\beta\theta)(\theta\zeta/\gamma)^p/p!. \tag{4.71}$$

Since the main contribution to the integrals arises from $|\zeta| \leqslant 1$, the resulting series is rapidly convergent for $\theta/\gamma \ll 1$.

It follows from N [Eqs. (8.23) and (8.26)] that

$$\frac{e^{i\pi/6}}{2\pi}\int_\Gamma \frac{\zeta^p}{\mathrm{Ai}^2(e^{2i\pi/3}\zeta)}\, d\zeta = pM_{p-1}, \tag{4.72}$$

where

$$pM_{p-1} = 1 \quad \text{for} \quad p = 0, \quad M_0 = 1.2551e^{i\pi/3},$$
$$M_1 = 0.5323e^{2i\pi/3}, \quad M_2 = 0.09352. \tag{4.73}$$

The values of the coefficients M_p are taken from Wu,[37] who also computed them for higher values of p.

Substituting (4.71) and (4.72) in (4.67), we find

$$F_{m,n}(\beta,\theta) = \sum_{p=0}^{\infty}\frac{(m+p)}{p!}M_{m+p-1}J_n^{(p)}(\beta\theta)\left(\frac{\theta}{\gamma}\right)^p. \tag{4.74}$$

Replacing the generalized Fock functions in (4.70)

[37] T. T. Wu, Phys. Rev. **104**, 1201 (1956).

by their expansions (4.74), we find

$$f_0(\beta,\theta) = i\left(\frac{\theta}{\sin\theta}\right)^{\frac{1}{2}}\left\{\frac{J_1(\beta\theta)}{\theta} + \left[\frac{M_0}{\gamma} - \frac{i}{M} + \tfrac{8}{15}M_1\gamma - \frac{iM_0(4N^2-3)}{6M^3}\gamma^2 + \mathcal{O}(\gamma^3)\right.\right.$$
$$\left. - \frac{e^{i\pi/3}}{\gamma}\sum_{m=1}^{\infty}(-1)^m\sum_n (a_n')^{-2}\exp(2im\pi\lambda_n)\right]J_0(\beta\theta)$$
$$\left. - \left[\frac{M_1}{\gamma} - \frac{iM_0}{M} + \frac{1}{2}\left(\tfrac{3}{5}M_2 - \frac{1}{M^2}\right)\gamma + \mathcal{O}(\gamma^2)\right]\frac{\theta}{\gamma}J_1(\beta\theta) + \mathcal{O}\left(\frac{\theta^2}{\gamma^2}\right)\right\}, \quad N>1, \quad 0\leq\theta\ll\gamma. \quad (4.75)$$

Here, we have approximated $J_0(\lambda_n\theta)\approx J_0(\beta\theta)$ in the first residue series of (4.70), and we have entirely neglected the contribution from the second residue series, which is indeed negligible under the present conditions.

For $N\to i\infty$, (4.75) agrees with N [Eq. (9.33)], to the order of accuracy computed there. The first term of (4.75), which corresponds to the forward diffraction peak, again dominates the amplitude for $\theta\ll\gamma$.

Finally, for $\theta\gg\gamma$, (4.70) goes over smoothly into (4.53). This has already been proved in N [Eq. (9.41)], for the dominant term in the amplitude, which is the same as here, so that the proof need not be repeated.

The results (4.53) and (4.70) give the value of $f_0(\beta,\theta)$ for all directions, $0\leq\theta\leq\pi$. We see that the domain $\theta\sim\gamma$ is a normal (Fock-type) transition region. In this region, tables of generalized Fock functions would be required for a numerical evaluation.

E. Behavior for $N<1$

Let us now take $N<1$. In this case, as shown in Fig. 8(b), all rays incident at an angle $\theta_1>\theta_t$ are totally reflected, where θ_t is the critical angle, given by (4.1). There is a corresponding shadow boundary at $\theta=\theta_t$, where

$$\theta_t = \pi - 2\theta_t = 2\cos^{-1}N. \quad (4.76)$$

The same shadow boundary, as will be seen later, appears in all the terms of the Debye expansion.

The existence of this shadow boundary leads to a subdivision into three different angular regions:

$$\begin{aligned} &\text{(i)} && \theta-\theta_t\gg\Delta\theta;\\ &\text{(ii)} && |\theta-\theta_t|\lesssim\Delta\theta;\\ &\text{(iii)} && \theta_t-\theta\gg\Delta\theta. \end{aligned} \quad (4.77)$$

We shall see that the width $\Delta\theta$ of the transition region is again given by (4.2), although it is not a normal transition. From the point of view of geometrical optics, region (iii) is where total reflection occurs, whereas only partial reflection takes place in (i). Furthermore, there is still a forward diffraction peak in region (iii), so that we still have to distinguish $\theta\gg\gamma$ and $\theta\lesssim\gamma$ within it.

As shown in Fig. 10, the distinction between regions (i) and (iii) is reflected in the position of the saddle point associated with (4.21). The saddle point $\bar\lambda$ is still given by (4.27), so that $\bar\lambda<\alpha$ in region (i) (point $\bar\lambda_1$ in Fig. 10) and $\bar\lambda>\alpha$ in region (iii) (point $\bar\lambda_2$ in Fig. 10). The path of integration Γ' crosses the real axis at the saddle point, at an angle of $-\pi/4$, and it must begin and end at infinity outside of the shaded regions in Fig. 10. [The asymptotic behavior of the integrand of (4.21) follows from Appendix B and from N (Appendices A and C). The shaded regions are those where the integrand diverges at infinity, where η_1 and η_2 are defined by (B2).] Thus, as we go through the transition region (ii), the path Γ' sweeps across the poles λ_n'; consequently, as had already been mentioned in Sec. 3D, there is no way to avoid the contributions from these poles.

Let us consider first the behavior of $f_0(\beta,\theta)$ in region (i), still using the representation (4.20)–(4.23). The corresponding path of integration Γ_1' in (4.21) (Fig. 10) does not differ in any way from the path for $N>1$, so that we obtain precisely the same result (4.35) as before. The only question to be considered is that of the domain of validity of this result.

The expression (4.29) for R_{22} depends upon the validity of the Debye asymptotic expansion for

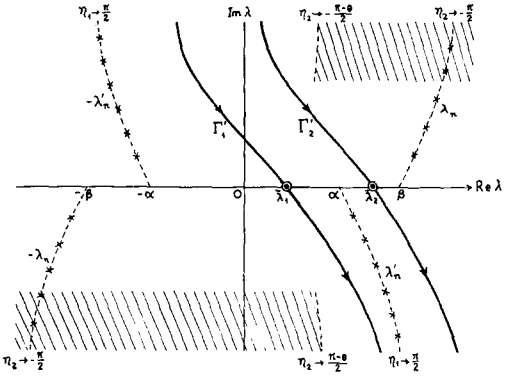

FIG. 10. For $N<1$, the path of integration in (4.21) must begin in the upper half-plane, to the left of the shaded region, and end in the lower half-plane, to the right of the shaded region, going over a saddle point ○ that, for $\theta>\theta_t$, is to the left of $\bar\lambda=\alpha$ (e.g., at $\bar\lambda_1$) and, for $\theta<\theta_t$, is to the right of $\bar\lambda=\alpha$ (e.g., at $\bar\lambda_2$). ×—poles.

[2 α]. Thus,

$$|\alpha - \lambda| \gg \alpha^{\frac{1}{3}} \tag{4.78}$$

must be satisfied within the relevant portion of the domain of integration. The distance of closest approach from $\lambda = \alpha$ to the path of integration is of the order of $\alpha - \bar{\lambda}$, so that (4.78) must be valid for $\lambda = \bar{\lambda}$. Taking into account (4.27) and (4.76), this leads to

$$\theta - \theta_t \gg N^{\frac{1}{3}}\gamma^2/M' \tag{4.79}$$

where M' is defined by (3.31). Exactly the same condition is found from the requirement that the first correction term in the WKB expansion (4.35), involving the denominator

$$\beta(N^2 - \cos^2\theta/2)^{\frac{3}{2}} = \beta(\cos^2(\theta_t/2) - \cos^2(\theta/2))^{\frac{3}{2}}, \tag{4.80}$$

must be small.

According to (1.1), the domain (4.79) falls within region (i). [It may overlap with (ii), depending on the value of N.] On the other hand, as we have seen in (4.52), the approximation (4.35) remains valid up to $\theta = \pi$.

The contribution $f_{0,\text{res}}$ from the poles λ_n is still given by (4.41), the only difference being that the substitution (3.30) must be made in the expression (3.29) for the poles. The physical interpretation remains unchanged: these terms correspond to the surface waves excited by the tangentially incident rays, and, as before, their damping is determined almost completely by the geometry.

In contrast with the case $N > 1$, however, the poles λ'_n now give a significant contribution, corresponding to an entirely new type of surface waves. The result for $f'_{0,\text{res}}$ is given by (4.23), where (4.46) is now to be replaced by

$$r'_{0n} \approx -(2N/M')\exp(-2iM'\beta + 2i\lambda'_n \cos^{-1} N), \tag{4.81}$$

so that (4.48) becomes

$$f'_{0\text{res}}(\beta, \theta) \approx \frac{2e^{i\pi/4}N^{\frac{3}{2}}}{M'}\left(\frac{2\pi}{\beta \sin\theta}\right)^{\frac{1}{2}} \exp(-2iM'\beta) \times \left\{\sum_n \exp(-i\lambda'_n\zeta^+_{1,0}) + \sum_{m=1}^{\infty}(-1)^m \times \sum_n [\exp(-i\lambda'_n\zeta^+_{1,m}) - i\exp(-i\lambda'_n\zeta^-_{1,m})]\right\}, \quad \pi - \theta \gg \beta^{-\frac{1}{2}}, \tag{4.82}$$

where

$$\zeta^{\pm}_{1,m} = 2m\pi - \theta_t \pm \theta, \quad m = 0, 1, 2, \cdots, \tag{4.83}$$

and θ_t is given by (4.76).

The geometrical interpretation of the angles $\zeta^+_{1,0}$ and $\zeta^-_{1,1}$ is shown in Fig. 11(a). The surface waves in

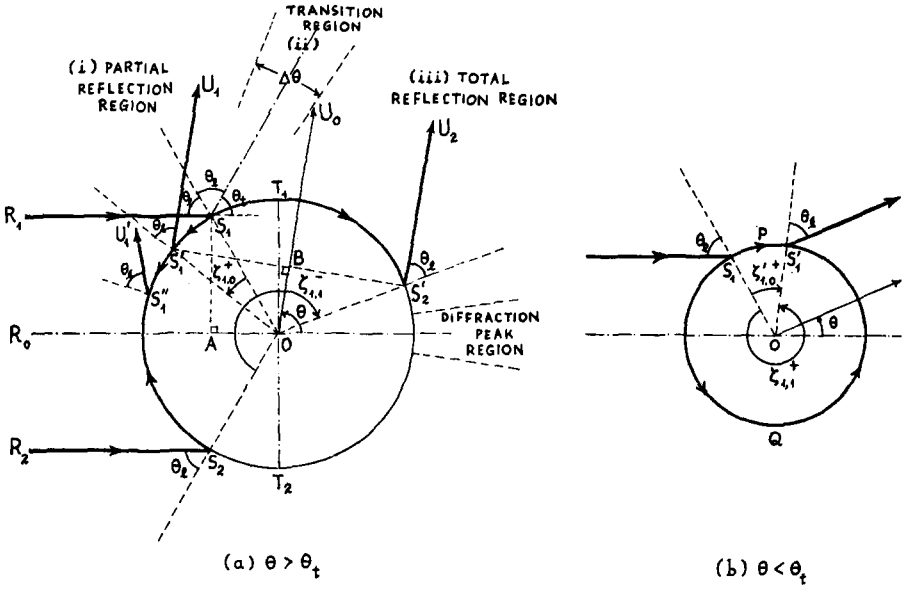

FIG. 11. Geometrical interpretation of (4.82) and (4.83). (a) The angles $\zeta^+_{1,0}$ and $\zeta^-_{1,1}$ correspond to the rays $R_1S_1S'_1U_1$ and $R_2S_2S'_2U_2$, respectively ($\theta > \theta_t$). The path difference with respect to the central path R_0OU_0 is $\overline{OA} + \overline{OB}$. The subdivision into regions is also indicated. The diffracted ray $R_1S_1S'_1S''_1U'_1$ appears in the second term in the Debye expansion [cf. Eq. (5.66)]. (b) For $\theta < \theta_t$, $\zeta^+_{1,0}$ is to be replaced by $\zeta^+_{1,1} = 2\pi + \zeta^+_{1,0}$. According to the geometrical theory of diffraction, the diffracted ray would propagate clockwise, as $S_1PS'_1$, corresponding $\zeta^+_{1,0} = 2\pi - \zeta^+_{1,1} = -\zeta^+_{1,0}$.

(4.82) are excited by the critically incident rays R_1S_1, R_2S_2. Their complex propagation constant λ'_n is given by (3.35), so that they travel along the surface on the inner side, with phase velocity slightly smaller than c/N and angular damping constant

$$\approx (\sqrt{3}/2)(\alpha/2)^{\frac{1}{3}}x_n.$$

In terms of diffracted rays, the surface ray excited by the critically incident ray R_1S_1 gives rise to the diffracted ray S'_1U_1 in the direction θ, leaving the surface at the critical angle θ_i, so that the arc $S_1S'_1$ travelled along the surface corresponds to the angle $\zeta^+_{1,0}$; similarly $\zeta^+_{1,m}$ includes m additional turns around the sphere. The path difference with respect to the central ray R_0OU_0 [Fig. 11(a)] is $\overline{OA} + \overline{OB} = 2a\cos\theta_i = 2M'a$, which accounts for the phase factor $\exp(-2iM'\beta)$ in (4.82). Similar considerations apply to the ray $R_2S_2S'_2U_2$.

These diffracted rays obey a peculiar "law of refraction": although the *magnitudes* of the angles of incidence and refraction are given by Snell's law, they have opposite signs: both upon entering and upon leaving the surface, *the incident and "refracted" rays lie on the same side of the normal!*

This result is in disagreement with the geometrical theory of diffraction.[16,33] According to this theory, the diffracted rays associated with the critically incident rays R_1S_1 and R_2S_2 would obey the ordinary law of refraction both at the point of excitation and at the point where they leave the surface. This is illustrated in Fig. 11(b), which refers to the case $\theta < \theta_i$: according to the geometrical theory of diffraction, the diffracted ray would travel *clockwise*, along the path $S_1PS'_1$, corresponding to the angle $\zeta'^+_{1,0} = -\zeta^+_{1,0}$; according to the present results, it follows the *anticlockwise* path $S_1QS'_1$, corresponding to the angle $\zeta^+_{1,1}$. Thus, although the entry and exit points are the same, the results are quite different.

In the case of a plane interface (Fig. 12), a critically incident ray RS gives rise, as is well known, to a surface wave SV travelling along the interface in the optically rare medium, so that the corresponding ray obeys Snell's law. At each point along its path (such as S', S'' in Fig. 12), the surface wave sheds rays back into the dense medium at the critical angle, again obeying Snell's law. This gives rise to a conical wave in the dense medium, the Schmidt head wave, which has been investigated theoretically and experimentally (Ref. 4, pp. 366 and 380).

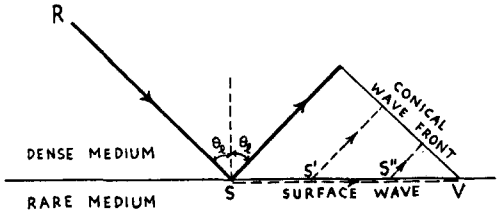

FIG. 12. The Schmidt head wave.

Thus, if we approximate the sphere surface locally by its tangent plane at the entry and exit points (as is done in geometrical optics), we are led to the prediction of the geometrical theory of diffraction. It seems at first sight very surprising that the surface waves actually found in (4.82) travel in the opposite sense around the sphere.

It was precisely to avoid the seemingly "unphysical" contributions from the poles λ'_n that Franz and Beckmann proposed their modified contours. However, as has already been seen in Sec. 3D, their proposal does not achieve its purpose, nor does it lead to the diffracted rays predicted by the geometrical theory of diffraction. Such rays would correspond to poles in the *first* quadrant, near $\lambda = \alpha$.

Chen[33] has tried to identify such poles with the Regge poles closest to $\lambda = \alpha$ in Fig. 4, by enclosing them with the contour C' *before* making the Debye expansion. However, as was mentioned in Sec. 3D, this is not allowed, because the Debye expansion diverges on C' (also, C' is not suitable for applying the saddle-point method). Furthermore, according to the discussion in Secs. 2 and 3, the Regge poles associated with the original partial-wave series have a very different physical interpretation as compared with those associated with the Debye expansion.

Streifer and Kodis[38] found surface waves similar to those of Fig. 11(a) in the case of a dielectric cylinder, but considered their physical interpretation unsatisfactory.

Since the path of integration in the saddle-point method must sweep across the poles λ'_n (Fig. 10), it is clear that one cannot obtain the geometrical-optics contribution without including also the contributions from these poles, so that any attempt to get rid of them is of no avail.

The interpretation of the surface waves found in (4.82) in terms of diffracted rays disagrees with the geometrical theory of diffraction only with respect to the sense of propagation around the sphere. There is, however, a very good physical reason why this should indeed be so.

Physically, the role played by the surface waves is to describe *the field penetration into shadow regions:* their exponential damping is characteristic of the shadow produced by a curved surface (cf. N, p. 83).

[38] W. Streifer and R. D. Kodis, Quart. Appl. Math. **22**, 193 (1964).

They are always excited at the border between lit and shadow regions on the surface. Therefore, one must expect that *surface waves always travel away from the shadow boundary into the shadow* (rather than into the lit region). Otherwise, a smooth transition between lit and shadow regions, with the exponential damping starting at the boundary and proportional to the angle of penetration into the shadow, would not be possible.

For an impenetrable sphere (N, p. 39), as well as for a transparent sphere with $N > 1$, the requirement of propagation into the shadow always leads to agreement with the geometrical theory of diffraction. For $N < 1$, however, the domain $\theta > \theta_t$ is a shadow region for transmitted rays [cf. Fig. 13(b)], and the requirement that the surface waves excited at S_1 and S_2 (Fig. 11) must propagate into the shadow leads precisely to the sense of propagation that we have found. The geometrical theory of diffraction would lead to surface waves propagating into the lit region, which is physically unacceptable.

Since the geometrical theory has met with considerable success in the treatment of a large class of problems, it would be interesting to modify its formulation, taking into account the physical requirements about the sense of propagation of surface waves. The local behavior of a ray is determined not only by the tangential plane, but also by the distinction between shadow and lit sides.

We also see now that, although $f'_{0,\mathrm{res}}(\beta, \theta)$ is negligible for $N > 1$, the expression (4.48) is simply the analytic continuation of the result (4.82) found for $N < 1$ [cf. Eq. (3.30)].

The domain where the residue series (4.82) is rapidly convergent is determined by the condition

$$|\mathrm{Im}\ \lambda'_1|\ \zeta^+_{1,0} \gg 1,$$

i.e., according to (3.35) and (4.83),

$$\theta - \theta_t \gg (N\beta)^{-\frac{1}{3}} \sim \gamma. \tag{4.84}$$

Finally, in order to obtain expressions that remain valid up to $\theta = \pi$, it is necessary to employ the uniform asymptotic expansion [N, Eq. (C11)] of the Legendre functions. Putting together all of the above results, we finally obtain

$$\begin{aligned} f_0(\beta, \theta) \approx & -\frac{1}{2}\left(\frac{[N^2 - \cos^2(\theta/2)]^{\frac{1}{2}} - \sin(\theta/2)}{[N^2 - \cos^2(\theta/2)]^{\frac{1}{2}} + \sin(\theta/2)}\right) \exp(-2i\beta \sin(\theta/2)) \\ & \times \left\{1 + \frac{i}{2\beta}\left[\frac{1}{\sin^3(\theta/2)} - \frac{2N^2 - \cos^2(\theta/2)}{(N^2 - \cos^2(\theta/2))^{\frac{3}{2}}}\right] + \mathcal{O}(\beta^{-2})\right\} - \frac{e^{i\pi/3}}{\gamma}\left(\frac{\pi - \theta}{\sin\theta}\right)^{\frac{1}{2}} \\ & \times \sum_{m=0}^{\infty}(-1)^m \sum_n (a'_n)^{-2} \exp[i(2m+1)\pi\lambda_n] J_0[\lambda_n(\pi - \theta)] + 4\pi i \frac{N^2}{M'}\left(\frac{\pi - \theta}{\sin\theta}\right)^{\frac{1}{2}} \exp(-2iM'\beta) \\ & \times \sum_{m=0}^{\infty}(-1)^m \sum_n \exp[i\lambda'_n\theta_t - i(2m+1)\pi\lambda'_n] J_0[\lambda'_n(\pi - \theta)], \quad N < 1, \quad \theta - \theta_t \gg \gamma. \end{aligned} \tag{4.85}$$

Let us now go over to region (iii) [cf. Eq. (4.77)], where, according to geometrical optics, total reflection takes place. We again have to treat separately the diffraction peak region $0 \leq \theta \ll \gamma$. For $\theta \gg \gamma$, we can still employ the representation (4.20)–(4.23), but the saddle-point path Γ'_2 for the evaluation of (4.21) is now on the other side of the line (Fig. 10) where the poles λ'_n are located. Thus, we have to take into account their additional residue-series contribution, and (4.21) becomes

$$\text{where} \qquad f_{0,g}(\beta, \theta) = \tilde{f}_{0,g}(\beta, \theta) - f'_{0,0}(\beta, \theta), \tag{4.86}$$

$$\tilde{f}_{0,g}(\beta, \theta) = -\frac{i}{\beta}\int_{\Gamma'_2} S_0(\lambda, \beta) Q^{(1)}_{\lambda-\frac{1}{2}}(\cos\theta)\lambda\, d\lambda, \tag{4.87}$$

$$\begin{aligned} f'_{0,0}(\beta, \theta) = & -\frac{2\pi}{\beta}\sum_n \lambda'_n r'_{0n} Q^{(1)}_{\lambda'_n-\frac{1}{2}}(\cos\theta) \\ & \approx 2e^{i\pi/4}\frac{N^{\frac{3}{2}}}{M'}\left(\frac{2\pi}{\beta\sin\theta}\right)^{\frac{1}{2}} \exp(-2iM'\beta) \\ & \times \sum_n \exp(-i\lambda'_n\zeta^+_{1,0}), \end{aligned} \tag{4.88}$$

and we have made use of (4.81) and N [Eq. (C7)]. The last term should be grouped together with $f'_{0,\mathrm{res}}(\beta, \theta)$, so that we have to make the following replacements in (4.20):

$$f_{0,g} \to \tilde{f}_{0,g}; \quad f'_{0,\mathrm{res}} \to \tilde{f}'_{0,\mathrm{res}} = f'_{0,\mathrm{res}} - f'_{0,0}, \tag{4.89}$$

where $f'_{0,\mathrm{res}}(\beta, \theta)$ is given precisely by (4.14). This follows from (4.23), (4.88), and the identity N [Eq. (6.33)].

According to (4.88), the substitution of $f'_{0,\mathrm{res}}$ by $\tilde{f}'_{0,\mathrm{res}}$ amounts precisely to subtracting out from (4.82) the residue series in $\zeta^+_{1,0}$, which would diverge for $\theta < \theta_t$. The first term in the remaining residue series $\tilde{f}'_{0,\mathrm{res}}$ then corresponds to the angle $\zeta^+_{1,1}$, as it should, according to Fig. 11(b). Thus, the residue series $\tilde{f}'_{0,\mathrm{res}}$ is rapidly convergent for all $\theta < \theta_t$.

The saddle-point evaluation of (4.87) is entirely similar to that which led to (4.35), except that, in (4.29), we have to make the substitution

$$(\alpha^2 - \lambda^2)^{\frac{1}{2}} \to -i(\lambda^2 - \alpha^2)^{\frac{1}{2}}. \tag{4.90}$$

Correspondingly, (4.35) is replaced by

$$\tilde{f}_{0,g}(\beta,\theta) = -\frac{1}{2}\left(\frac{[\cos^2(\theta/2)-N^2]^{\frac{1}{2}} - i\sin(\theta/2)}{[\cos^2(\theta/2)-N^2]^{\frac{1}{2}} + i\sin(\theta/2)}\right)\exp(-2i\beta\sin(\theta/2))$$
$$\times\left\{1+\frac{i}{2\beta}\left[\frac{1}{\sin^3(\theta/2)} + i\frac{(2N^2-\cos^2(\theta/2))}{(\cos^2(\theta/2)-N^2)^{\frac{3}{2}}}\right] + \mathcal{O}(\beta^{-2})\right\},$$
$$N<1, \quad \theta_t-\theta \gg N^{\frac{1}{3}}\gamma^2/M', \quad \theta \gg \gamma, \quad (4.91)$$

where the restriction on $\theta_t - \theta$ arises in the same way as (4.79). As ought to be expected, we find the unimodular Fresnel reflection coefficient associated with total reflection [cf. Eq. (4.36)].

On the other hand, nothing changes in the residue series associated with the poles λ_n, so that we finally obtain [cf. (4.41)]

$$f_0(\beta,\theta) \approx -\frac{1}{2}\left(\frac{[\cos^2(\theta/2)-N^2]^{\frac{1}{2}} - i\sin(\theta/2)}{[\cos^2(\theta/2)-N^2]^{\frac{1}{2}} + i\sin(\theta/2)}\right)\exp(-2i\beta\sin(\theta/2))$$
$$\times\left\{1+\frac{i}{2\beta}\left[\frac{1}{\sin^3(\theta/2)} + i\frac{(2N^2-\cos^2(\theta/2))}{(\cos^2(\theta/2)-N^2)^{\frac{3}{2}}}\right] + \mathcal{O}(\beta^{-2})\right\} + \tfrac{1}{2}e^{i\pi/12}\left(\frac{\gamma}{\pi\sin\theta}\right)^{\frac{1}{2}}$$
$$\times\left\{-i\sum_n (a_n')^{-2}\exp(i\lambda_n v_0^+) + \sum_{m=1}^{\infty}(-1)^m\sum_n (a_n')^{-2}[\exp(i\lambda_n v_m^-) - i\exp(i\lambda_n v_m^+)]\right\}$$
$$+ 2e^{-i\pi/4}\frac{N^{\frac{3}{2}}}{M'}\left(\frac{2\pi}{\beta\sin\theta}\right)^{\frac{1}{2}}\exp(-2iM'\beta)\sum_{m=1}^{\infty}(-1)^m\sum_n[\exp(-i\lambda_n'\zeta_{1,m}^+) + i\exp(-i\lambda_n'\zeta_{1,m}^-)],$$
$$N<1, \quad \theta_t-\theta \gg \gamma, \quad \theta \gg \gamma. \quad (4.92)$$

In the region $0 \leq \theta \lesssim \gamma$, where the forward diffraction peak is contained, $f_0(\beta,\theta)$ is still given by (4.70), provided that we make the substitution (3.30) and that (4.46) is replaced by (4.81) in the residue series at the poles λ_n'.

There remains only for us to consider the transition region (ii) in (4.77):

$$|\theta-\theta_t| \lesssim \gamma. \quad (4.93)$$

In this region, the approximation (4.29) for R_{22} is no longer valid within the range of the saddle point: the Debye asymptotic expansions have to be replaced by [cf. (3.33)]

$$[2\alpha] \approx e^{i\pi/3}\left(\frac{2}{\alpha}\right)^{\frac{1}{3}}\ln' \mathrm{Ai}(e^{-2i\pi/3}\zeta), \quad (4.94)$$

where

$$\zeta = (2/\alpha)^{\frac{1}{3}}(\lambda-\alpha). \quad (4.95)$$

The main contribution to the integral in (3.21) still comes from the neighborhood of the saddle point

$$\bar{\lambda} = \beta\cos(\theta/2) \approx \beta\cos(\theta_t/2) = N\beta = \alpha, \quad (4.96)$$

so that we may replace λ by α in slowly varying factors. Thus, (4.29) is replaced by

$$R_{22}(\lambda,\beta) \approx \frac{1+\kappa^2\ln'\mathrm{Ai}(e^{-2i\pi/3}\zeta)}{1-\kappa^2\ln'\mathrm{Ai}(e^{-2i\pi/3}\zeta)} \quad (4.97)$$

in first approximation, where

$$\kappa^2 = e^{-i\pi/6}N^{\frac{2}{3}}\gamma/M'; \quad |\kappa^2| \ll 1. \quad (4.98)$$

The remaining approximations employed in (4.31) are still valid.

As θ ranges through the transition region (4.93), the saddle-point path of integration sweeps across the poles, as shown in Fig. 10. Let us make the change of variable (4.30) and expand everything around the saddle point:

$$w-\theta/2 = e^{-i\pi/4}u[\beta\sin(\theta/2)]^{-\frac{1}{2}};$$
$$\zeta = \bar{\zeta} - \sqrt{2}\,e^{-i\pi/3}u/\kappa, \quad (4.99)$$

where

$$\bar{\zeta} \approx \frac{M'}{N^{\frac{1}{3}}}\frac{(\theta_t-\theta)}{\gamma^2}. \quad (4.100)$$

Then, we finally get

$$f_{0,g}(\beta,\theta) \approx \tfrac{1}{2}\exp(-2i\beta\sin(\theta/2))\left\{1+\frac{2\kappa^2}{\sqrt{\pi}}\int_{-\infty}^{\infty}\exp(-u^2)\frac{\ln'\mathrm{Ai}(e^{-2i\pi/3}\bar{\zeta}+\sqrt{2}\,u/\kappa)}{1-\kappa^2\ln'\mathrm{Ai}(e^{-2i\pi/3}\bar{\zeta}+\sqrt{2}\,u/\kappa)}\,du\right\}$$
$$-2e^{i\pi/4}\frac{N^{\frac{3}{2}}}{M'}\left(\frac{2\pi}{\beta\sin\theta}\right)^{\frac{1}{2}}\exp(-2iM'\beta)\sum_{n\geq n_0}\exp(-i\lambda_n'\zeta_{1,0}^+), \quad N<1, \quad |\theta-\theta_t| \lesssim \gamma \quad (4.101)$$

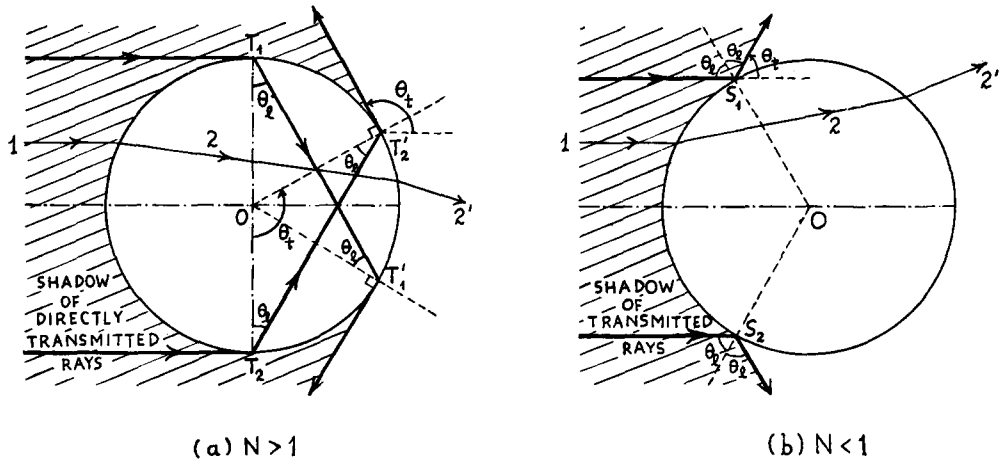

FIG. 13. Structure of the lit and shadow regions in the geometrical-optics approximation, for the second term of the Debye expansion, corresponding to directly transmitted rays, such as 2'. (a) $N > 1$; (b) $N < 1$. In both cases, the shadow boundary is $\theta_i = \pi - 2\theta_t$, where θ_t is the critical angle.

where n_0 is the last pole that has been swept by the path of integration. When all the poles have been swept (e.g., for $\theta < \theta_i$), their total contribution is given by (4.88), so that the terms in (4.82) that would be poorly converging are gradually subtracted out. Otherwise, (4.82) and the corresponding expression for $f_{0,\mathrm{res}}(\beta, \theta)$ remain valid.

The first term (unity) in the expression within curly brackets in (4.101) is the dominant one. The other term, according to (4.98), is a small correction, which contains the effects due to the poles not yet subtracted out, as well as the corrections to the reflection coefficient. In fact, within the present order of approximation, the poles correspond to the roots of the denominator in the integrand. For $\theta > \theta_i$, there may be several poles within the range of the saddle-point.

The asymptotic expansion of integrals containing poles in the neighborhood of a saddle point has been investigated by several authors (cf. e.g., Ref. 39). The transition term representing the effect of the poles can be expressed in terms of error functions with complex argument. We shall not carry out this procedure explicitly for (4.101).

As will be seen later, the structure of the transition region is actually quite complicated, because all higher-order terms in the Debye expansion lead to the same shadow boundary for $N < 1$, so that all their contributions should be taken into account.

This concludes the discussion of the asymptotic behavior of $f_0(\beta, \theta)$. We see that it can be determined for all values of θ, $0 \leq \theta \leq \pi$, both for $N > 1$ and for $N < 1$.

[39] B. L. van der Waerden, Appl. Sci. Res. **B2**, 33 (1950).

5. THE SECOND TERM OF THE DEBYE EXPANSION

A. Preliminary Considerations

The second term of the Debye expansion is given by either one of the equivalent representations (3.23) and (3.26), with $p = 1$. In the geometrical-optics approximation, it is associated with rays that are directly transmitted through the sphere, without any internal reflection, like the ray 2' in Fig. 5.

The structure of the lit and shadow regions for this class of rays is shown in Fig. 13(a) for $N > 1$ and in Fig. 13(b) for $N < 1$. In both cases, there is a shadow region (shown shaded in Fig. 13), which is inaccessible to directly transmitted rays. For $N > 1$, the shadow boundary corresponds to transmitted rays associated with tangentially incident rays at T_1 and T_2 [Fig. 13(a)]. According to geometrical optics, these rays are critically refracted and reemerge tangentially at T_1' and T_2', respectively. For $N < 1$, the shadow boundary is associated with the critically incident rays at S_1 and S_2, which are totally reflected; it is the same one already found for the first term of the Debye expansion and shown in Fig. 8(b).

The direction of the shadow boundary is given in both cases by [cf. Eq. (4.76)]

$$\theta_i = \pi - 2\theta_t, \tag{5.1}$$

where θ_t is the critical angle. Notice, however, that, while θ_t is given by (4.1) for $N < 1$, it is given by

$$\sin \theta_t = 1/N \tag{5.2}$$

for $N > 1$.

Thus, we expect to find three different regions, as in (4.77):

$$\begin{aligned} &\text{(i)} && \theta - \theta_t \gg \Delta\theta; \\ &\text{(ii)} && |\theta - \theta_t| \leqslant \Delta\theta; \\ &\text{(iii)} && \theta_t - \theta \gg \Delta\theta, \end{aligned} \tag{5.3}$$

where $\Delta\theta$ is the angular width of the transition domain (ii) between the shadow region (i) and the lit region (iii). We shall see that this is a normal transition, so that

$$\Delta\theta \sim \gamma. \tag{5.4}$$

In the shadow region (i), the amplitude can be reduced to a pure residue series. Since this region extends up to $\theta = \pi$, we employ the representation (3.26). Changing λ to $-\lambda$ in the sum from $m = -\infty$ to -1, and taking into account (3.10), we find that (3.26) becomes

$$f_1(\beta, \theta) = -\frac{1}{\beta}\sum_{m=0}^{\infty}(-1)^m\int_{-\infty}^{\infty} U(\lambda, \beta)P_{\lambda-\frac{1}{2}}(-\cos\theta) \times \exp[i(2m+1)\pi\lambda]\lambda\, d\lambda, \tag{5.5}$$

where $U(\lambda, \beta)$ is given by (3.24).

The asymptotic behavior of $U(\lambda, \beta)$ as $|\lambda| \to \infty$ in the upper half-plane is shown in Fig. 14. We see that

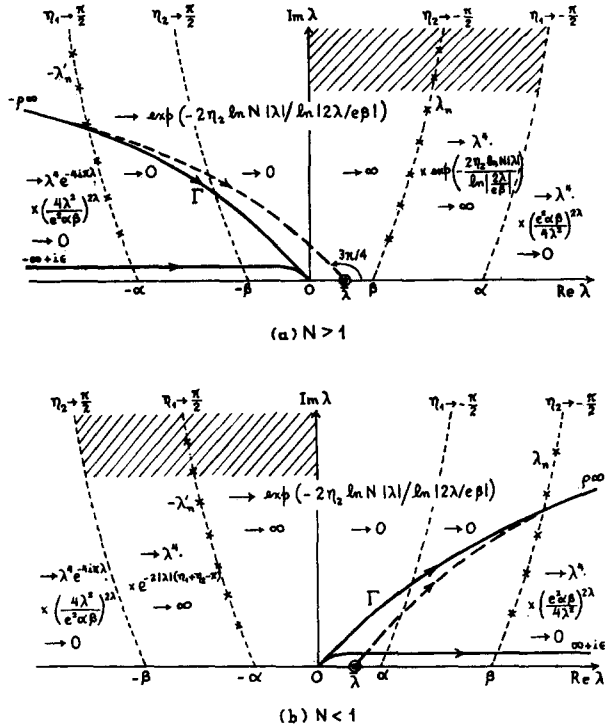

FIG. 14. Asymptotic behavior of $U(\lambda, \beta)$ [cf. Eq. (3.24)] as $|\lambda| \to \infty$ in different regions of the λ plane. (a) $N > 1$; (b) $N < 1$. $U \to \infty$ in the shaded regions and $U \to 0$ elsewhere (apart from the poles). The paths of integration in (5.11) and (5.15) are replaced by symmetric paths from $-\rho\infty$ to $\rho\infty$ prior to the saddle-point evaluation; one-half of these paths is shown. ×—poles; ⊙—saddle point; — — — steepest descent path.

$U \to 0$ everywhere, except in the shaded regions in the neighborhood of the imaginary axis, where it diverges like

$$\exp(c\,|\lambda|/\ln|\lambda|), \quad c = \text{const} > 0.$$

On the other hand, according to N [Eq. (C8)], $e^{i\pi\lambda}P_{\lambda-\frac{1}{2}}(-\cos\theta)$ behaves like $e^{i\lambda\theta}$ as $|\lambda| \to \infty$ in the upper half-plane, so that, for any $\theta > 0$, the path of integration in (5.5) can be closed at infinity, reducing the integrals to pure residue series:

$$f_1(\beta, \theta) = f_{1,\text{res}}(\beta, \theta) + f'_{1,\text{res}}(\beta, \theta), \tag{5.6}$$

where

$$f_{1,\text{res}}(\beta, \theta) = -\frac{2\pi i}{\beta}\sum_{m=0}^{\infty}(-1)^m\sum_n \text{residue}\,\{\lambda U(\lambda, \beta) \times \exp[i(2m+1)\pi\lambda]P_{\lambda-\frac{1}{2}}(-\cos\theta)\}_{\lambda_n}, \tag{5.7}$$

$$f'_{1,\text{res}}(\beta, \theta) = -\frac{2\pi i}{\beta}\sum_{m=0}^{\infty}(-1)^m\sum_n \text{residue}\,\{\lambda U(\lambda, \beta) \times \exp[i(2m+1)\pi\lambda]P_{\lambda-\frac{1}{2}}(-\cos\theta)\}_{-\lambda_n'}. \tag{5.8}$$

[Actually, of course, we have to consider a sequence of contours passing between the poles, as was done in N (Sec. IV). For a more careful discussion of this point, see Ref. 40.] This representation will be employed in the shadow region (i).

In the lit region (iii), we start from (5.5). We shift the path of integration to a straight line above the real axis (from $-\infty + i\epsilon$ to $\infty + i\epsilon$, $\epsilon > 0$), and we substitute the identity N [Eq. (C6)]:

$$P_{\lambda-\frac{1}{2}}(-\cos\theta) = -ie^{i\pi\lambda}P_{\lambda-\frac{1}{2}}(\cos\theta) + 2i\cos(\pi\lambda)Q^{(2)}_{\lambda-\frac{1}{2}}(\cos\theta). \tag{5.9}$$

[This shift is necessary because of the singularities of $Q^{(2)}_{\lambda-\frac{1}{2}}(\cos\theta)$ on the negative real axis.] Taking into account also the identity

$$\sum_{m=0}^{\infty}(-1)^m\cos(\pi\lambda)\exp[i(2m+1)\pi\lambda] = \tfrac{1}{2}, \quad \text{Im}\,\lambda > 0, \tag{5.10}$$

valid over the new path of integration, we find

$$f_1(\beta, \theta) = -\frac{i}{\beta}\int_{-\infty+i\epsilon}^{\infty-i\epsilon} U(\lambda, \beta)Q^{(2)}_{\lambda-\frac{1}{2}}(\cos\theta)\lambda\, d\lambda - \frac{2\pi}{\beta}\sum_{m=0}^{\infty}(-1)^m\sum_n \text{residues}\,\{\lambda U(\lambda, \beta)P_{\lambda-\frac{1}{2}}(\cos\theta) \times \exp[2i(m+1)\pi\lambda]\}_{\lambda_n, -\lambda_n'}. \tag{5.11}$$

In (5.11), the integrals containing $P_{\lambda-\frac{1}{2}}(\cos\theta)$ have been reduced to residue series at the poles

[40] R. F. Goodrich and N. D. Kazarinoff, Proc. Cambridge Phil. Soc. **59**, 167 (1963).

λ_n, $-\lambda_n'$ by closing the path of integration at infinity in the upper half-plane. This is allowed, according to Fig. 14, due to the extra convergence factor $e^{i\pi\lambda}$ in the first term of (5.9). Furthermore, in the integral containing $Q^{(2)}_{\lambda-\frac{1}{2}}(\cos\theta)$, the path of integration has been shifted from $(-\infty + i\epsilon,\ \infty + i\epsilon)$ to a path symmetric about the origin $(-\infty + i\epsilon,\ \infty - i\epsilon)$, by crossing the *positive* real axis, which is allowed, because $Q^{(2)}_{\lambda-\frac{1}{2}}(\cos\theta)$ is regular there.

If we now split the path of integration at the origin and change λ to $-\lambda$ over one-half of it, making use of the identity

$$Q^{(2)}_{\lambda-\frac{1}{2}}(\cos\theta) - Q^{(2)}_{-\lambda-\frac{1}{2}}(\cos\theta) = i\tan(\pi\lambda)P_{\lambda-\frac{1}{2}}(\cos\theta), \tag{5.12}$$

which follows from (5.9), we find

$$-\frac{i}{\beta}\int_{-\infty+i\epsilon}^{\infty-i\epsilon} U(\lambda,\beta)Q^{(2)}_{\lambda-\frac{1}{2}}(\cos\theta)\lambda\,d\lambda = \frac{1}{\beta}\int_0^{\infty-i\epsilon} U(\lambda,\beta)P_{\lambda-\frac{1}{2}}(\cos\theta)\tan(\pi\lambda)\lambda\,d\lambda. \tag{5.13}$$

Substituting this in (5.11), we see that the resulting expression is regular down to $\theta = 0$.

By an entirely similar procedure, but employing, instead of (5.9), the identity N [Eq. (C5)],

$$_{-\frac{1}{2}}(-\cos\theta) = ie^{-i\pi\lambda}P_{\lambda-\frac{1}{2}}(\cos\theta) - 2i\cos(\pi\lambda)Q^{(1)}_{\lambda-\frac{1}{2}}(\cos\theta), \tag{5.14}$$

we find

$$f_1(\beta,\theta) = -\frac{i}{\beta}\int_{-\infty-i\epsilon}^{\infty+i\epsilon} U(\lambda,\beta)Q^{(1)}_{\lambda-\frac{1}{2}}(\cos\theta)\lambda\,d\lambda + \frac{2\pi}{\beta}\sum_{m=0}^{\infty}(-1)^m\sum_n \text{residues}\,\{\lambda U(\lambda,\beta)P_{\lambda-\frac{1}{2}}(-\cos\theta) \times \exp[-2i(m+1)\pi\lambda]\}_{-\lambda_n,\lambda_n'}, \tag{5.15}$$

where the residues are now taken at the poles in the lower half-plane, $\lambda = -\lambda_n$, $\lambda = \lambda_n'$. Similarly to (5.13), we have

$$-\frac{i}{\beta}\int_{-\infty-i\epsilon}^{\infty+i\epsilon} U(\lambda,\beta)Q^{(1)}_{\lambda-\frac{1}{2}}(\cos\theta)\lambda\,d\lambda = -\frac{1}{\beta}\int_0^{\infty+i\epsilon} U(\lambda,\beta)P_{\lambda-\frac{1}{2}}(\cos\theta)\tan(\pi\lambda)\lambda\,d\lambda. \tag{5.16}$$

The above expressions could also have been obtained by starting from (3.23) instead of (3.26).

We shall see that the representations (5.11) and (5.13) are appropriate in the lit region for $N > 1$, whereas (5.15) and (5.16) will be employed for $N < 1$. Let us start by considering the behavior of the amplitude in the shadow region for $N > 1$.

B. Behavior for $N > 1$ in the Shadow Region $(\theta - \theta_t \gg \gamma)$

In this region, we shall employ the representations (5.6)–(5.8). According to (5.7), (3.24), (3.5), and (3.8), we have

$$f_{1,\,\text{res}}(\beta,\theta) = \frac{32i}{\pi\beta^3}\sum_{m=1}^{\infty}(-1)^m\sum_n \text{residue}\left\{\frac{c_{1m}(\lambda,\beta,\theta)}{[d(\lambda,\beta)]^2}\right\}_{\lambda_n}, \tag{5.17}$$

where $d(\lambda,\beta)$ is given by (4.38) and

$$c_{1m}(\lambda,\beta,\theta) = \frac{\lambda\exp[i(2m+1)\pi\lambda]P_{\lambda-\frac{1}{2}}(-\cos\theta)}{[H^{(1)}_\lambda(\beta)H^{(2)}_\lambda(\alpha)]^2}. \tag{5.18}$$

A similar expression is valid for $f'_{1,\text{res}}(\beta,\theta)$, with λ_n replaced by $-\lambda_n'$. In both cases, the poles are double poles.

The residue of the expression within curly brackets in (5.17) at a double pole is given by (cf. Ref. 29, Appendix II)

$$\text{residue}\left\{\frac{c_{1m}(\lambda,\beta,\theta)}{[d(\lambda,\beta)]^2}\right\}_{\lambda_n} = \frac{c_{1m}}{\dot{d}^2}\left(\frac{\dot{c}_{1m}}{c_{1m}} - \frac{\ddot{d}}{\dot{d}}\right)_{\lambda_n}, \tag{5.19}$$

where the dots denote partial derivatives with respect to λ and all quantities in the second member are to be evaluated at the poles λ_n.

The evaluation can be carried out by employing the asymptotic expansions N, Eq. (A16) for $H^{(2)}_\lambda(\alpha)$, N, Eq. (C11) for $P_{\lambda-\frac{1}{2}}(-\cos\theta)$ and the expansions for $H^{(1)}_\lambda(\beta)$ and its derivatives given in Appendix A. Retaining only the dominant term in each of these expressions and neglecting corrections of order γ, we find the following final result. [The evaluation of the dominant term in the residue-series contribution at the poles λ_n for an arbitrary term of the Debye expansion will be carried out in Paper II (Appendix C).]

$$f_{1,\text{res}}(\beta,\theta) \approx 2i\frac{e^{i\pi/3}}{\gamma M}\left(\frac{\pi-\theta}{\sin\theta}\right)^{\frac{1}{2}}\exp(2iM\beta) \times\sum_{m=0}^{\infty}(-1)^m\sum_n(a_n')^{-2}\exp\{i\lambda_n[(2m+1)\pi-\theta_t]\} \times\{[(2m+1)\pi-\theta_t]J_0[\lambda_n(\pi-\theta)] + i(\pi-\theta)J_1[\lambda_n(\pi-\theta)]\},\quad \theta-\theta_t\gg\gamma,\quad \theta\le\pi, \tag{5.20}$$

where θ_t is given by (5.1), (5.2), i.e.,

$$\theta_t = 2\cos^{-1}(1/N). \tag{5.21}$$

In particular, for $\pi - \theta \gg \beta^{-1}$, this result can be simplified by inserting the asymptotic expansions for the Bessel functions, which lead to

$$f_{1,\mathrm{res}}(\beta, \theta) \approx -\frac{e^{i\pi/12}}{M}\left(\frac{\gamma}{\pi \sin\theta}\right)^{\frac{1}{2}} \times \exp(2iM\beta)\Big\{\sum_n (a_n')^{-2}\zeta_{1,0}^{+} \exp(i\lambda_n\zeta_{1,0}^{+}) + \sum_{m=1}^{\infty}(-1)^m \sum_n (a_n')^{-2}[\zeta_{1,m}^{+}\exp(i\lambda_n\zeta_{1,m}^{+}) + i\zeta_{1,m}^{-}\exp(i\lambda_n\zeta_{1,m}^{-})]\Big\}, \quad \theta - \theta_t \gg \gamma, \quad \pi - \theta \gg \beta^{-1}, \quad (5.22)$$

where

$$\zeta_{1,m}^{\pm} = 2m\pi - \theta_t \pm \theta, \quad (5.23)$$

as in (4.83) [but note that θ_t is now given by (5.21) instead of (4.76)!].

By analogy with (4.43), this result can be rewritten as follows (cf. also Ref. 29):

$$f_{1,\mathrm{res}}(\beta, \theta) = -\frac{i}{(\sin\theta)^{\frac{1}{2}}}\exp(2iM\beta)\Big\{-i\sum_n D_n^2 D_{21}D_{12} \times \int_0^{\zeta_{1,0}^{+}} \exp(i\lambda_n\zeta_{1,0}^{+})\,d\varphi + \sum_{m=1}^{\infty}(-1)^m \sum_n D_n^2 D_{21}D_{12} \times \Big[\int_0^{\zeta_{1,m}^{-}} \exp(i\lambda_n\zeta_{1,m}^{-})\,d\varphi - i\int_0^{\zeta_{1,m}^{+}} \exp(i\lambda_n\zeta_{1,m}^{+})\,d\varphi\Big]\Big\}, \quad (5.24)$$

where D_n^2 is given by (4.45) and

$$D_{21}D_{12} = 2/M. \quad (5.25)$$

The physical interpretation of these results in terms of diffracted rays is illustrated in Fig. 15. The incident rays tangential to the sphere at T_1 and T_2, after penetrating into the sphere at the critical angle θ_t, reemerge tangentially at T_1' and T_2', respectively, defining the shadow boundary. At the points of emergence, they launch surface waves, travelling from the shadow boundary into the shadow. A typical diffracted ray of this type is $T_2T_2'T_2''B$ in Fig. 15.

However, before penetrating into the sphere, a ray can also describe part of its path as a surface wave. Rays of this type are generated by diffracted rays associated with the first term of the Debye expansion (Fig. 9), which, after critical refraction into the sphere, reemerge as surface waves, to complete the remainder of their path along the surface, before leaving it tangentially in the direction of observation. A typical example is $T_2\hat{T}_2'\hat{T}_2''T_2''B$ in Fig. 14.

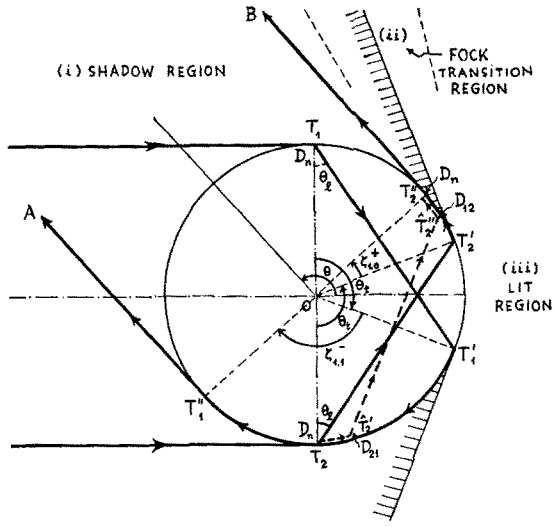

FIG. 15. Physical interpretation of (5.22) and (5.24). The limiting rays T_1T_1' and T_2T_2' that define the shadow boundaries excite surface waves propagating into the shadow, generating the diffracted rays $T_1T_1'T_1''A$ and $T_2T_2'T_2''B$ in the direction θ. The corresponding angles described along the surface are $\zeta_{1,1}^{-}$ and $\zeta_{1,0}^{+}$, respectively. There are infinitely many other possible paths for diffracted rays belonging to this class. One such path, $T_2\hat{T}_2'\hat{T}_2''T_2''B$, corresponding to the same angle $\zeta_{1,0}^{+}$, is shown in broken line. The subdivision into regions is also indicated.

Since the total angle $\zeta_{1,m}^{\pm}$ described along the surface can be broken up into two parts in an infinite number of ways, there is an infinite class of diffracted rays of this type, and the resultant amplitude is the sum of all their contributions. The contribution from all paths such that an angle between φ and $\varphi + d\varphi$ is described before critical refraction is proportional to $d\varphi$. Since the maximum value of φ is the total angle $\zeta_{1,m}^{\pm}$ described, this accounts for the integrals appearing in (5.24).

The factor D_n^2 arises from the excitation of the diffracted wave (e.g., at T_2) and its reconversion into a tangential ray (e.g., at T_2''). The factors D_{21} and D_{12} represent the transmission coefficients of surface waves into the sphere (e.g., at $\hat{T}_2'$) and out of the sphere (e.g., at $\hat{T}_2''$), respectively.

The factor $\exp(2iM\beta)$ represents the phase shift corresponding to the "shortcut" through the sphere (e.g., T_1T_1' or $\hat{T}_2'\hat{T}_2''$). The factor $-i$ corresponds to the phase decrease by $\pi/2$ experienced by a diffracted ray such as $T_1T_1'T_1''A$ as it passes through the pole T_2, which is a focal point for diffracted rays.

According to (5.8), $f_{1,\mathrm{res}}'(\beta, \theta)$ is given by an expression identical to (5.17)–(5.19), except that the residues are now to be evaluated at the poles $-\lambda_n'$. Employing the asymptotic expansion corresponding to (A1) for $H_\lambda^{(2)}(\alpha)$, the Debye asymptotic expansion given in N (Fig. 15), for $H_\lambda^{(1)}(\beta)$, and N [Eq. (C11)] for $P_{\lambda-\frac{1}{2}}(-\cos\theta)$, and keeping only the dominant terms,

we find, with the help of (3.33)–(3.35),

$$f'_{1,\mathrm{res}}(\beta,\theta) \approx 2e^{-i\pi/3}\frac{N^{\frac{7}{3}}}{\gamma M}\left(\frac{\pi-\theta}{\sin\theta}\right)^{\frac{1}{2}}\exp(2M\beta)\sum_{m=0}^{\infty}(-1)^m\sum_n(a'_n)^{-2} \times\exp\{-i\lambda'_n[(2m+1)\pi-2i\cosh^{-1}N]\} \times\{[(2m+1)\pi-2i\cosh^{-1}N]J_0[\lambda'_n(\pi-\theta)] - i(\pi-\theta)J_1[\lambda'_n(\pi-\theta)]\}, \quad \theta-\theta_t\gg\gamma,\quad \theta\le\pi. \tag{5.26}$$

In particular, for $\pi-\theta\gg\alpha^{-1}$, this becomes

$$f'_{1,\mathrm{res}}(\beta,\theta) \approx e^{-i\pi/3}\frac{N^{\frac{11}{6}}}{M}\left(\frac{\gamma}{\pi\sin\theta}\right)^{\frac{1}{2}} \times\exp(2M\beta)\Big\{\sum_n(a'_n)^{-2}(\theta-2i\cosh^{-1}N) \times\exp[-i\lambda'_n(\theta-2i\cosh^{-1}N)-i(\pi/4)] +\sum_{m=1}^{\infty}(-1)^m\sum_n(a'_n)^{-2}[(2m\pi+\theta-2i\cosh^{-1}N) \times\exp[-i\lambda'_n(2m\pi+\theta-2i\cosh^{-1}N)-i(\pi/4)] -(2m\pi-\theta-2i\cosh^{-1}N) \times\exp[-i\lambda'_n(2m\pi-\theta-2i\cosh^{-1}N)+i(\pi/4)]]\Big\}, \quad \theta-\theta_t\gg\gamma,\quad \pi-\theta\gg\alpha^{-1}. \tag{5.27}$$

By comparing these results with (5.20)–(5.22), we see again, as for (4.48), that $f'_{1,\mathrm{res}}(\beta,\theta)$ is exponentially small and may therefore be neglected. For $N<1$, we shall see that the situation is just the reverse; (5.26)–(5.27) represent the analytic continuation of the results for that case.

Finally, let us remark that the damping factor for the least strongly damped terms in (5.22) is proportional to [cf. Eq. (3.29)]:

$$\exp(-\mathrm{Im}\,\lambda_n\zeta^+_{1,0})\sim\exp[-(\sqrt{3}/2)x_n(\theta-\theta_t)/\gamma],$$

so that the residue series is rapidly convergent for $\theta-\theta_t\gg\gamma$.

C. Behavior for $N>1$ in the Lit Region $(\theta_t-\theta\gg\gamma)$

In this region, we employ the representation (5.11), where the integral is to be evaluated by the saddle-point method. For this purpose, the path of integration is first deformed from $(-\infty+i\epsilon,\ \infty-i\epsilon)$ into a new path Γ from $-\rho\infty$ to $\rho\infty$, symmetric about the origin, one half of which is shown in Fig. 14(a). This brings it closer to the steepest descent path, represented by the curve in broken line in Fig. 14(a), which will be discussed below. [The steepest descent path crosses the real axis between $\lambda=0$ and $\lambda=\beta$, at an angle of $-\pi/4$, as will be seen later. It must curve away from the imaginary axis as $|\lambda|\to\infty$, to get into the regions where the integrand goes to zero [cf. Fig. 14, where an additional factor $e^{i\lambda\theta}$ has to be introduced, corresponding to

$$Q^{(2)}_{\lambda-\frac{1}{2}}(\cos\theta)].$$

Its exact shape in the intermediate region is difficult to determine and need not be considered here.]

In this process, we sweep across poles λ'_n and $-\lambda'_n$ with the lower and upper halves of the contour, respectively, so that (5.11) becomes

$$f_1(\beta,\theta)=f_{1,g}(\beta,\theta)+\tilde{f}_{1,\mathrm{res}}(\beta,\theta)+\tilde{f}'_{1,\mathrm{res}}(\beta,\theta), \tag{5.28}$$

where

$$f_{1,g}(\beta,\theta)=-\frac{i}{\beta}\int_\Gamma U(\lambda,\beta)Q^{(2)}_{\lambda-\frac{1}{2}}(\cos\theta)\lambda\,d\lambda, \tag{5.29}$$

$$\tilde{f}_{1,\mathrm{res}}(\beta,\theta)=-\frac{2\pi}{\beta}\sum_{m=0}^{\infty}(-1)^m\sum_n\text{residue} \times\{\lambda UP_{\lambda-\frac{1}{2}}(\cos\theta)\exp[2i(m+1)\pi\lambda]\}_{\lambda_n}, \tag{5.30}$$

$$\tilde{f}'_{1,\mathrm{res}}(\beta,\theta) =-\frac{2\pi}{\beta}\sum_{m=0}^{\infty}(-1)^m\sum_n\text{residue} \times\{\lambda UP_{\lambda-\frac{1}{2}}(\cos\theta)\exp[2i(m+1)\pi\lambda]\}_{-\lambda_{n'}} +\frac{2\pi i}{\beta}\sum_{n=1}^{n_0}\text{residue}\{\lambda UP_{\lambda-\frac{1}{2}}(\cos\theta)\tan(\pi\lambda)\}_{-\lambda_{n'}}, \tag{5.31}$$

where the last term in (5.31) is the sum of the contributions from the $2n_0$ poles swept by the upper and lower halves of the contour together, and we have made use of (5.12).

The residue series (5.30) differs from (5.7) only by the substitution

$$iP_{\lambda-\frac{1}{2}}(-\cos\theta)\to e^{i\pi\lambda}P_{\lambda-\frac{1}{2}}(\cos\theta).$$

Accordingly, (5.20) is replaced by

$$\tilde{f}_{1,\mathrm{res}}(\beta,\theta) \approx\frac{2e^{i\pi/3}}{\gamma M}\left(\frac{\theta}{\sin\theta}\right)^{\frac{1}{2}}\exp(2iM\beta)\sum_{m=0}^{\infty}(-1)^m\sum_n(a'_n)^{-2} \times\exp\{i\lambda_n[(2m+2)\pi-\theta_t]\} \times\{[(2m+2)\pi-\theta_t]J_0(\lambda_n\theta)+i\theta J_1(\lambda_n\theta)\}, \quad \theta_t-\theta\gg\gamma,\quad \theta\gtrsim 0. \tag{5.32}$$

In particular, for $\theta \gg \beta^{-1}$, this becomes

$$\tilde{f}_{1,\mathrm{res}}(\beta, \theta) \approx -\frac{e^{i\pi/3}}{M}\left(\frac{\gamma}{\pi \sin\theta}\right)^{\frac{1}{2}} \exp(2iM\beta) \cdot \times \sum_{m=1}^{\infty}(-1)^m \sum_n (a_n')^{-2}[\zeta_{1,m}^{+} \exp(i\lambda_n \zeta_{1,m}^{+} - i(\pi/4)) + \zeta_{1,m}^{-} \exp(i\lambda_n \zeta_{1,m}^{-} + i(\pi/4))], \quad \theta_t - \theta \gg \gamma, \quad \theta \gg \beta^{-1}. \quad (5.33)$$

This differs from (5.22) only by the omission of the series in $\zeta_{1,0}^{+}$, which would not converge rapidly in this region. Physically, this omission corresponds to the fact that, in order to reach a direction θ in the lit region, a surface wave excited at T_2' (Fig. 15) must describe an angle $\zeta_{1,1}^{+} = 2\pi - \zeta_{1,0}^{+}$, rather than $\zeta_{1,0}^{+}$.

In the last residue series of (5.31), we can apply the approximation

$$\tan(\pi\lambda) \approx i,$$

valid in the neighborhood of the poles $-\lambda_n'$. We then find

$$\tilde{f}_{1,\mathrm{res}}'(\beta, \theta) \approx -2e^{i\pi/6}\frac{N^{\frac{7}{3}}}{\gamma M}\left(\frac{\theta}{\sin\theta}\right)^{\frac{1}{2}} \times \exp(2M\beta)\left\{\sum_{m=1}^{\infty}(-1)^m \sum_n (a_n')^{-2} \times \exp[-i\lambda_n'(2m\pi - 2i\cosh^{-1}N)] \times [(2m\pi - 2i\cosh^{-1}N)J_0(\lambda_n'\theta) - i\theta J_1(\lambda_n'\theta)] + i\sum_{n=1}^{n_0}(a_n')^{-2}\exp(-2\lambda_n'\cosh^{-1}N) \times [2\cosh^{-1}N J_0(\lambda_n'\theta) + \theta J_1(\lambda_n'\theta)], \quad \theta_t - \theta \gg \gamma, \quad \theta \geq 0, \quad (5.34)$$

which is again negligible as compared with $\tilde{f}_{1,\mathrm{res}}(\beta, \theta)$ [cf. Eq. (5.27)].

Finally, let us evaluate $f_{1,g}(\beta, \theta)$. The integral (5.29) has a saddle point on the real axis, between $\lambda = 0$ and $\lambda = \beta$, so that we may employ asymptotic expansions for the integrand similar to those employed in connection with (4.31). With the change of variables

$$\lambda = \beta \sin w_1 = \alpha \sin w_2, \quad (5.35)$$

we find

$$f_{1,g}(\beta, \theta) = -2e^{i\pi/4}N\left(\frac{2\beta}{\pi \sin\theta}\right)^{\frac{1}{2}}\int B(w_1, \beta, \theta) \times \exp[i\beta\delta(w_1, \theta)]\, dw_1, \quad (5.36)$$

where

$$\delta(w_1, \theta) = 2[N\cos w_2 - \cos w_1 + (w_2 - w_1 + \theta/2)\sin w_1], \quad (5.37)$$

$$B(w_1, \beta, \theta) = \frac{(\sin w_1)^{\frac{1}{2}}\cos^2 w_1 \cos w_2}{(N\cos w_2 + \cos w_1)^2} \times \left\{1 + \frac{i}{\beta}\left[\frac{1}{4\cos w_1}(1 + \tfrac{5}{3}\tan^2 w_1) - \frac{1}{4N\cos w_2}(1 + \tfrac{5}{3}\tan^2 w_2) - \frac{\tan^2 w_2}{\cos^2 w_1} \times (N\cos w_2 - \cos w_1) - \frac{\cot\theta}{8\sin w_1}\right] + \mathcal{O}(\beta^{-2})\right\}, \quad (5.38)$$

and the path of integration is the image of Γ [Fig. 14(a)] in the w_1 plane.

Taking into account the relation

$$dw_2/dw_1 = \cos w_1/(N\cos w_2), \quad (5.39)$$

we find from (5.37) that the location of the saddle point is determined by

$$\bar{w}_1 = \theta_1, \quad \bar{w}_2 = \theta_2, \quad (5.40)$$

where

$$\theta_1 - \theta_2 = \theta/2, \quad \sin\theta_1 = N\sin\theta_2. \quad (5.41)$$

The corresponding saddle point in the λ plane is

$$\bar{\lambda} = kp = \beta\sin\theta_1, \quad (5.42)$$

where p is the impact parameter of the incident ray AB (Fig. 16) which, after two refractions (angles θ_1, θ_2) and no reflection, emerges in the direction θ, according to the laws of geometrical optics.

It is possible to solve (5.41) to express $\sin\theta_1$ directly in terms of θ:

$$\sin\theta_1 = (N/\tau)\sin(\theta/2), \quad (5.43)$$

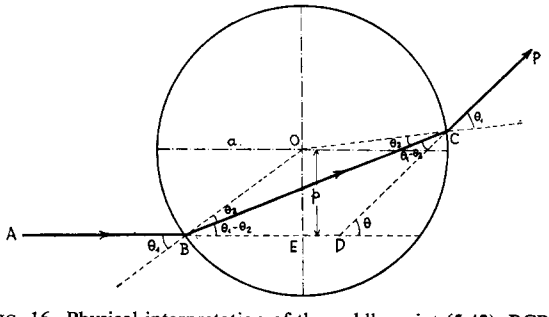

FIG. 16. Physical interpretation of the saddle point (5.42). BCP is the directly transmitted ray corresponding to the incident ray AB according to geometrical optics. The impact parameter associated with this ray is $\overline{OE} = p = \bar{\lambda}/k = a\sin\theta_1$, where $\theta = 2(\theta_1 - \theta_2)(N > 1)$.

where

$$\tau = (1 - 2N\cos(\theta/2) + N^2)^{\frac{1}{2}}. \qquad (5.44)$$

The steepest descent path crosses the real w_1 axis at an angle of $-\pi/4$. The corresponding path in the λ plane is represented by the curve in broken line in Fig. 14(a).

The saddle-point evaluation of (5.36) can now proceed by applying (4.34). A straightforward but rather lengthy calculation finally leads to the result

$$f_{1,g}(\beta,\theta) = -\left(\frac{\sin\theta_1}{\sin\theta}\right)^{\frac{1}{2}} \frac{(2N\cos\theta_1\cos\theta_2)^{\frac{3}{2}}}{(\cos\theta_1 + N\cos\theta_2)^2} \times \frac{\exp[2i\beta(N\cos\theta_2 - \cos\theta_1)]}{(N\cos\theta_2 - \cos\theta_1)^{\frac{1}{2}}} \times \left\{1 - \frac{i\mathcal{F}(\theta)}{16\beta\cos\theta_1} + \mathcal{O}(\beta^{-2})\right\}, \quad \theta_t - \theta \gg \gamma, \qquad (5.45)$$

where

$$\mathcal{F}(\theta) = 2\cot\theta_1\left[\cot\theta - \frac{\cot\theta_1}{2(1-\chi)}\right] - \frac{9}{1-\chi} + 15\chi - 6 + (\chi-1)(8\chi^2 + 5\chi + 8)\tan^2\theta_1, \qquad (5.46)$$

and [cf. Eq. (5.39)]:

$$\chi = \cos\theta_1/(N\cos\theta_2). \qquad (5.47)$$

Let us now discuss the domain of validity of (5.45). It must clearly fail near the shadow boundary, $\theta \to \theta_t$, because the Debye asymptotic expansions for $H_\lambda^{(1,2)}(\beta)$ employed in (5.36)–(5.38) are then no longer valid. We must have $\beta - \tilde{\lambda} \gg \beta^{\frac{1}{3}}$. According to (5.41), this implies $\theta_t - \theta \gg \gamma$, which is the condition given in (5.45). The same condition is found from the requirement that the first correction term $\mathcal{F}(\theta)/\beta\cos\theta_1$ in (5.45) must remain small as θ_1 approaches $\pi/2$.

At the other extreme, near $\theta = 0$, the derivation of (5.45) is again unjustified, because the asymptotic expansion N, Eq. (C7), for $Q^{(2)}_{\lambda-\frac{1}{2}}(\cos\theta)$ in (5.29) is no longer valid. However, it is found that (5.45) approaches a finite limit as $\theta \to 0$, namely,

$$f_{1,g}(\beta,0) = -\frac{2N^2}{(N-1)(N+1)^2}\exp[2i(N-1)\beta] \times \left\{1 + \frac{i}{\beta}\left[1 - \frac{1}{N} + \frac{1}{2(N-1)}\right] + \mathcal{O}(\beta^{-2})\right\}. \qquad (5.48)$$

The proper way to evaluate $f_{1,g}(\beta,\theta)$ near $\theta = 0$ is to apply the transformation (5.13) to (5.29), to substitute $P_{\lambda-\frac{1}{2}}(\cos\theta)$ by N, Eq. (C9), expanding the integrand around $\lambda = 0$, from where the dominant contribution arises, and to employ the techniques developed in N (Sec. IX.C and Appendix F). The result for $\theta = 0$ is identical to (5.48), showing that (5.45) is, in fact, uniformly valid down to $\theta = 0$ [a similar situation was found for (4.35)].

The result (5.45) depends implicitly on θ through (5.41). The dependence can be made explicit with the help of (5.43). The final result is

$$f_{1,g}(\beta,\theta) = -\frac{2N^2}{(N^2-1)^2} \times \frac{[(N\cos(\theta/2) - 1)(N - \cos(\theta/2))]^{\frac{3}{2}}}{(\cos(\theta/2))^{\frac{1}{2}}} \frac{\exp(2i\tau\beta)}{\tau^2} \times \left\{1 - \frac{i\tau}{16\beta(N\cos(\theta/2) - 1)}\left[\frac{2(N\cos(\theta/2) - 1)}{N\sin(\theta/2)} \times \left(\cot\theta - \frac{(N\cos(\theta/2) - 1)(N - \cos(\theta/2))}{2\tau^2\sin(\theta/2)}\right) - \frac{9}{1-\chi} + 15\chi - 6 + 8(\chi-1) \times (\chi^2 + \tfrac{5}{8}\chi + 1)\frac{N^2\sin^2(\theta/2)}{(N\cos(\theta/2) - 1)^2}\right] + \mathcal{O}(\beta^{-2})\right\}, \quad \theta_t - \theta \gg \gamma, \quad \theta \geq 0, \qquad (5.49)$$

where τ is given by (5.44) and [cf. Eq. (5.47)]

$$\chi = \frac{N\cos(\theta/2) - 1}{N(N - \cos(\theta/2))}. \qquad (5.50)$$

The dominant term, represented by the factor outside of the curly brackets, agrees with the result found by Rubinow [Ref. 12, Eq. (53)]. As observed by Rubinow, the corresponding contribution to the differential scattering cross section,

$$\left(\frac{d\sigma}{d\Omega}\right)_1 = a^2|f_{1,g}(\beta,\theta)|^2 = \frac{4a^2N^4}{\cos(\theta/2)(N^2-1)^4} \times \frac{[(N\cos(\theta/2) - 1)(N - \cos(\theta/2))]^3}{(N^2 - 2N\cos(\theta/2) + 1)^2}, \qquad (5.51)$$

differs from the prediction of classical mechanics for square-well scattering only by a factor

$$t = (T_{21}T_{12})^2 = \left[\frac{2\cos\theta_1}{(\cos\theta_1 + N\cos\theta_2)}\frac{2N\cos\theta_2}{(\cos\theta_1 + N\cos\theta_2)}\right]^2 = \frac{16N^2}{(N^2-1)^4}[(N\cos(\theta/2) - 1)(N - \cos(\theta/2))]^2, \qquad (5.52)$$

which represents the transmissivity of the well (T_{21} and T_{12} are given by the well-known Fresnel formulas).

However, it must be kept in mind that this is by no means the only quantum effect: there are other contributions to the differential cross section from the remaining terms of the Debye expansion (in particular, from the forward diffraction peak in f_0), as well as interference terms.

D. Behavior for $N > 1$ in the Penumbra Region ($|\theta - \theta_t| \lesssim \gamma$)

Let us now go over to the transition region (ii) of (5.3), $|\theta - \theta_t| \lesssim \gamma$ (penumbra). In this region, as was mentioned following (5.47), the above evaluation of $f_{1,g}(\beta, \theta)$ breaks down, because the Debye expansions for $H_\lambda^{(1,2)}(\beta)$ employed in (5.36)–(5.38) are no longer valid. With this single exception, all the results derived in Sec. 5C remain valid in the present region, so that we only need to consider $f_{1,g}$.

Since the dominant contribution to (5.29) in the penumbra region arises from the domain $|\lambda| - \beta = O(\beta^{\frac{1}{3}})$, the appropriate expansions for $H_\lambda^{(1,2)}(\beta)$ in (3.24), as well as for $[1\,\beta]$ and $[2\,\beta]$ in $T_{21}T_{12}$, are those given in Appendix A and already employed in Sec. 4D. We shall keep only the dominant term in each expansion. For $H_\lambda^{(2)}(\beta)/H_\lambda^{(1)}(\beta)$, the result is given by (4.54); for T_{21}, by (3.5) and (4.58), and we find

$$T_{12} \approx 2. \tag{5.53}$$

Finally, we get

$$f_{1,g}(\beta, \theta) \approx -\frac{e^{5i\pi/12}\gamma}{\pi\beta M(2\pi \sin\theta)^{\frac{1}{2}}} \times \int \exp\left[2i((\alpha^2 - \lambda^2)^{\frac{1}{2}} - \lambda \cos^{-1}(\lambda/\alpha)) + i\lambda\theta\right] \frac{\sqrt{\lambda}\, d\lambda}{A^2(\zeta)}, \tag{5.54}$$

where ζ and $A(\zeta)$ are given by (4.55) and (4.56), respectively. The path of integration in the ζ plane is chosen to be the same as in (4.65)–(4.66), so that the dominant contribution arises from $|\zeta| \lesssim 1$. Accordingly, the integrand may be expanded around $\lambda = \beta$. This leads to the final expression

$$f_{1,g}(\beta, \theta) \approx -2\frac{e^{i\pi/4}}{M}\frac{\exp\left[2iM\beta + i\beta(\theta - \theta_t)\right]}{(2\pi\beta \sin\theta)^{\frac{1}{2}}} f(s), \qquad |\theta - \theta_t| \lesssim \gamma, \tag{5.55}$$

where

$$s = (\theta - \theta_t)/\gamma \tag{5.56}$$

and

$$f(s) = \frac{e^{i\pi/6}}{2\pi}\int_\Gamma \frac{\exp(is\zeta)}{A^2(\zeta)}\, d\zeta \tag{5.57}$$

is the Fock function already defined in N [Eq. (8.23)]. The path Γ runs from $e^{2i\pi/3}\infty$ to 0 and from 0 to ∞ (cf. N, Fig. 10).

Thus, we find a normal (Fock-type) transition from light to shadow, described by $f(s)$. In the shadow region, $s \gg 1$, (5.55) becomes, according to N [Eq. (8.24)],

$$f_{1,g}(\beta, \theta) \approx -\frac{e^{i\pi/12}}{M}\left(\frac{\gamma}{\pi \sin\theta}\right)^{\frac{1}{2}} \exp(2iM\beta) \times \sum_n (a_n')^{-2}(\theta - \theta_t) \exp\left[i(\beta + e^{i\pi/3}x_n/\gamma)(\theta - \theta_t)\right], \qquad \theta - \theta_t \gg \gamma, \tag{5.58}$$

which, according to (3.29) and (5.23), corresponds to the residue series in $\zeta_{1,0}^+$ in (5.22) as it should [see the remarks following (5.33)].

On the other hand, for $s < 0$, $|s| \gg 1$, the Fock function (5.57) can be evaluated by the saddle-point method, with the following result:

$$f(s) \approx \sqrt{\pi}\, e^{-i\pi/4}|s|^{\frac{3}{2}} \exp\left[-(i/12)s^3\right], \qquad s < 0, \quad |s| \gg 1. \tag{5.59}$$

Substituting this in (5.55), we find, in the lit region,

$$f_{1,g}(\beta, \theta) \approx -\frac{(\theta_t - \theta)^{\frac{3}{2}}}{M(\sin\theta)^{\frac{1}{2}}} \times \exp\left\{2iM\beta - i\beta\left[(\theta_t - \theta) - \tfrac{1}{24}(\theta_t - \theta)^3\right]\right\}, \qquad \theta_t - \theta \gg \gamma. \tag{5.60}$$

Again, this agrees with the dominant term of (5.49), provided that, as in previous cases, we do not try to push the Fock-function representation too far into the lit region: its domain of validity is just sufficient to produce a smooth transition.

Finally, since $f(0) = 1$ [cf. N, Eq. (8.26)], we find, at the shadow boundary,

$$f_{1,g}(\beta, \theta_t) \approx -\frac{e^{i\pi/4}N}{(\pi\beta)^{\frac{1}{2}}M^{\frac{3}{2}}}\exp(2iM\beta). \tag{5.61}$$

This completes the evaluation of the second term of the Debye expansion for $N > 1$.

E. Behavior for $N < 1$

For $N < 1$, according to Fig. 13(b), we again have to consider three regions: shadow, penumbra, and lit region, defined precisely as in (5.3) [however, θ_t is now given by (4.76)!]. We shall see that the width of the penumbra region is given by

$$\Delta\theta \sim \gamma' = (2/\alpha)^{\frac{1}{3}} = \gamma/N^{\frac{1}{3}}. \tag{5.62}$$

Let us consider first the shadow region, $\theta - \theta_t \gg \gamma'$. The amplitude is again a pure residue series, given by (5.6)–(5.8), and the evaluation of the residues again proceeds according to (5.17)–(5.19). For $f'_{1,\mathrm{res}}(\beta, \theta)$, the main difference with respect to (5.26) is that $H_\lambda^{(1,2)}(\beta)$ is now given by N, Eq. (A16). Accordingly,

the result differs from (5.26) only by the substitutions [cf. Eqs. (4.46) and (4.81)]:

$$M \to -iM', \quad \cosh^{-1} N \to -i \cos^{-1} N = -i\theta_t/2. \tag{5.63}$$

Thus, we find

$$f'_{1,\mathrm{res}}(\beta, \theta) \approx 2e^{i\pi/6} \frac{N^2}{\gamma' M'} \left(\frac{\pi - \theta}{\sin \theta}\right)^{\frac{1}{2}} \exp(-2iM'\beta) \times \sum_{m=0}^{\infty} (-1)^m \sum_n (a'_n)^{-2} \exp\{-i\lambda'_n[(2m+1)\pi - \theta_t]\} \times \{[(2m+1)\pi - \theta_t] J_0[\lambda'_n(\pi - \theta)] - i(\pi - \theta) J_1[\lambda'_n(\pi - \theta)]\}, \quad \theta - \theta_t \gg \gamma', \quad \theta \leq \pi. \tag{5.64}$$

[The evaluation of the dominant term in the residue-series contribution at the poles λ'_n for an arbitrary term of the Debye expansion will be carried out in Paper II (Appendix D).]

In particular, for $\pi - \theta \gg \alpha^{-1}$, we find [cf. Eq. (5.27)]

$$f'_{1,\mathrm{res}}(\beta, \theta) \approx \frac{e^{-i\pi/12} N^2}{M'} \left(\frac{\gamma'}{\pi \sin \theta}\right)^{\frac{1}{2}} \exp(-2iM'\beta) \times \left\{ \sum_n (a'_n)^{-2} \zeta^+_{1,0} \exp(-i\lambda'_n \zeta^+_{1,0}) + \sum_{m=1}^{\infty} (-1)^m \sum_n (a'_n)^{-2} \times [\zeta^+_{1,m} \exp(-i\lambda'_n \zeta^+_{1,m}) - i\zeta^-_{1,m} \exp(-i\lambda'_n \zeta^-_{1,m})] \right\}, \quad \theta - \theta_t \gg \gamma', \quad \pi - \theta \gg \alpha^{-1}. \tag{5.65}$$

By comparing this result with (4.82), we see that it can be rewritten as follows:

$$f'_{1,\mathrm{res}}(\beta, \theta) \approx 2e^{i\pi/4} \frac{N^2}{M'} \left(\frac{2\pi}{N\beta \sin \theta}\right)^{\frac{1}{2}} \exp(-2iM'\beta) \times \left\{ \sum_n \mathcal{D}_n \zeta^+_{1,0} \exp(-i\lambda'_n \zeta^+_{1,0}) + \sum_{m=1}^{\infty} (-1)^m \sum_n [\mathcal{D}_n \zeta^+_{1,m} \exp(-i\lambda'_n \zeta^+_{1,m}) - i\mathcal{D}_n \zeta^-_{1,m} \exp(-i\lambda'_n \zeta^-_{1,m})] \right\}, \quad \theta - \theta_t \gg \gamma', \quad \pi - \theta \gg \alpha^{-1}, \tag{5.66}$$

where

$$\mathcal{D}_n = e^{-i\pi/3}/2\pi a'^2_n \gamma'. \tag{5.67}$$

Each term in (5.66) differs from the corresponding term in (4.82) only by a factor

$$\mathcal{D}_n \zeta^{\pm}_{1,m} = \mathcal{D}_n \int_0^{\zeta_{1,m}^{\pm}} d\varphi. \tag{5.68}$$

This result can be physically interpreted as follows [Figs. 11(a) and 17]. The diffracted rays shown in Fig. 11(a) travel along the *inner* side of the surface, so that they cannot make any "shortcuts" such as those found for $N > 1$ (Fig. 15). Their only possible interaction with the surface is to produce a ray in the exterior region leaving the surface at the critical angle,

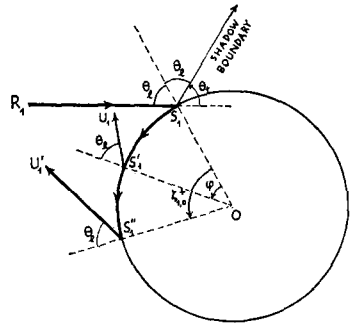

FIG. 17. Physical interpretation of the diffracted rays in (5.66); $S_1 S'_1 S''_1 U'_1$ is a typical diffracted ray of this class.

such as $S'_1 U_1$ in Figs. 11(a) and 17. Each time a surface wave associated with the first term of the Debye expansion does this, it excites further surface waves by a kind of "internal diffraction," and these are precisely the contributions found in (5.66). They have had one additional interaction with the surface as compared with (4.82), in agreement with the general physical interpretation of the Debye expansion given in Sec. 3A. We see that $\mathcal{D}_n$ represents the *internal diffraction coefficient*.

A typical diffracted ray of this class is $S_1 S'_1 S''_1 U'_1$ in Fig. 17. The angle φ described by the "parent" surface wave up to the point of excitation S'_1 can take any value between 0 and $\zeta^{\pm}_{1,m}$, so that we again have an infinity of possible paths and must sum all their contributions. This leads to the integral in (5.68) [cf. the similar discussion for (5.24)].

To obtain the contribution from the residue series at the poles λ_n, it suffices to analytically continue (5.22) to $N < 1$, by making the substitutions

$$M \to -iM', \quad \cos^{-1} \frac{1}{N} \to -i \cosh^{-1} \frac{1}{N}. \tag{5.69}$$

This leads to

$$f_{1,\mathrm{res}}(\beta, \theta) \approx -\frac{e^{i\pi/3}}{M'} \left(\frac{\gamma}{\pi \sin \theta}\right)^{\frac{1}{2}} \exp(2M'\beta) \times \left(\sum_n (a'_n)^{-2} (\theta + 2i \cosh^{-1}(1/N)) \times \exp[i\lambda_n(\theta + 2i \cosh^{-1}(1/N))] + \sum_{m=1}^{\infty} (-1)^m \sum_n (a'_n)^{-2} \left\{ (2m\pi + \theta + 2i \cosh^{-1}(1/N)) \times \exp[i\lambda_n(2m\pi + \theta + 2i \cosh^{-1}(1/N))] + i(2m\pi - \theta + 2i \cosh^{-1}(1/N)) \times \exp[i\lambda_n(2m\pi - \theta + 2i \cosh^{-1}(1/N))] \right\} \right), \quad \theta - \theta^t \gg \gamma', \quad \pi - \theta \gg \alpha^{-1}. \tag{5.70}$$

These terms play the same role here that (5.27) played for $N > 1$. We can regard them as arising from

refraction of the surface waves excited by the tangentially incident rays (Fig. 9), which, as we have seen in Sec. 4E, are still given by (4.41) for $N < 1$. However, this is refraction with grazing angle of incidence, i.e., well beyond the critical angle, so that the corresponding angle of refraction is complex, corresponding to evanescent waves in the optically rare medium, as in total reflection. This gives rise to strong damping and makes (5.70) exponentially small, and therefore negligible, in comparison with (5.65), which, consequently, describes the total amplitude in the shadow region.

Thus, for the second term of the Debye expansion, the poles λ_n and λ'_n interchange their roles as we go over from $N > 1$ to $N < 1$. For $N > 1$ ($N < 1$), the contribution from the poles $\lambda_n(\lambda'_n)$ is dominant, and that from the other set of poles is exponentially small in comparison, although both contributions can be analytically continued in N from one case to the other. The two sets of poles play complementary roles, and λ'_n is just as important for $N < 1$ as λ_n is for $N > 1$.

Let us consider next the lit region, $\theta_t - \theta \gg \gamma'$. In this region, we must employ the representation (5.15)–(5.16) instead of (5.11)–(5.13). In order to apply the saddle-point method, the path of integration in (5.15) is first deformed into the path Γ shown in Fig. 14(b). In this process, it sweeps across poles λ_n and $-\lambda_n$ (say $2n_0$ of them), so that we get [cf. Eq. (5.28)]

$$f_1(\beta, \theta) = f_{1,g}(\beta, \theta) + \tilde{f}_{1,\mathrm{res}}(\beta, \theta) + \tilde{f}'_{1,\mathrm{res}}(\beta, \theta), \quad (5.71)$$

with

$$f_{1,g}(\beta, \theta) = -\frac{i}{\beta}\int_\Gamma U(\lambda, \beta) Q^{(1)}_{\lambda-\frac{1}{2}}(\cos\theta)\lambda\, d\lambda, \quad (5.72)$$

$$\tilde{f}_{1,\mathrm{res}}(\beta, \theta) = \frac{2\pi}{\beta}\left\{-i\sum_{n=1}^{n_0}\text{residue}\,[\lambda U P_{\lambda-\frac{1}{2}}(\cos\theta)\tan(\pi\lambda)]_{\lambda_n} + \sum_{m=0}^{\infty}(-1)^m\sum_n \text{residue}\,[\lambda U P_{\lambda-\frac{1}{2}}(\cos\theta)e^{2i(m+1)\pi\lambda}]_{\lambda_n}\right\}, \quad (5.73)$$

$$\tilde{f}'_{1,\mathrm{res}}(\beta, \theta) = \frac{2\pi}{\beta}\sum_{m=0}^{\infty}(-1)^m\sum_n \text{residue} \times \{\lambda U P_{\lambda-\frac{1}{2}}(\cos\theta)\exp[2i(m+1)\pi\lambda]\}_{-\lambda_n'}. \quad (5.74)$$

We now find

$$\tilde{f}'_{1,\mathrm{res}}(\beta, \theta) \approx 2e^{i\pi/6}\frac{N^2}{\gamma' M'}\left(\frac{\theta}{\sin\theta}\right)^{\frac{1}{2}}\exp(-2iM'\beta) \times \sum_{m=0}^{\infty}(-1)^m\sum_n (a'_n)^{-2}\exp\{-i\lambda'_n[2(m+1)\pi - \theta_t]\} \times \{i[2(m+1)\pi - \theta_t]J_0(\lambda'_n\theta) + \theta J_1(\lambda'_n\theta)\}, \quad \theta_t - \theta \gg \gamma', \quad \theta \geq 0. \quad (5.75)$$

In particular, for $\theta \gg \alpha^{-1}$,

$$\tilde{f}'_{1,\mathrm{res}}(\beta, \theta) \approx \frac{e^{-i\pi/12}N^2}{M'}\left(\frac{\gamma'}{\pi\sin\theta}\right)^{\frac{1}{2}}\exp(-2iM'\beta) \times \sum_{m=1}^{\infty}(-1)^m\sum_n (a'_n)^{-2}[\zeta^+_{1,m}\exp(-i\lambda'_n\zeta^+_{1,m}) - i\zeta^-_{1,m}\exp(-i\lambda'_n\zeta^-_{1,m})], \quad \theta_t - \theta \gg \gamma', \quad \theta \gg \alpha^{-1}, \quad (5.76)$$

which differs from (5.65) only by the omission of the series in $\zeta^+_{1,0}$, as it should [see the comments following (5.33)].

On the other hand,

$$\tilde{f}_{1,\mathrm{res}}(\beta, \theta) \approx \frac{2e^{i\pi/12}}{\gamma M'}\left(\frac{\theta}{\sin\theta}\right)^{\frac{1}{2}}\exp(2M'\beta) \times \left\{\sum_{n=1}^{n_0}(a'_n)^{-2}\exp(-2\lambda_n\cosh^{-1}(1/N)) \times [2\cosh^{-1}(1/N)J_0(\lambda_n\theta) + \theta J_1(\lambda_n\theta)] + \sum_{m=1}^{\infty}(-1)^m\sum_n (a'_n)^{-2} \times \exp(2im\pi\lambda_n - 2\lambda_n\cosh^{-1}(1/N)) \times [(2im\pi - 2\cosh^{-1}(1/N))J_0(\lambda_n\theta) - \theta J_1(\lambda_n\theta)]\right\}, \quad \theta_t - \theta \gg \gamma', \quad \theta \geq 0, \quad (5.77)$$

which is negligible in comparison with $\tilde{f}'_{1,\mathrm{res}}(\beta, \theta)$.

Finally, let us consider the "geometrical-optic" contribution $f_{1,g}(\beta, \theta)$, given by (5.72). This differs from (5.29) by having $Q^{(1)}_{\lambda-\frac{1}{2}}$ instead of $Q^{(2)}_{\lambda-\frac{1}{2}}$ and by the different path of integration. With the same change of variables (5.35), the saddle point is found to be determined by [cf. Eqs. (5.40) and (5.41)]:

$$\bar{w}_1 = \theta_1, \quad \bar{w}_2 = \theta_2, \quad (5.78)$$

where

$$\theta_2 - \theta_1 = \frac{\theta}{2}, \quad \sin\theta_1 = N\sin\theta_2. \quad (5.79)$$

This agrees with the laws of geometrical optics for $N < 1$ ($\theta_1 < \theta_2$), and it is the reason why it was necessary to employ the representation (5.15) instead of (5.11).

The steepest descent path now crosses the real axis at an angle of $\pi/4$ [Fig. 14(b)]. Thus, we have to employ N, Eq. (6.12), rather than N, Eq. (6.21). Making appropriate changes in the calculation that led to (5.45), we finally obtain

$$f_{1,g}(\beta, \theta) = \left(\frac{\sin\theta_1}{\sin\theta}\right)^{\frac{1}{2}}\frac{(2N\cos\theta_1\cos\theta_2)^{\frac{3}{2}}}{(\cos\theta_1 + N\cos\theta_2)^2} \times \frac{\exp[-2i\beta(\cos\theta_1 - N\cos\theta_2)]}{(\cos\theta_1 - N\cos\theta_2)^{\frac{1}{2}}} \times \left\{1 - \frac{i\mathcal{F}(\theta)}{16\beta\cos\theta_1} + O(\beta^{-2})\right\}, \quad (5.80)$$

where

$$\mathcal{F}(\theta) = 2\cot\theta_1\left[\frac{\cot\theta_1}{2(\chi-1)} - \cot\theta\right] + \frac{9}{\chi-1} + 15\chi - 6 + 8(\chi-1)(\chi^2 + \tfrac{5}{8}\chi + 1)\tan^2\theta_1, \quad (5.81)$$

and χ is still given by (5.47).

With the help of (5.43), this result can also be expressed directly in terms of the angle θ. We find

$$f_{1,g}(\beta,\theta) = \frac{2N^2}{(1-N^2)^2}\frac{[(1-N\cos(\theta/2))(\cos(\theta/2)-N)]^{\frac{3}{2}}}{(\cos(\theta/2))^{\frac{1}{2}}}\frac{\exp(-2i\tau\beta)}{\tau^2}$$
$$\times\left(1 - \frac{i\tau}{16\beta(1-N\cos(\theta/2))}\left\{\frac{2(1-N\cos(\theta/2))}{N\sin(\theta/2)}\left[\frac{(1-N\cos(\theta/2))(\cos(\theta/2)-N)}{2\tau^2\sin(\theta/2)} - \cot\theta\right]\right.\right.$$
$$\left.\left. + \frac{9}{\chi-1} + 15\chi - 6 + 8(\chi-1)(\chi^2+\tfrac{5}{8}\chi+1)\frac{N^2\sin^2(\theta/2)}{(1-N\cos(\theta/2))^2}\right\} + \mathcal{O}(\beta^{-2})\right),$$
$$\theta_t - \theta \gg \gamma', \quad \theta \geq 0, \quad (5.82)$$

where τ and χ are again given by (5.44) and (5.50), respectively. The result is also uniformly valid down to $\theta = 0$. It differs from (5.49) only by the over-all sign factor and by the replacement $\tau \to -\tau$. This gives the correct continuation for $N < 1$, as can be verified by checking that, for $\theta = 0$, Eq. (5.82) becomes identical to (5.48).

The last region that remains to be considered is the penumbra region, $|\theta - \theta_t| \lesssim \gamma'$. In this region, we must employ the expansions of Appendix A for $H_\lambda^{(1,2)}(\alpha)$. By a procedure entirely similar to that which led to (5.55), we find

$$f_{1,g}(\beta,\theta) \approx 2e^{-i\pi/4}\frac{N^{\frac{3}{2}}}{M'}$$
$$\times \frac{\exp[-2iM'\beta - iN\beta(\theta-\theta_t)]}{(2\pi\beta\sin\theta)^{\frac{1}{2}}}\bar{f}(s'), \quad |\theta-\theta_t| \lesssim \gamma', \quad (5.83)$$

where

$$s' = (\alpha/2)^{\frac{1}{3}}(\theta-\theta_t) = (\theta-\theta_t)/\gamma' \quad (5.84)$$

and

$$\bar{f}(s) = \frac{e^{-i\pi/6}}{2\pi}\int_{\bar{\Gamma}}\frac{\exp(-is\zeta)}{\bar{A}^2(\zeta)}\,d\zeta, \quad (5.85)$$

where $\bar{A}(\zeta)$ is defined by (4.56) and the path $\bar{\Gamma}$ consists of a straight line from $e^{-2i\pi/3}\infty$ to 0 and the real axis from 0 to ∞. By comparing (5.85) with (5.57), we find that they are complex conjugate:

$$\bar{f}(s) = [f(s)]^* \quad (5.86)$$

The behavior of $\bar{f}(s)$ for $|s| \gg 1$ therefore follows immediately from the corresponding behavior of $f(s)$. In this way, we also find that (5.83) gives rise to a smooth transition between shadow and lit region. Note that it is a normal (Fock-type) transition, similar to that found for $N > 1$. This behavior differs from that found in the same region for the first term of the Debye expansion [cf. Eq. (4.101)]. As has already been mentioned, all terms in the Debye expansion give rise to the same transition region for $N < 1$, so that the behavior of the complete amplitude within this region is quite complicated.

This concludes the discussion of the behavior of the second term in the Debye expansion. We see that the modified Watson transformation indeed enables us to determine the high-frequency behavior of the first two terms in any direction θ, both for $N > 1$ and for $N < 1$. The behavior of the remaining terms will be discussed in Paper II.

ACKNOWLEDGMENTS

Part of the research described in this paper was carried out during the author's stay at the Institute for Advanced Study, in 1964–65. The author is indebted to the late Professor J. R. Oppenheimer for his hospitality and encouragement. He also wishes to thank Professor E. Wolf for his hospitality at the University of Rochester, where the remainder of the work was performed.

This research was partially supported by grants from the National Science Foundation, the Air Force Office of Scientific Research, and the Air Force Cambridge Research Laboratories.

APPENDIX A: ASYMPTOTIC EXPANSIONS FOR THE POLES AND AUXILIARY FORMULAS FOR THE COMPUTATION OF RESIDUES

The following asymptotic expansions for $H_\lambda^{(1)}(x)$, $H_\lambda'^{(1)}(x)$, valid when $|\lambda - x| = \mathcal{O}(x^{\frac{1}{3}})$, $x \gg 1$, have been derived by Schöbe[41]:

$$H_\lambda^{(1)}(x) = 2e^{-i\pi/3}\left(\frac{2}{x}\right)^{\frac{1}{3}}\sum_{n=0}^{\infty}(-1)^n\left(\frac{2}{x}\right)^{2n/3}[P_n(\xi)\,\mathrm{Ai}(-\xi) - e^{-i\pi/3}Q_n(\xi)\,\mathrm{Ai}'(-\xi)], \quad (A1)$$

$$H_\lambda'^{(1)}(x) = -2e^{-i\pi/3}\left(\frac{2}{x}\right)^{\frac{2}{3}}\sum_{n=0}^{\infty}(-1)^n\left(\frac{2}{x}\right)^{2n/3}[\bar{P}_n(\xi)\,\mathrm{Ai}(-\xi) - e^{-i\pi/3}\bar{Q}_n(\xi)\,\mathrm{Ai}'(-\xi)], \quad (A2)$$

[41] W. Schöbe, Acta Math. 92, 265 (1954).

where

$$\xi = e^{-i\pi/3}\left(\frac{2}{x}\right)^{\frac{1}{3}}(\lambda - x), \tag{A3}$$

and

$$\begin{aligned} P_0(\xi) &= 1, & Q_0(\xi) &= 0, \\ P_1(\xi) &= e^{i\pi/3}\frac{\xi}{15}, & Q_1(\xi) &= -e^{-i\pi/3}\frac{\xi^2}{60}, \\ P_2(\xi) &= e^{-i\pi/3}\left(\frac{\xi^5}{7200} - \frac{13\xi^2}{1260}\right), & Q_2(\xi) &= -\frac{\xi^3}{420} + \frac{1}{140}, \end{aligned} \tag{A4}$$

$$\begin{aligned} \bar{P}_0(\xi) &= 0, & \bar{Q}_0(\xi) &= 1, \\ \bar{P}_1(\xi) &= -\frac{\xi^3}{60} - \frac{1}{10}, & \bar{Q}_1(\xi) &= -e^{i\pi/3}\frac{\xi}{15}, \\ \bar{P}_2(\xi) &= -e^{i\pi/3}\left(\frac{\xi^4}{3360} + \frac{\xi}{60}\right), & \bar{Q}_2(\xi) &= e^{-i\pi/3}\left(\frac{\xi^5}{7200} + \frac{19\xi^2}{2520}\right). \end{aligned} \tag{A5}$$

The corresponding expansions for $H_\lambda^{(2)}(x)$, $H_\lambda'^{(2)}(x)$ are obtained by changing the sign of i everywhere in the above expressions.

By employing a slightly different version of these results, Streifer and Kodis[28] found the following improved asymptotic expansion for the poles (3.29):

$$\lambda_n = \beta + e^{i\pi/3}\xi_n/\gamma, \tag{A6}$$

where $\gamma \ll 1$ [cf. Eq. (2.49)] is the expansion parameter, and

$$\xi_n = x_n - \delta_n, \tag{A7}$$

with x_n defined by (2.54) [nth zero of Ai $(-x)$], and

$$\begin{aligned} \delta_n = {} & -e^{i\pi/3}\frac{x_n^2}{60}\gamma^2 - e^{-i\pi/3}\left(\frac{x_n^3}{1400} - \frac{1}{140}\right)\gamma^4 - \left(\frac{281x_n^4}{4536000} - \frac{29x_n}{12600}\right)\gamma^6 \\ & + e^{i\pi/6}\frac{\gamma}{M}\Bigg[1 + e^{i\pi/3}\frac{x_n}{6}\left(1 + \frac{1}{M^2}\right)\gamma^2 - e^{-i\pi/3}\frac{x_n^2}{20} \\ & \times \left(\frac{3}{2M^4} + \frac{13}{9M^2} - \frac{1}{18}\right)\gamma^4 - \frac{e^{-i\pi/6}}{M}\frac{x_n}{36}\left(\frac{1}{M^4} + \frac{2}{M^2} + 1\right)\gamma^5\Bigg] + \mathcal{O}(\gamma^7), \end{aligned} \tag{A8}$$

where $M = (N^2 - 1)^{\frac{1}{2}}$, as in (2.53). The corresponding result for $N < 1$ (which was actually the case considered in Ref. 28) is obtained by the substitution (3.30): $M = -iM' = -i(1 - N^2)^{\frac{1}{2}}$. Notice that $\delta_n = \mathcal{O}(\gamma)$, so that $|\delta_n| \ll 1$.

The first three terms of (A8), which do not depend on N, correspond to the Regge poles [N, Eq. (3.5)] for an impenetrable sphere, i.e., the roots of $H_\lambda^{(1)}(\beta) = 0$. They can formally be obtained by letting $N \to i\infty$, corresponding to an infinitely high potential barrier. The remaining terms in (A8) represent the effect of a finite refractive index.

For the evaluation of the residue series appearing in the first three terms of the Debye expansion, the values of $H_\lambda^{(1)}(\beta)$, $H_\lambda'^{(1)}(\beta)$ and their derivatives up to third order with respect to λ, taken at the poles λ_n, are required. The corresponding asymptotic expansions may be obtained from (A1)–(A5) with the help of the following formulas, which follow from (A3):

$$\dot{\xi} = e^{-i\pi/3}\gamma, \quad \dot{A} = -e^{-i\pi/3}\gamma A', \quad \dot{A}' = e^{-i\pi/3}\gamma\xi A, \tag{A9}$$

where the dots denote partial derivatives with respect to λ and we have introduced the abbreviations

$$A = \text{Ai}\,(-\xi), \quad A' = \text{Ai}'\,(-\xi), \quad \xi = e^{-i\pi/3}\gamma(\lambda - \beta). \tag{A10}$$

We then find the following results:

$$H_\lambda^{(1)}(\beta) = 2e^{-i\pi/3}\gamma\left\{A + \frac{\gamma^2}{15}e^{i\pi/3}\left(\frac{\xi^2}{4}A' - \xi A\right) + \frac{\gamma^4}{20}e^{-i\pi/3}\left[\frac{1}{7}\left(\frac{\xi^3}{3} - 1\right)A' + \frac{\xi^2}{9}\left(\frac{\xi^3}{40} - \frac{13}{7}\right)A\right] + O(\gamma^6)\right\}, \quad \text{(A11)}$$

$$H_\lambda'^{(1)}(\beta) = -2e^{i\pi/3}\gamma^2\left\{A' + \frac{\gamma^2}{15}e^{i\pi/3}\left[\xi A' - \left(\frac{\xi^3}{4} + \frac{3}{2}\right)A\right] + \frac{\gamma^4}{60}e^{-i\pi/3}\left[\frac{\xi^2}{6}\left(\frac{\xi^3}{20} + \frac{19}{7}\right)A' - \xi\left(\frac{\xi^3}{56} + 1\right)A\right] + O(\gamma^6)\right\}, \quad \text{(A12)}$$

$$\dot{H}_\lambda^{(1)}(\beta) = 2e^{i\pi/3}\gamma^2\left\{A' - \frac{\gamma^2}{15}e^{i\pi/3}\left[\frac{3\xi}{2}A' + \left(\frac{\xi^3}{4} - 1\right)A\right] - \frac{\gamma^4}{180}e^{-i\pi/3}\left[\xi^2\left(\frac{22}{7} - \frac{\xi^3}{40}\right)A' + \xi\left(\frac{31}{56}\xi^3 - 5\right)A\right] + O(\gamma^6)\right\}, \quad \text{(A13)}$$

$$\dot{H}_\lambda'^{(1)}(\beta) = -2\gamma^3\left\{\xi A + \frac{\gamma^2}{30}e^{i\pi/3}\left[\left(\frac{\xi^3}{2} + 5\right)A' + \frac{\xi^2}{2}A\right] + \frac{\gamma^4}{60}e^{-i\pi/3}\left[\frac{10}{21}\xi\left(\frac{\xi^3}{8} + 4\right)A' + \left(\frac{\xi^6}{120} + \frac{8}{21}\xi^3 - 1\right)A\right] + O(\gamma^6)\right\}, \quad \text{(A14)}$$

$$\ddot{H}_\lambda^{(1)}(\beta) = 2\gamma^3\left\{\xi A + \frac{\gamma^2}{30}e^{i\pi/3}\left[\left(\frac{\xi^3}{2} - 5\right)A' - \frac{9}{2}\xi^2 A\right] - \frac{\gamma^4}{180}e^{-i\pi/3}\left[\frac{\xi}{7}\left(79 - \frac{19}{4}\xi^3\right)A' - \left(\frac{\xi^6}{40} - \frac{75}{14}\xi^3 + 5\right)A\right] + O(\gamma^6)\right\}, \quad \text{(A15)}$$

$$\ddot{H}_\lambda'^{(1)}(\beta) = 2\gamma^4 e^{-i\pi/3}\left\{\xi A' - A - \frac{\gamma^2}{30}e^{i\pi/3}\left[\xi^2 A' + \xi\left(\frac{\xi^3}{2} + 6\right)A\right] + O(\gamma^4)\right\}, \quad \text{(A16)}$$

$$\dddot{H}_\lambda^{(1)}(\beta) = -2\gamma^4 e^{-i\pi/3}\left\{\xi A' - A - \frac{\gamma^2}{30}e^{i\pi/3}\left[6\xi^2 A' - \xi\left(14 - \frac{\xi^3}{2}\right)A\right] + O(\gamma^4)\right\}, \quad \text{(A17)}$$

$$\dddot{H}_\lambda'^{(1)}(\beta) = -2\gamma^5 e^{i\pi/3}\left\{2A' + \xi^2 A + \frac{\gamma^2}{30}e^{i\pi/3}\left[\xi\left(\frac{\xi^3}{2} + 4\right)A' - 3(\xi^3 + 2)A\right] + O(\gamma^4)\right\}. \quad \text{(A18)}$$

To evaluate these expressions at the pole λ_n, it suffices to replace ξ by ξ_n, which is given by (A7)–(A8). Since $|\delta_n| \ll 1$, the Taylor expansion of the Airy functions around $\xi = x_n$ may be employed, with the results

$$A_n = \mathrm{Ai}(-\xi_n) = \delta_n a_n'\left(1 - \frac{x_n}{6}\delta_n^2 + \tfrac{1}{12}\delta_n^3 + \frac{x_n^2}{120}\delta_n^4 - \frac{x_n}{120}\delta_n^5 + \cdots\right), \quad \text{(A19)}$$

$$A_n' = \mathrm{Ai}'(-\xi_n) = a_n'\left(1 - \frac{x_n}{2}\delta_n^2 + \tfrac{1}{8}\delta_n^3 + \frac{x_n^2}{24}\delta_n^4 - \frac{x_n}{20}\delta_n^5 + \cdots\right), \quad \text{(A20)}$$

where $a_n' = \mathrm{Ai}'(-x_n)$, as in (4.40), and we have employed the differential equation of the Airy functions,

$$\mathrm{Ai}''(z) = z\,\mathrm{Ai}(z). \quad \text{(A21)}$$

The denominator that gives rise to the poles is [cf. Eq. (4.38)]:

$$d(\lambda, \beta) = [1\ \beta] - N[2\ \alpha] \quad \text{(A22)}$$

and the value of its partial derivatives with respect to λ, up to third order, at the poles λ_n is also required for the evaluation of residues.

In the neighborhood of the poles, we have, by N, Eq. (A16):

$$[2\ \alpha] = -i\frac{(N^2 - \omega^2)^{\frac{1}{2}}}{N} - \frac{N\gamma^3}{4(N^2 - \omega^2)} + O(\gamma^6), \quad \text{(A23)}$$

where

$$\omega = \lambda/\beta. \tag{A24}$$

The partial derivatives of [2 α] with respect to λ can be readily evaluated from this expression. Those of [1 β], on the other hand, can be expressed in terms of (A11)–(A18) by means of the following formulas:

$$[1\dot{\ }\beta] = \frac{1}{H_\lambda^{(1)}(\beta)}\{\dot{H}_\lambda'^{(1)}(\beta) - [1\ \beta]\dot{H}_\lambda^{(1)}(\beta)\}, \tag{A25}$$

$$[1\ddot{\ }\beta] = \frac{1}{H_\lambda^{(1)}(\beta)}\{\ddot{H}_\lambda'^{(1)}(\beta) - [1\ \beta]\ddot{H}_\lambda^{(1)}(\beta)\} - 2\frac{\dot{H}_\lambda^{(1)}(\beta)}{H_\lambda^{(1)}(\beta)}[1\dot{\ }\beta], \tag{A26}$$

$$[1\dddot{\ }\beta] = \frac{1}{H_\lambda^{(1)}(\beta)}\{\dddot{H}_\lambda'^{(1)}(\beta) - [1\ \beta]\dddot{H}_\lambda^{(1)}(\beta)\} - 3\frac{\ddot{H}_\lambda^{(1)}(\beta)}{H_\lambda^{(1)}(\beta)}[1\ddot{\ }\beta] - 3\frac{\dot{H}_\lambda^{(1)}(\beta)}{H_\lambda^{(1)}(\beta)}[1\dot{\ }\beta], \tag{A27}$$

where, at the poles, [1 β] can be computed from (3.27) and (A23):

$$[1\ \beta]_{\lambda_n} = N[2\ \alpha]_{\lambda_n}. \tag{A28}$$

APPENDIX B: ASYMPTOTIC BEHAVIOR OF THE SPHERICAL REFLECTION AND TRANSMISSION COEFFICIENTS

We collect in this appendix the main results required in the text about the asymptotic behavior of $S(\lambda, \beta)$ and of the spherical reflection and transmission coefficients (3.4)–(3.8) as $|\lambda| \to \infty$. The derivation is omitted: it is based upon the formulas for the asymptotic behavior of cylindrical functions given in N (Appendix A).

The results are presented graphically in Figs. 18–21. The expression given in each region of the λ plane represents the asymptotic behavior of the corresponding function in that region. Inessential factors, such as constants, are omitted.

The notation is the same as in N (Appendix A): when $|\lambda| \to \infty$ along directions approaching the positive or negative imaginary axis, we take, respectively,

$$\lambda = \pm\sigma|\lambda|, \quad \sigma = \exp[i(\pi/2 + \epsilon)], \tag{B1}$$

and we define

$$\eta_1 = \epsilon \ln\left|\frac{2\lambda}{e\alpha}\right|, \quad \eta_2 = \epsilon \ln\left|\frac{2\lambda}{e\beta}\right|. \tag{B2}$$

The asymptotic behavior of $S(\lambda, \beta)$ is given in Fig. 18, and that of all the spherical reflection and transmission coefficients can be obtained from Figs. 19 and 20. Finally, Fig. 21 shows the asymptotic behavior of $\rho = R_{11}H_\lambda^{(1)}(\alpha)/H_\lambda^{(2)}(\alpha)$, the expansion parameter in the Debye expansion [cf. Eq. (3.15)].

All the results shown refer to the case $N > 1$. However, it is not difficult to adapt them to the case $N < 1$.

APPENDIX C: REDUCTION TO GENERALIZED FOCK FUNCTIONS

To reduce the first two integrals in (4.64) to the generalized Fock functions (4.67), we first note that, by (4.63),

$$(1 + \tfrac{1}{2}\zeta\gamma^2)J_0 = \frac{\gamma}{\theta}\frac{d}{d\zeta}[(1 + \tfrac{1}{2}\zeta\gamma^2)J_1], \tag{C1}$$

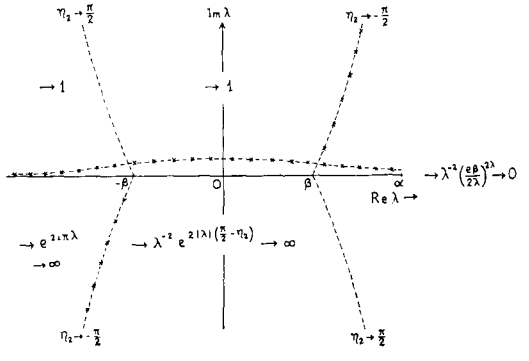

FIG. 18. Asymptotic behavior of $1 - S(\lambda, \beta)$ as $|\lambda| \to \infty$ in different regions of the λ plane. ×—poles ($N > 1$).

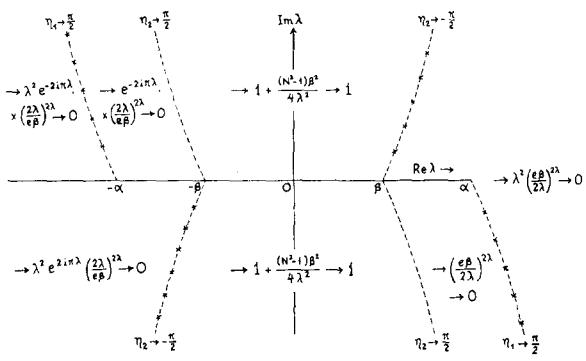

FIG. 19. Asymptotic behavior of $T_{21}(\lambda, \beta) = 1 + R_{22}(\lambda, \beta)$ as $|\lambda| \to \infty$ in different regions of the λ plane. ×—poles ($N > 1$).

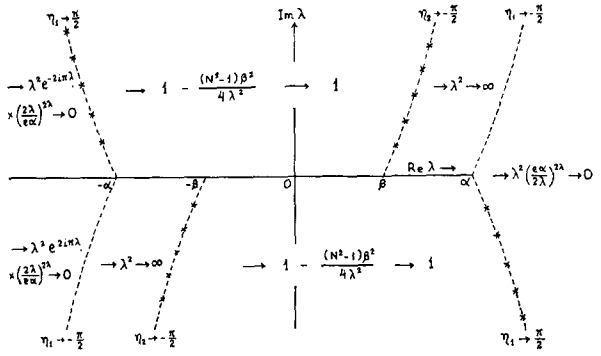

FIG. 20. Asymptotic behavior of $T_{12}(\lambda, \beta) = 1 + R_{11}(\lambda, \beta)$ as $|\lambda| \to \infty$ in different regions of the λ plane. ×—poles ($N > 1$).

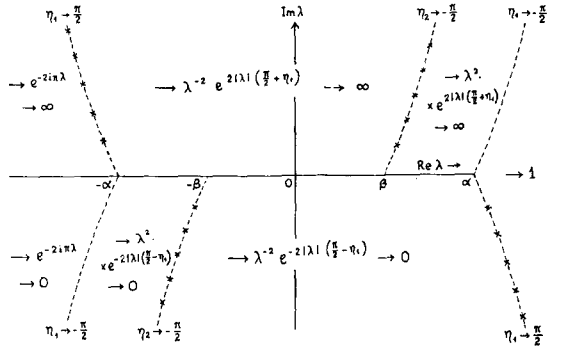

FIG. 21. Asymptotic behavior of $\rho(\lambda, \beta) = R_{11}(\lambda, \beta)H_\lambda^{(1)}(\alpha)/H_\lambda^{(2)}(\alpha)$ as $|\lambda| \to \infty$ in different regions of the λ plane. Note that $|\rho| < 1$ along the real axis. ×—poles ($N > 1$).

where, unless otherwise indicated, the argument of the Bessel functions is always the same as in (4.63). We then find, by partial integration,

$$e^{2i\pi/3}\int_{\sigma_1\infty}^{0}(1 + \tfrac{1}{2}\zeta\gamma^2)J_0\frac{\bar{A}}{A}\,d\zeta$$
$$= e^{2i\pi/3}\frac{\gamma}{\theta}J_1(\beta\theta) + \frac{e^{i\pi/6}}{2\pi}\frac{\gamma}{\theta}\int_{\sigma_1\infty}^{0}(1 + \tfrac{1}{2}\zeta\gamma^2)\frac{J_1}{A^2}\,d\zeta, \quad \text{(C2)}$$

where the Wronskian relation (4.57) has been employed.

A similar transformation can be performed for the second integral in (4.64), with the help of the Wronskian relation [N, Eq. (D2)]. Putting together the results, we obtain

$$e^{2i\pi/3}\int_{\sigma_1\infty}^{0}(1 + \tfrac{1}{2}\zeta\gamma^2)J_0\frac{\bar{A}}{A}\,d\zeta$$
$$+ e^{i\pi/3}\int_0^{\infty}(1 + \tfrac{1}{2}\zeta\gamma^2)J_0\frac{\mathrm{Ai}(\zeta)}{A}\,d\zeta$$
$$= -\frac{\gamma}{\theta}J_1(\beta\theta) + \frac{\gamma}{\theta}[F_{0,1}(\beta, \theta) + \tfrac{1}{2}\gamma^2F_{1,1}(\beta, \theta)], \quad \text{(C3)}$$

where $F_{m,n}$ is defined by (4.67).

Similarly, by partial integration, we find

$$\frac{e^{-i\pi/6}}{2\pi}\int_\Gamma\frac{A'}{A^3}J_0\,d\zeta = \frac{\theta}{2\gamma}F_{0,1}(\beta, \theta). \quad \text{(C4)}$$

It follows from the differential equation (A21) of the Airy functions that

$$\frac{A'^2}{A^4} = \tfrac{1}{3}e^{2i\pi/3}\frac{\zeta}{A^2} - \frac{1}{3}\frac{d}{d\zeta}\left(\frac{A'}{A^3}\right). \quad \text{(C5)}$$

Thus, by partial integration, we get

$$\frac{1}{2\pi}\int_\Gamma\frac{A'^2}{A^4}J_0\,d\zeta$$
$$= \frac{i}{3}F_{1,0}(\beta, \theta) + e^{i\pi/6}\frac{\theta^2}{12\gamma^2}[F_{0,0}(\beta, \theta) - F_{0,2}(\beta, \theta)], \quad \text{(C6)}$$

where we have employed the relation

$$J_1' = \tfrac{1}{2}(J_0 - J_2).$$

Finally, we have

$$\frac{1}{2\pi}\int_\Gamma\zeta^2\frac{A'}{A^3}J_0\,d\zeta = -e^{i\pi/6}\left[F_{1,0}(\beta, \theta) - \frac{\theta}{2\gamma}F_{2,1}(\beta, \theta)\right]. \quad \text{(C7)}$$